2022

Advancing liver-stage malaria *in vitro* models for drug discovery

Francisca Maria de Andrade Terras Arez Durisic

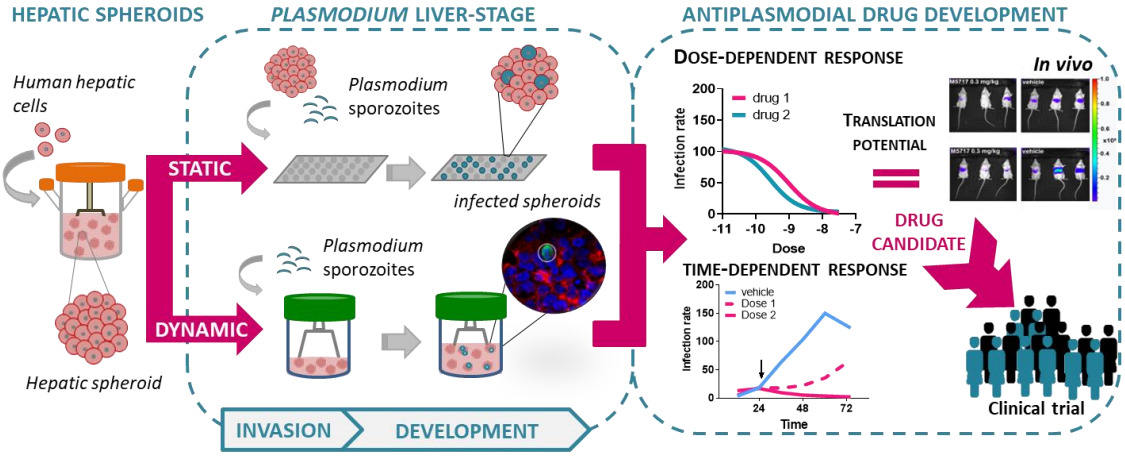

Dissertation presented to obtain the **Ph.D. degree in Bioengineering**

Oeiras, April, 2022

INSTITUTO DE TECNOLOGIA QUÍMICA E BIOLÓGICA ANTÓNIO XAVIER | UNIVERSIDADE NOVA DE LISBOA

Advancing liver-stage malaria *in vitro* models for drug discovery

Francisca Arez

Dissertation presented to obtain the Ph.D. degree in Bioengineering

Instituto de Tecnologia Química e Biológica António Xavier | Universidade Nova de Lisboa

Oeiras, April, 2022

Advancing liver-stage malaria *in vitro* models for drug discovery

Francisca Arez

The work developed in this thesis was supervised by:

- Main supervisor: Paula M. Alves, Ph.D., Instituto de Biologia Experimental e Tecnológica (iBET) and Instituto de Tecnologia Química e Biológica António Xavier, Universidade Nova de Lisboa (ITQB NOVA)

- Co-supervisor: Miguel Prudêncio, Ph.D., Instituto de Medicina Molecular João Lobo Antunes, Faculdade de Medicina, Universidade de Lisboa (iMM JLA)

Financial support from:

Fundação para a Ciência e Tecnologia (FCT), Ph.D. Grants:

PD/BD/128371/2017
COVID/BD/151635/2021

Merck KGaA Darmstadt, Germany

Fundação para a Ciência e Tecnologia/Ministério da Ciência, Tecnologia e Ensino Superior (FCT/MCTES, Portugal) through national funds to iNOVA4Health (UIDB/04462/2020 and UIDP/04462/2020) and the Associate Laboratory LS4FUTURE (LA/P/0087/2020).

Advancing liver-stage malaria *in vitro* models for drug discovery

Instituto de Tecnologia Química e Biológica António Xavier | Universidade Nova de Lisboa

Acknowledgments

I would like to acknowledge all the people directly or indirectly involved in this thesis.

I thank to my supervisor Paula Alves, for engaging in this challenging project with me, giving me the opportunity to grow as an independent researcher. Thank you for discussing with me the project directions, overcoming the obstacles arising throughout these years (which were not few) and for your great problem-solving ability. Thank you for always making the time, even when swamped with all your responsibilities.

To my co-supervisor Miguel Prudêncio, thank you for introducing me to the malaria field and for bringing me into your team. Thank you for your prompt availability and for your dedication to this project. But mostly, thank you for all your scientific rigor, written, spoken and in the experimental work. Thank you for your attention to detail.

I express my enormous gratitude to Catarina Brito, a member of my thesis committee. Thank you for being a team member and a boss, who helped me growing as a scientist, as a colleague and as a person. Thank you, for the continuous guidance, for your knowledge, for pushing me further, for presenting me with challenges that made me grow as a scientist but also for knowing when I need help and moral support. In summary, thank you for your management and for making me the scientist I am today. I also thank you for your friendship throughout these years.

A special thanks to Thomas Spangenberg, the other member of my thesis committee and without whom this project would never be possible. Thank you for the fruitful discussions, ideas, for always motivating the team and for enabling the clinical translational outcomes of this thesis, a part of this work that is special to me.

I am also thankful to Prof Manuel Carrondo and Dr Beatrice Greco for initiating this collaboration, putting together this great team and for the provocative comments that helped this project thrive.

I have to thank to the two other people also involved in this project, and that that contributed to the scientist and professional I have become. Forever my friends Sofia Rebelo and Daniel Simão. Thank you for teaching me from scratch the technical skills I first acquired in my academic career and in the beginning of this project. Thank you for your criticism, scientific discussions, and management of my expectations besides your friendship. To Sofia, I thank further for the guidance in this project that today is my PhD, for your leadership skills that I so much tried to absorb while working by your side, and reproduce throughout the time you were not directly involved in the project. Thank you for being always my buffer, for your positive perspective when my view is clouded with negativism or lost, but most importantly, for never giving up on me. This thesis is in part yours also.

Thank you, Isabella Ramella Gal, my lab hero, unstoppable as no other, without whom the ending of the project and my thesis writing would not be as easy and fruitful as it was.

I thank to all team members from iMM JLA, Lisboa that made the project a success: Marta Machado, for her contagious enthusiasm, Diana Fontinha for her scientific rigor and calm personality, which was a good balance in the team, for the kindness of Helena Cabaço, always willing to give us a hand, making things look easy no matter the amount of work they are.

To my other friends at iBET, I thank specially to Marta Silva, Ana Paula Terrasso, Mafalda Dias, Rita Costa, Marta Estrada, Catarina Pinto, João Sá, and João Vidigal for all the laughs, pranks, scientific discussions, and good sense of humor, which were very important to maintain our youth and good mental health.

I acknowledge all the Advanced Cell Models lab members during my PhD for the good laboratory environment and to all the ACTU members that in some way made my days happier.

A special thanks to my PhD friends “Las Marotas”, for all the counseling, problem sharing and solving throughout these years and crazy (good) friendship.

As last but important notes, I thank to my husband for all the support, for making me leave work at normal hours. To my daughter, for reminding me every day that the PhD is not the hardest thing I have done in these 5 years. To all my babysitters, you know who you are and how important you were for me to have a thesis document written at this day.

Ao resto da minha família agradeço o apoio e amor incondicional que me deram durante esta etapa da minha vida.

Abstract

The malaria drug pipeline has been highly affected by the fast-developing rate of *Plasmodium* resistance to the currently available drugs. There are two promising and complementary approaches being explored to mitigate drug resistance. One is focused on the drugs, and includes the development of drugs exploiting novel targets and the combination of drug partners presenting the same pharmacokinetic properties but distinct modes of action. The other approach is to explore the life cycle of the parasite and target the hepatic stage of the *Plasmodium* life cycle. This phase precedes the symptomatic phase of malaria, and is essential for the development of the disease. Despite promising, drugs targeting the hepatic phase are scarce, highlighting the need for preclinical models recapitulating the complete *Plasmodium* liver-stage of infection and more predictive of the host's drug response. Three-dimensional (3D) models have been shown in the last decades to be powerful tools in the preclinical evaluation of drug toxicity and host drug response compared to the conventional 2D cultures, and are progressively being adopted by the scientific community and pharma industry.

The work developed in this thesis aimed to fill in the gaps in the drug development of anti-plasmodial drugs targeting the liver-stage, ultimately contributing for the enrichment of the anti-plasmodial drugs progressing in the malaria pipeline. Firstly, we developed a preclinical model of the liver-stage of the *Plasmodium* life cycle (Chapter 2), employing immortalized human hepatic cell lines and the murine *Plasmodium berghei* (*Pb*), typically employed in malaria murine models. We explored 3D cell culture approaches and stirred-tank culture systems, achieving a model that has major advantages over the current state-of-the-art: 1) long-term maintenance of the viability, polarization,

phenotype, and biosynthetic functions of the hepatic cells (at least up to 4 weeks), allowing follow-up of reactivation of the parasite to address drug resistance; 2) recapitulation of the complete hepatic development of *Pb* sporozoites into red-blood-cell infective merozoites; and, 3) scalability of the culture system, which allows the feeding of platforms with higher throughput. Due to the ability of maintaining cultures for extended periods of time, the model is potentially interesting for targeting human *Plasmodium* species that have longer hepatic life cycles, and that may form hypnozoites, which are dormant hepatic forms responsible for patient relapse.

The work described in chapters 2 and 3, contributes directly to the enrichment of the malaria drug pipeline. We have applied the developed 3D infection model in drug development, in the preclinical evaluation of the activity of a novel drug candidate under clinical development by Merck, the M5717. The drug was assessed as monotherapy (chapter 2) and in combination with an approved-malaria drug, pyronaridine (chapter 3). The results obtained *in vitro* for drug efficacy and safety were in accordance with those obtained in *in vivo* studies. Importantly, the data obtained for the M5717 monotherapy replicated what was observed in the mice model and was applied in the extrapolation that defined the dose of a Phase I clinical trial. These data open opportunities to reduce the use of animal models in malaria drug discovery. In summary, the work presented in this thesis goes beyond the development of the infection model, demonstrating its predictive power and impact in the preclinical stage of anti-plasmodial drug development.

Finally, chapter 4 described the first steps aiming at the translation of the infection platform into human infectious *Plasmodium* species, such as *P. falciparum* and *P. vivax*, the two main species responsible for the higher morbidity and mortality of malaria. This translation will allow addressing drugs for which the active form is a product of the

hepatic metabolization and assess their long-term effects including drug resistance and disease relapse (targeting hypnozoites).

Overall, this thesis paves the way for the introduction of human 3D cell models in the malaria drug discovery pipeline, ultimately contributing to the development of new effective chemoprotective drugs targeting the liver-stage of *Plasmodium* infection, including the latent forms that evade the action of most anti-plasmodial drugs.

Keywords: *Plasmodium,* liver, Malaria, spheroids, drug discovery, M5717, translational.

Resumo

O reportório de fármacos dirigidos à malária tem sido fortemente afetado pelo rápido desenvolvimento de resistência por parte do parasita da malária, *Plasmodium*, aos fármacos disponíveis até à data. De forma a mitigar o desenvolvimento de resistência a fármacos duas abordagens promissoras e complementares têm sido implementadas. Uma focada no desenvolvimento de fármacos com novos mecanismos de ação e a combinação de fármacos que possuam mecanismos de ação diferentes, mas propriedades farmacocinéticas semelhantes. A outra abordagem consiste em explorar o ciclo de vida do parasita e direcionar as terapias para a fase hepática da infeção por *Plasmodium*. A fase hepática do ciclo de vida deste parasita precede a fase associada aos sintomas da malária e é obrigatória para a evolução desta doença, como tal constitui um alvo promissor para terapia direcionada. Apesar de promissora, por ter um carácter assintomático a fase hepática tem sido menos explorada, pelo que poucos fármacos são eficazes nesta fase da infeção. Como tal, há necessidade de desenvolver novos modelos celulares pré-clínicos capazes de recapitular da fase hepática da infeção de *Plasmodium* e prever com precisão a resposta do hospedeiro e patogénio a novos fármacos. Nas últimas décadas, modelos celulares tri-dimensionais (esferóides) têm-se revelado plataformas poderosas na avaliação de toxicidade e na previsão da resposta do hospedeiro a novos fármacos. Como tal, tanto na comunidade científica como na comunidade farmacêutica têm-se tornado uma alternativa aos modelos pre-clínicos convencionais, como culturas bi-dimensionais em monocamadas.

O trabalho desenvolvido no âmbito desta tese tem como objetivo contribuir para o desenvolvimento de fármacos contra a malária, contribuindo em última instância para o enriquecimento do reportório de

fármacos existentes, especificamente contra a fase hepática da infeção. Primeiramente, desenvolveu-se um modelo celular pre-clínico que mimetiza a fase hepática completa da infecção de *Plasmodium* (capítulo 2), utilizando linhas celulares humanas imortalizadas e *P. berghei*, uma espécie murina de *Plasmodium*, que *in vitro* infecta células hepáticas humanas. Para a construção de um modelo tri-dimensional foram usados sistemas de cultura agitados, permitindo o desenvolvimento de um modelo com vantagens relativamente aos modelos pre-clínicos disponíveis de momento: 1) a manutenção por um extenso período de cultura de hepatócitos em esferóides com viabilidade celular, fenótipo hepático e funções biosintéticas (pelo menos 4 semanas) permitindo seguir a reativação dos parasitas e detetar a resistência a fármacos; 2) recapitulação da fase hepática completa da infeção de *Plasmodium*, até à geração e libertação de parasitas denominados merozoítos, capazes de estabelecer a fase da infeção associada aos sintomas; e 3) a capacidade escalonável do sistema de cultura, que permite alimentar plataformas com maior capacidade de *high throughput*. A capacidade de manutenção de culturas por longos períodos de tempo é especialmente interessante para estudar espécies de *Plasmodium* que infetam humanos, com fases hepáticas de infeção mais longas (~7 dias), e que formem hipnozoítos, formas dormentes do parasita responsáveis pelas reincidências da doença, normalmente meses após a infeção primária.

O trabalho descrito nos capítulos 2 e 3 contribui diretamente para o reportório de fármacos contra a fase hepática da infeção de *Plasmodium*. As plataformas desenvolvidas no capítulo 2 foram utilizadas para a avaliação da segurança e eficácia de um fármaco em desenvolvimento clínico pela Merck, M5717. Este fármaco foi avaliado em monoterapia (capítulo 2) e em combinação com um fármaco já aprovado contra malária, pironaridina (capítulo 3). Os resultados de

segurança e eficácia obtidos *in vitro*, foram confirmados em modelos animais. Mais importante, os dados gerados relativamente à monoterapia de M5717 foram posteriormente aplicados numa simulação que serviu de base para estabelecer doses a aplicar numa primeira fase de ensaios clínicos. Para além do desenvolvimento do modelo, este trabalho demonstra o poder de previsão que os esferóides oferecem e o impacto na redução do número de modelos animais necessários na fase pre-clínica de desenvolvimento de fármacos contra a malária.

Finalmente, o capítulo 4 descreve os primeiros passos para a translação da plataforma de infeção desenvolvida para espécies de *Plasmodium* infeciosas em humanos, nomeadamente *P. falciparum* e *P. vivax,* as duas espécies responsáveis pela maioria de casos e mortes causados por esta doença. A translação para estas espécies passa pelo uso de hepatócitos primários, o que permitirá estudar e desenvolver fármacos para os quais o efeito requer a metabolização no composto ativo. Para além disso, esta plataforma permitirá o estudo do efeito farmacológico ao longo do tempo, incluindo o desenvolvimento de resistência e reincidência da doença.

Em conclusão, esta tese abre o caminho para a introdução de modelos celulares 3D no desenvolvimento de fármacos contra a malária, contribuindo em última instância para o desenvolvimento de novos fármacos eficazes na eliminação de parasitas na fase hepática da infeção, incluindo as formas latentes (hipnozoítos) que escapam à eficácia da maioria dos fármacos disponíveis.

Palavras-chave: *Plasmodium*, fase hepática, malária, esferóides, desenvolvimento de fármacos, M5717, translacional.

Thesis publications

Arez F.*, Rebelo SP.*, Fontinha D.*, Simão D., Martins TR., Machado M., Fischli C., Oeuvray C., Badolo L., Carrondo MJT., Rottmann M., Spangenberg T., Brito C., Greco B., Prudêncio M., Alves PM., (2019) Flexible 3D Cell-Based Platforms for the Discovery and Profiling of Novel Drugs Targeting Plasmodium Hepatic Infection. ACS Infectious Diseases. DOI: 10.1021/acsinfecdis.9b00144.

Fontinha D.*, Arez F.*, Ramella IG., Nogueira G., Moita D., Baeurle THH., Brito C., Spangenberg T., Alves PM., Prudêncio M., (2021) Pre-erythrocytic Activity of M5717 in Monotherapy and Combination in Preclinical Plasmodium Infection Models. ACS Infectious Diseases. DOI: 10.1021/acsinfecdis.1c00640

Khandelwal, A., Arez, F., Alves, P. M., Badolo, L., Brito, C., Fischli, C., Fontinha, D., Oeuvray, C., Prudêncio, M., Rottmann, M., Wilkins, J., Yalkinoglu, Ö., Bagchus, W. M., & Spangenberg, T. (2022). Translation of liver stage activity of M5717, a Plasmodium elongation factor 2 inhibitor: from bench to bedside. Malaria Journal, 21(1), 151. DOI: 10.1186/s12936-022-04171-0

Other publications

Arez F., Rodrigues AF., Brito C. and Alves PM., (2021) Bioengineered Liver Cell Models of Hepatotropic Infections. Viruses. DOI: 10.3390/v13050773.

Table of Contents

List of abbreviations

a.u. - arbitrary units

ALB - Albumin

Alb – Albumin

ATO – atovaquone

BC - bile canaliculi

BD – Bile duct

C_{av} - average plasma concentration

CV – central vein

CD81 – tetraspanin CD81

CSP - circumsporozite protein

CYP450 - cytochrome P450 enzymes

DNA – desoxyribonucleic acid

ECM – extracellular matrix

EEF - exoerythocytic form

eEF2 - elongation factor 2

ESC – embryonic stem cells

FBS – faetal bovine serum

FDA – fluorescein diacetate

FELASA - Federation of European Laboratory Animal Science Associations

FPR – false positive rate

FSG- Fish-skin gelatin

G6PD - glucose-6-phosphate dehydrogenase

GAPDH - glyceraldehyde 3-phosphate dehydrogenase

GFP – green fluorescent protein

HA – hepatic artery

HBV - hepatitis B virus

HCV - hepatitis C virus

HGF – hepatocyte growth factor

HLC -hepatocyte-like cells

HNF4α - hepatocyte nuclear factor 4 alpha

hpi – hours post-infection

HSC - hepatic stellate cells

HSP70 – heat shock protein 70

HSPGs - heparan-sulfate proteoglycans

I.V. - intravenous

IC50 - half maximal inhibitory concentration

KC – kupffer cells

LC-MS - Liquid chromatography-mass spectrometry

LDLR - low-density lipoprotein receptor

LPS - lipopolysaccharide

LSEC – liver sinusoidal endothelial cells

Luc – luciferase

Lumina – live bioluminescence

MalDA - Malaria Drug Accelerator

MFI – mean fluorescence intensity

MIC - minimum inhibitory concentration

MMV – Medicines for Malaria Venture

MPCC - micropatterned co-cultures

MRP2 - multidrug resistance-associated protein 2

MSP-1 – Merozoite surface protein

NPC – non-parenchymal cells

NTCP - Na^+-taurocholate cotransporting polypeptide

O.C.T.- optimum cutting temperature

P. berghei – Plasmodium berghei

P. cynomolgy – Plasmodium cynomolgi

P. falciparum – Plasmodium falciparum

P. ovale – Plasmodium ovale

P. vivax – Plasmodium vivax

P. yoelii – Plasmodium yoelii

Pb – P. berghei

PBS - phosphate-buffered saline

pen/strep – penicillin-streptomycin

PHH – primary human hepatocytes

PI4K - phosphatidylinositol 4-kinases

PPP – public-private partnerships

PV – Portal vein

PVM - parasitophorous vacuole membrane

PXR - pregnane-x-receptor

Pyro - pyronaridine

RNA – ribonucleic acid

RT-qPCR – real-time quantitative polymerase chain reaction

S.D. – standard deviation

S.E.M - standard error of the mean

SACC – self-assembling co-cultures

Spz – sporozoites

SR-BI - scavenger receptor class B type 1

TJ – tight junctions

TRAP - thrombospondin-related anonymous protein

TX-100 – Triton X-100

UIS4 up-regulated in infective sporozoites 4

ZO-1 – zonula occludens-1

Chapter I

General introduction and thesis aims

Author contributions: Chapter outline, FA; Chapter writing, FA; Chapter revision and editing, MP, CB and PMA

Table of contents

Liver Microenvironment and Hepatocyte-specific Traits

The liver is a central organ in the human body, with critical roles in homeostasis, metabolism, detoxification, and clearance of exogenous microorganisms.

The functional units of the human liver are its two lobules, which are composed by the portal triads (portal vein, bile duct, and hepatic artery) and the surrounding hepatocytes, linearly arranged towards the central vein (Figure I.1A).

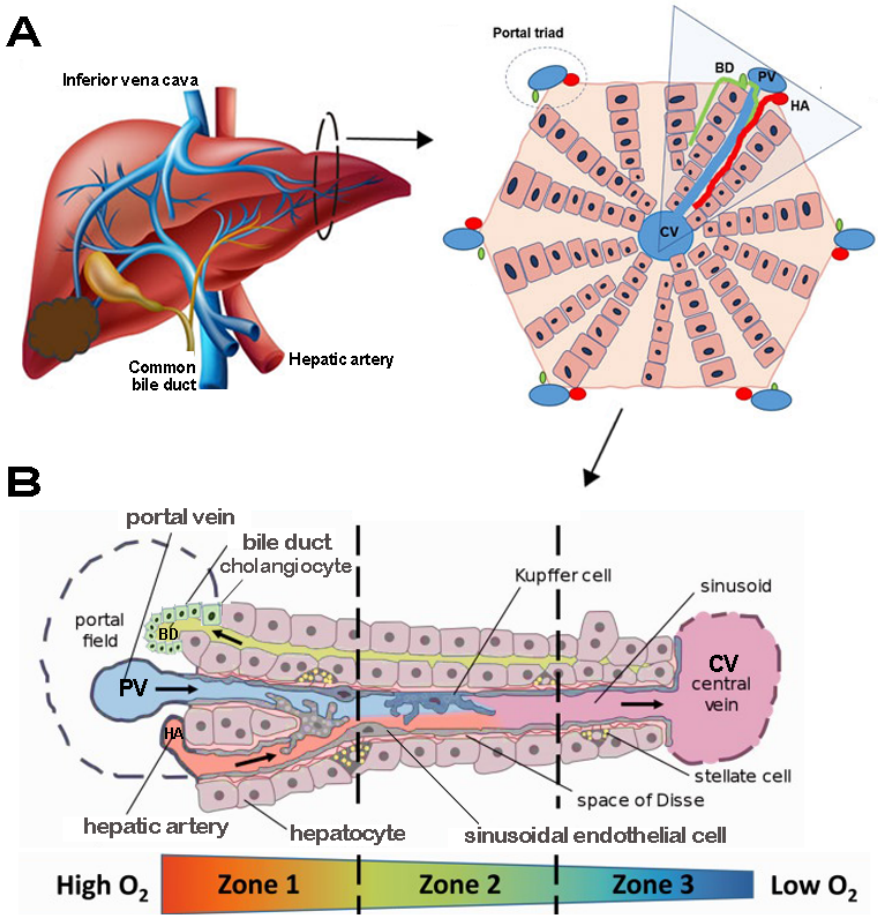

Figure I.1 - Schematic representation of the liver tissue architecture and cellular organization. (A) Scheme of the two liver lobules and the hexagonal-shaped hepatocytes linearly arranged towards the central vein (CV) and portal

triad (Bile duct - BD, Portal vein – PV and hepatic artery – HA). **(B)** Representation of the liver cell population, highlighting the hepatocyte zonation resulting from the higher to lower oxygen supply from the PV to the CV. Image adapted from (Lee-Montiel et al. 2017; Xu 2021).

Being parenchymal cells, hepatocytes are responsible for the major liver functions, including the carbohydrate and lipid metabolism, detoxification, protein synthesis, and self-replication. In addition, around 40% of the liver cells are non-parenchymal cells (NPC) that support and maintain hepatocyte functionality (Figure I.1B). Among them, the liver sinusoidal endothelial cells (LSEC, approximately 50 % of the NPC) form the fenestrated lining of the hepatic sinusoid allow the exchange of proteins and particles between plasma and the cell types of the liver, while maintaining barrier functions (Trefts et al. 2018); Kupffer cells (KC, 20 % of the NPC), the liver-resident macrophages recognize and mount the innate immune response in the liver (Racanelli and Rehermann 2006); and hepatic stellate cells (HSC, 1% of the NPC) or liver stromal cells, are involved in the biosynthesis of the liver extracellular matrix (ECM), scarring after liver injury and storage of vitamin A (Trefts et al. 2018). Other NPC populations include the liver dendritic cells, cholangiocytes, and intrahepatic lymphocytes that comprise the T cells, B cells and natural killer cells. Each of these cell types cooperatively regulate hepatic function at multiple levels (Racanelli and Rehermann 2006; Trefts et al. 2018).

Contributing to the liver architecture and microenvironment, the ECM confers mechanical coherence and resistance to the liver. In the adult liver, the most common ECM proteins are collagens, particularly collagen I and IV, followed by the glycoproteins laminin and fibronectin, and proteoglycans. Although their expression varies throughout liver development, collagen IV is more abundantly localized in the basement membrane with laminin, whereas the interstitial space is composed

mostly by collagen I and fibronectin (Ueno et al. 2003). Both the parenchyma cells and NPCs express ECM, which plays specific roles in major biological functions such as cell proliferation, migration, differentiation, and gene expression (Ueno et al. 2003). The importance of the ECM is highlighted by the diverse number of liver diseases that result in its remodeling and stiffening, as well as by its effect on the cell culture of primary human hepatocytes (discussed below) (Pampaloni et al. 2007).

The liver presents a unique organization due to the dual supply of nutrients from the portal vein (approximately 75%) and oxygen from the hepatic artery (approximately 25%) (Figure I.1B) (Kalra et al. 2022), which influence the phenotype of hepatocytes. As a result of their proximity to the portal triad, hepatocytes are exposed to gradients of oxygen, nutrients, and signaling cues that define their heterogeneity, or spatial zonation (Figure I.1B). The spatial zonation results on hepatocyte subpopulations with distinct phenotypes, including number of chromosomes, expression profiles of RNA and proteins, and metabolic roles. These subpopulations have complementary functions: the more perfused/oxygenated hepatocytes (periportal, or zone 1 hepatocytes, Figure I.1B) are largely involved in oxidative metabolism, such as beta-oxidation, gluconeogenesis, bile and cholesterol formation and amino acid catabolism, whereas the less oxygenated and more distant from the portal triad mostly have a role in detoxification, xenobiotic biotransformation, ketogenesis, glycolysis, lipogenesis, glycogen synthesis, and glutamine formation (perivenous, or zone 3 hepatocytes, Figure I.1B) (Jungermann 1986; Braeuning et al. 2006). Although these zones are normally described as discrete, hepatic zonation is a flexible trait, as mid-lobular hepatocytes (pericentral, or from zone 2 hepatocytes) can assume the functional role of periportal and

perivenous hepatocytes in response to liver injury (Wei et al. 2021; He et al. 2021).

As epithelial cells, hepatocytes form a crucially important cell layer that separates sinusoidal blood from the canalicular bile (Figure I.1), two countercurrent flow systems (Treyer and Müsch 2013). To sustain the simultaneous secretion of canalicular bile and the secretion of serum proteins into the blood, hepatocytes present a highly complex polarity characterized by multiple cell membrane domains (apical and basolateral) segregated by tight junctions (TJ) (Figure I.2).

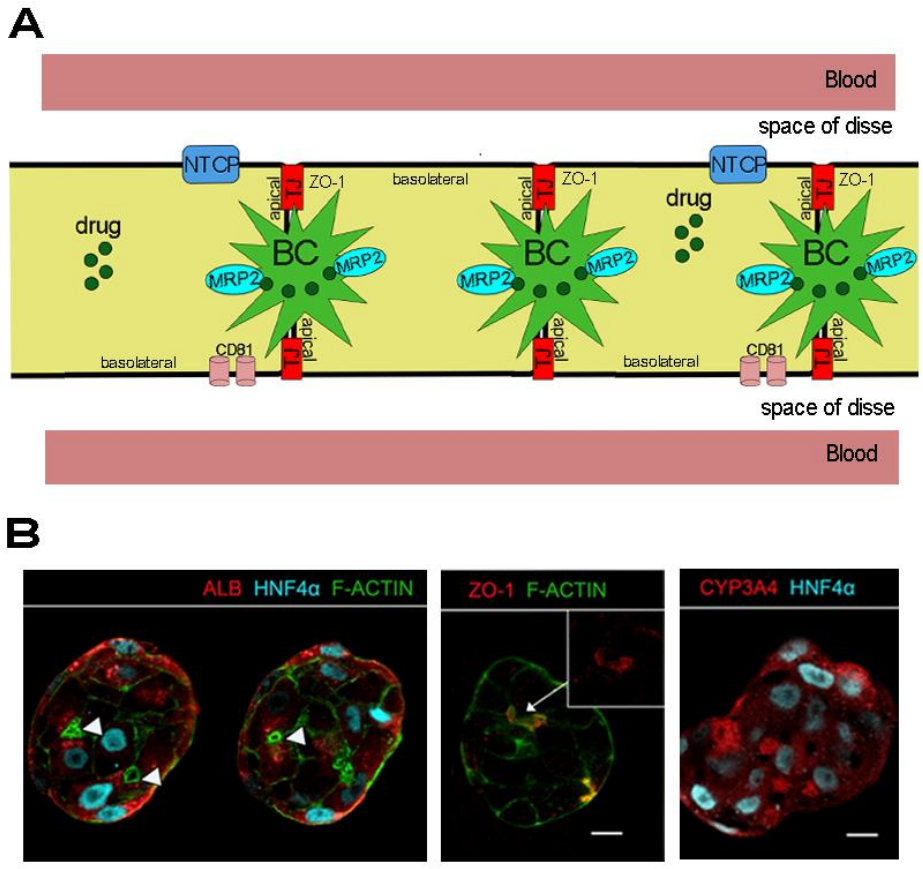

Figure I.2 - Hepatocyte-specific traits. (A) Schematic representation of the hepatocyte polarity discriminating the apical and basolateral membrane domains, separated by tight junctions (TJ). The specific localization of

hepatocyte receptors in the basolateral domain (Na^+-taurocholate cotransporting polypeptide, NTCP and tetraspanin CD81), and the formation of bile canulicular lumens (BC) in the apical membranar domain with the localization of multidrug resistance-associated protein 2 (MRP2) are represented. **(B)** Representative images of hepatocyte specific traits in *in vitro* 3D cultures of the hepatic cell line HepaRG (Rebelo et al. 2015). The F-actin intercellular localization demonstrates the formation of bile canulicular lumens (identified with white arrows), the expression of hepatocyte specific proteins (hepatocyte nuclear factor 4α, HNF4α and albumin, ALB) are represented in the left panel. The middle panel shows the localization of zonula occludens-1 (ZO-1), one of the constituents of hepatocytes tight junctions and the right panel demonstrates the expression of the phase I metabolizing enzyme CYP3A4.

The apical poles of two adjacent hepatocytes form a continuous apical membrane delineating small lumens, the bile canaliculi (BC), that harbor numerous transport proteins, such as multidrug resistance-associated protein 2 (MRP2, Figure I.2A), to excrete bile salts from the cell (Gissen and Arias 2015). The basolateral domain, which contacts the sinusoidal blood, contains a subset of ABC transporters and solute transporters that mediate retrieval of bile acids and other biliary components from the circulation, such as the Na^+-taurocholate cotransporting polypeptide (NTCP, Figure I.2A) (Gissen and Arias 2015). Furthermore, it is in the basolateral membrane that receptors such as low-density lipoprotein receptor (LDLR), scavenger receptor class B type 1 (SR-BI) and tetraspanin CD81 (CD81), are expressed, facilitating the entry of hepatitis C virus (HCV) and *Plasmodium falciparum* (Silvie et al. 2003; Schulze et al. 2019), two of the more incident hepatotropic pathogens.

The formation of BC is an important feature of polarized hepatocytes and the accumulation of actin filaments on their membrane is essential for their functional organization (Figure I.2B) (Ishii et al.

1991). TJ segregate the basolateral and apical domains of hepatocytes (Figure I.2A) and are composed of transmembrane proteins, such as occludins, claudins and junctional adhesion molecules (catenins and cadherins). Zona ocluden proteins (e.g. ZO-1), the first proteins cloned from TJ, link the transmembrane proteins to the actin cytoskeleton being concentrated in the TJ of highly polarized cells (Fanning et al. 1998). ZO-1 is frequently used *in vitro* as a marker of hepatocyte polarity (Figure I.2B)(Rebelo et al. 2015; Gaskell et al. 2016). The TJ are crucial for the maintenance of hepatocyte-hepatocyte interactions, which are required for maintaining cell polarity and the expression of phase I metabolizing enzymes (cytochrome P450, CYP450), essential for the response of hepatocytes to a xenobiotic insult (Hamilton et al. 2001). One of the triggering factors important for the establishment of TJ is the hepatocyte nuclear factor 4-alpha (HNF4α), which induced the expression of claudin and occludin proteins and subsequent polarization of murine embryonal carcinoma cells (Chiba et al. 2003). Besides its role in hepatocyte polarization, HNF4α is one of the most important transcription factors in the maintenance of hepatocyte differentiation and function by activating most hepatocyte-specific genes. Unlike other liver transcription factors (Chiba et al. 2003), the loss of HNF4α in mice virtually abolished the expression of genes encoding for apolipoproteins, metabolic proteins and serum factors, as well as transcription factors involved in hepatocyte gene profile (Li et al. 2000). Furthermore, by regulating the expression of pregnane-x-receptor (PXR), a transcription factor responsible for the induction of proteins involved in the three phases of xenobiotic metabolism, HNF4α indirectly affects this major function of the hepatocytes. Due to its essential roles in hepatocyte maturity and function HNF4α is widely used as a marker of hepatocyte identity (Figure I.2B).

As previously mentioned, hepatocyte polarity is crucial for their adequate function. One of these functions is the secretion of proteins into the blood flow. One of the most abundant proteins in the plasma and secreted exclusively by the hepatocytes is albumin. Albumin contains binding sites with high affinity to many compounds, such as xenobiotics, affecting drug pharmacokinetics (Tesseromatis and Alevizou 2008). As albumin is exclusively synthesized by hepatocytes, its concentration reflects hepatic protein synthesis and is one of the most widely used measures of hepatocytes and liver biosynthetic function (Figure I.2B).

Finally, hepatocytes are effector cells in xenobiotic metabolism, one of the most important functions of the liver. This function is accomplished by the abundant hepatocyte expression of metabolizing enzymes, such as CYP450 (Figure I.2B), transferases and drug transporters, responsible for catalyzing reactions in the different phases of drug biotransformation. Drug biotransformation consists in sequential chemical modifications towards better drug excretion, often resulting in the inactivation of the compound's pharmacological activity. This process occurs in phases, being the first phase mostly carried out by the CYP450 isoforms, with the aim of functionalizing the active compounds with polar groups through oxidation, reduction, and hydrolysis reactions (Sevior et al. 2012). From all CYP families, CYP1, CYP2 and CYP3 are known to play important roles in the metabolism of the majority of the drugs. Specifically, the isoforms CYP3A4, CYP2C9, CYP1A2, CYP2D6, CYP2C19 and CYP2E1 are responsible for the metabolism of 90% of xenobiotics (Manikandan and Nagini 2018). Important for drug development, CYP450s possess a broad spectrum of substrates, allowing competition of different substrates for the same enzyme binding site, which may lead to CYP450 inhibition and low drug metabolism. Therefore, these enzymes constitute major players in the metabolism-

based drug–drug interactions. The inhibition of any CYP450 may be clinically significant. However, due to polymorphisms of CYP450 within the population, their effect is not always straightforward (Sevior et al. 2012), highlighting their required assessment during the preclinical development of drug candidates, or in the establishment of hepatic *in vitro* models for such purpose (Figure I.2B). The products of phase I enzymes become substrates of the phase II metabolizing enzymes, which catalyze conjugation reactions making use of endogenous co-factors, such as glucuronate, sulfate, glutathione, or amino acids. The drugs after phase I and II biotransformation are more hydrophilic and less toxic, being more easily excreted through the action of membrane efflux pumps, including multidrug resistance transporters (often termed phase III metabolizing enzymes). Similar to biotransformation enzymes, genetic polymorphisms occur in drug transporters. Additionally, their activity levels may be altered by drug–drug interactions causing their inhibition or induction (Sevior et al. 2012). Hence, the expression and activity of the metabolizing enzymes involved in these three phases are a common trait to be evaluated and recapitulated in *in vitro* hepatic models for drug testing purposes.

Malaria: The *Plasmodium* Life Cycle

Malaria is one of the deadliest human infectious diseases worldwide, having caused 627 000 deaths in 2020 alone, almost 70 thousand more than in 2019 (WHO 2021). Today, the burden falls disproportionately on children in tropical regions younger than 5 years old and living in sub-Saharan Africa (WHO 2021). In humans, five *Plasmodium* species can cause the disease: *P. falciparum, P. vivax, P. ovale, P. malariae and P. knowlesi* (Prudêncio et al. 2011). *P. falciparum* and *P. vivax* are the two most prevalent parasite species in the malaria cases reported worldwide (WHO 2021). Malaria is transmitted during a

bite of a female *Anopheles* mosquito, upon which sporozoites residing in the mosquito's salivary glands are released into the mammalian host's skin (Amino et al. 2006) (Figure I.3).

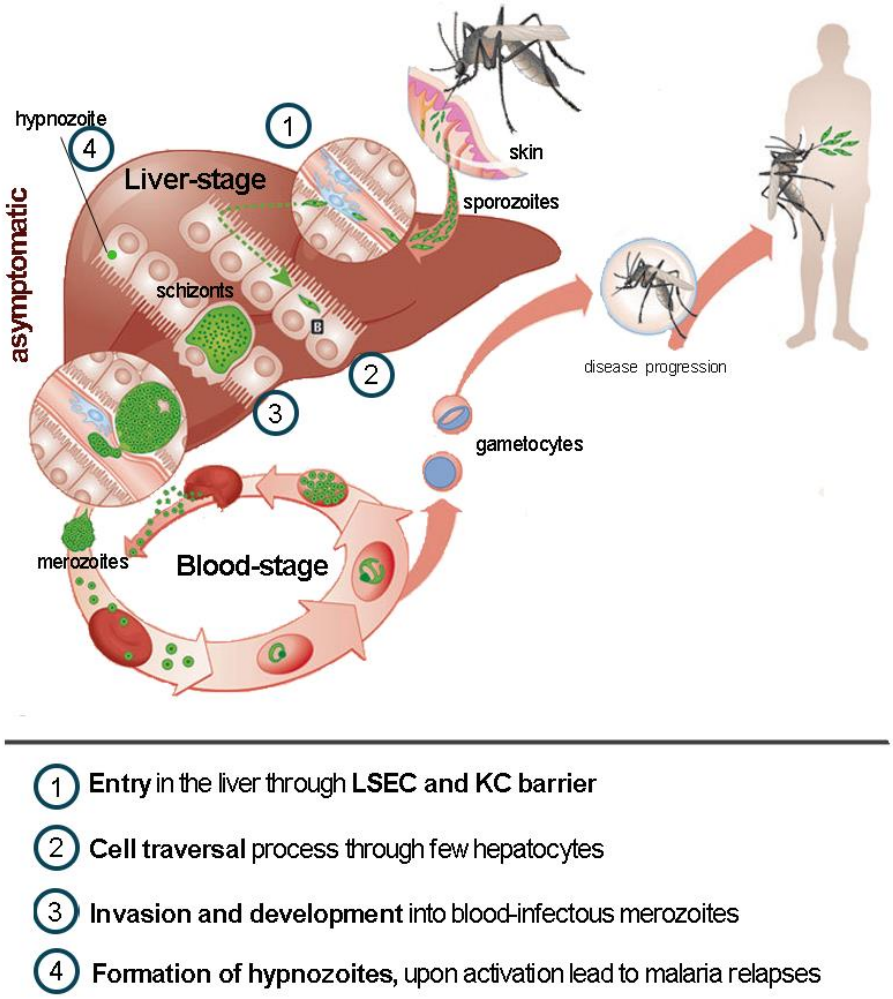

Figure I.3 - *Plasmodium* life cycle. Schematic representation of the *Plasmodium* life cycle highlighting the 4 important processes occurring during the asymptomatic liver-stage of infection: (1) sporozoite traversal of liver sinusoidal endothelial cells (LSEC) and Kupffer Cells (KC) barrier into the parenchyma; (2) cell traversal process preceding the productive invasion of one hepatocyte; (3) invasion and development of sporozoites into blood-infectious merozoites inside the invaded hepatocyte; (4) persistence of hypnozoite forms

in the case of P. *vivax* and P. *ovale* infections. Image adapted from (Portugal et al. 2011).

Within the dermis, the parasites use their gliding motility, typical of apicomplexan protozoans (King 1988), to enter blood vessels and, in a smaller percentage, lymph nodes (Amino et al. 2006). Most sporozoites travel through the blood stream reaching the liver, whereas those that get trapped in the lymph nodes develop abnormally, ultimately being degraded (Amino et al. 2006). In the liver, *Plasmodium* sporozoites cross the first physical barrier composed by LSEC and KC (Figure I.3). Through a process termed cell traversal, essential for parasite's evasion from KC phagocytic activity, parasites irreversibly disrupt the KC membrane and reach the parenchymal cells (Tavares et al. 2013). In the parenchyma, parasites traverse several hepatocytes in a transient cell traversal process (reversible rupture) until productively invading one, which is characterized by parasite internalization into a parasitophorous vacoule through an invagination process. Unlike cell traversal, productive invasion does not imply the rupture of the host cell membrane, allowing the parasite to develop inside a parasitophorous vacuole (PV) in the intact host cell (Mota et al. 2002). Within the PV, each sporozoite transforms into a spherical exoerythocytic form (EEF) (Bano et al. 2007), which undergoes asexual replication and differentiation (the schizontal phase, Figure I.3) into thousands of blood-infectious merozoites (Prudêncio et al. 2006). Merozoites are released into the blood stream inside merosomes, completing the asymptomatic liver-stage of infection (Figure I.3). In the blood, merozoites initiate a cyclic infection of red blood cells (Figure I.3), such as erythrocytes or reticulocytes, according to the *Plasmodium species*. This is the stage of infection associated to the major clinical symptoms and during which sexual forms, gametocytes, are originated and can be further uptake during another mosquito blood meal, leading to the disease

transmission (Figure I.3). All human-infective *Plasmodium* species transit and mature through these stages. However, *P. vivax* and *P. ovale* possess the unique ability to form long lasting latent parasitic forms, termed hypnozoites, in the mammalian liver (Figure I.3). Hypnozoites can be activated weeks to months after the primary infection, causing recurrent disease relapses (Imwong et al. 2007). While in latency, these parasitic forms are not targeted by most of the available drug therapies, hampering malaria eradication.

Non-human *Plasmodium* parasite species as models of infection

Whereas *Plasmodium* blood-stages have been recognized as early as 1880s, it was only half a century later that liver forms of the parasite were first identified (reviewed by Prudêncio et al. 2011). This is, in part, associated with the limited access to human infectious *Plasmodium* species, which can be obtained from wild mosquitoes or from patient clinical isolates. For both, the use in research requires complex and time-consuming paperwork and are of limited availability outside of the endemic areas. With the aim of having a regular source of human infectious parasites, the implementation of *in vitro* cultures of erythrocytic stages of *P. falciparum* and *P. vivax* was attempted early (Bass and Johns 1912). Nevertheless, the infectivity of *P. vivax* is hard to maintain in culture and their restricted access have limited this procedure optimization.

As in most instances, *Plasmodium* parasites from non-human hosts are an attractive alternative for the study of this disease. *P. berghei* and *P. yoelii* are rodent *Plasmodium* parasites, that share the characteristics of the liver-stage development with primate-infective *Plasmodium* species, albeit in a shorter timeline (Figure I.4, 48 to 68 h

for the complete liver-stage development of parasites *in vitro*) (reviewed by Prudêncio et al. 2011).

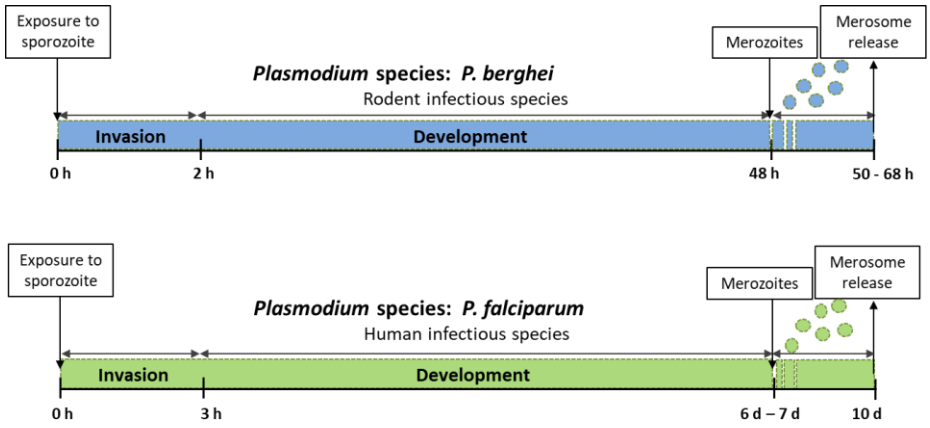

Figure I.4 - *In vitro* timeline of *Plasmodium* liver-stage infection. Schematic representation of the *Plasmodium* liver-stage development *in vitro*, highlighting the timeline for parasite productive invasion, development into detectable merozoites and release of merosome into the cultures supernatants for rodent- (blue) and human- (green) infective *Plasmodium* species.

Although selectively infecting hepatocytes in rodent hosts, *P. berghei* and *P. yoelii* sporozoites can invade and develop inside diverse human hepatic cells *in vitro* (Tavares et al. 2017), providing testing settings of *in vitro* liver-stage cultures in human host cells in addition to the *in vivo* pathology setting. As such, rodent *Plasmodium* species have been crucial and widely used for unveiling important molecular players and pathogen-hepatocyte interactions occurring in the liver-stage of *Plasmodium* infection.

Sporozoite gliding, the spiral movement that allows sporozoite motility is produced by the binding of parasite surface proteins to the surface of the target cells. The circumsporozoite protein (CSP) is the most abundant protein on the sporozoite surface and it is suggested to

have multiple and crucial roles in sporozoite gliding, interactions with the host cells and sporozoite development. Employing the *P. berghei* mouse model, it has been reported that the inhibition of CSP with monoclonal antibodies renders inhibition of gliding motility, compromising sporozoites infectivity (Potocnjak et al. 1980). Due to its important role in this movement, CSP is often used *in vitro*, to detect the parasite's gliding capacity through CSP shedding during gliding (King 1988). Another protein secreted during the gliding stages, and to which mutations have rendered impairment of *P. berghei* sporozoite motility, is thrombospondin-related anonymous protein (TRAP) (Yoshida et al. 1981; Sultan et al. 1997). Both CSP and TRAP were shown to be conserved among diverse *Plasmodium* species, including *P. vivax* and *P. falciparum*, as well as the rodent *Plasmodium* species *P. berghei* and *P.yoelii* (McCutchan et al. 1996; Templeton and Kaslow 1997).

The KC receptor CD68 was another surface protein to be discovered as an entry gate of the parasite in the liver employing a *P. berghei* mouse model (Cha et al. 2015). CD68 was shown to be involved in the internalization of sporozoites by binding to the parasite's glyceraldehyde 3-phosphate dehydrogenase (GAPDH) exposed on the surface of sporozoites (Cha et al. 2016). Yet, the functional significance of this interaction remains unknown, as parasites were previously reported to bind directly to liver heparan-sulfate proteoglycans (HSPGs) expressed by HSC in the space of Disse and hepatocytes (Frevert et al., 1993). Furthermore, HSPGs were later shown to be involved in the shift between traversal and invasive phenotype of *P. berghei* sporozoites (Coppi et al. 2007).

The role of cell traversal in productive invasion, as well as the factors required for productively invading hepatocytes, are yet to be fully understood. Employing both *P. yoelli* and *P. berghei* mouse models, cell traversal was initially proposed to activate sporozoites for productive

invasion, possibly via exposure to cytoplasmic components, such as the hepatocyte growth factor (HGF) (Mota et al., 2002). Later, Risco-Castillo et al., 2015 showed that cell traversal-deficient sporozoites infected hepatocytes *in vitro* with efficiency and kinetics similar to those of wild-type parasites, refuting the previous hypothesis. Currently, it is consensual that cell traversal and productive invasion depend on distinct parasite effectors and most likely constitute mechanistically independent processes (reviewed by Loubens et al., 2021). The host receptors CD81 and SR-B1 were identified as players in sporozoite productive invasion, rendering differential permissiveness to different *Plasmodium* species (Silvie et al. 2003, 2006; Foquet et al. 2015; Langlois et al. 2020). *P. yoelii,* sporozoites strictly depend on CD81 to infect cells (Silvie et al. 2003; Manzoni et al. 2017). In the presence of CD81-expressing cells, both *P. yoelii* and *P. berghei* sporozoites become competent for productive invasion (Risco-Castillo et al. 2015; Manzoni et al. 2017). However, *P. berghei* sporozoites are able to use SR-B1 as an alternative entry pathway in the absence of CD81 (Langlois et al. 2020).

P. falciparum depends on CD81 for infection, and antibodies against CD81, but not SR-B1, completely inhibit invasion of primary human hepatocytes (Silvie et al. 2003; Dumoulin et al. 2015; Foquet et al. 2015; Manzoni et al. 2017). Nevertheless, CD81 overexpressed in human hepatocyte cell lines is not enough to render these cells permissiveness to *P. falciparum* infection, indicating that other factors in addition to CD81 are required for productive invasion in this species (Dumoulin et al., 2015; Silvie et al., 2006).

One common feature to productive invasion by all *Plasmodium* parasites is the invagination of sporozoites into a parasitophorous vacuole. One of the proteins found to be part of the parasitophorous vacuole membrane (PVM) and essential for parasite productive invasion

is the up-regulated in infectious sporozoites 4 (UIS4) protein (Mueller et al. 2005). UIS4 is expressed exclusively in infective sporozoites and developing liver-stages and localizes to the PVM. The knockout of *UIS4* in *P. berghei* sporozoites generated parasites that are not able to progress through their life cycle further than hepatocyte invasion (Mueller et al. 2005). This protein is therefore a marker widely used to assess parasite invasion *in vitro,* together with proteins expressed abundantly by the parasite, such as the surface CSP or the intracellular heat shock protein 70 (HSP70), one of the major chaperone classes expressed in *P. falciparum* with immunogenic role, and widely conserved across all *Plasmodium* species.

Besides their importance in unravelling biological processes and players of *Plasmodium* infection, animal models are proven tools for drug discovery. Several anti-plasmodial drugs were, and continue to be, validated in rodent models of infection before proceeding to human parasites. *P. berghei* mouse models constitute infection models part of the drug discovery and development process (discussed below), in view of their proven use in the prediction of treatment outcomes for human infections.

Due to the particular ability of *P. vivax* and *P. ovale* to form latent forms of the parasite, these species liver-stages cannot be accurately mimicked employing the rodent *Plasmodium* species, which are not able to form hypnozoites. Instead, *P. cynomolgi*, the simian counterpart of *P. vivax*, is employed. This specie is having high genome homology with *P. vivax* and the potential for causing malaria relapses. The continuous *in vitro* culture of *P. cynomolgi* erythrocytic stages has been accomplished in 1981, culturing rhesus monkey erythrocytes in RPMI 1640 culture medium (Nguyen-Dinh et al. 1981). Further developments of such procedures were carried on until recently (Chua et al. 2019), making this *Plasmodium* species the a widely used surrogate model to

interrogate *P. vivax* liver-stage (Tachibana et al. 2012; Joyner et al. 2015).

Malaria Drug Development: The case study of M5717

Drug development is the process of bringing a novel drug from the "bench to bedside" and it takes around 10 to 15 years, being a process highly time consuming and highly costly. Currently, the average price of bringing one drug to the market is approximately 2 billion dollars (Deloitte 2022).

The workflow of this process is depicted in Figure I.5. It starts with drug discovery, followed by drug testing in preclinical and clinical settings until the market approval by the regulatory agencies (FDA U.S Food & Drug Administration 2022). However, few of the drugs that start enter the process end up in the market, most of them failing in the preclinical phase (Dowden and Munro 2019).

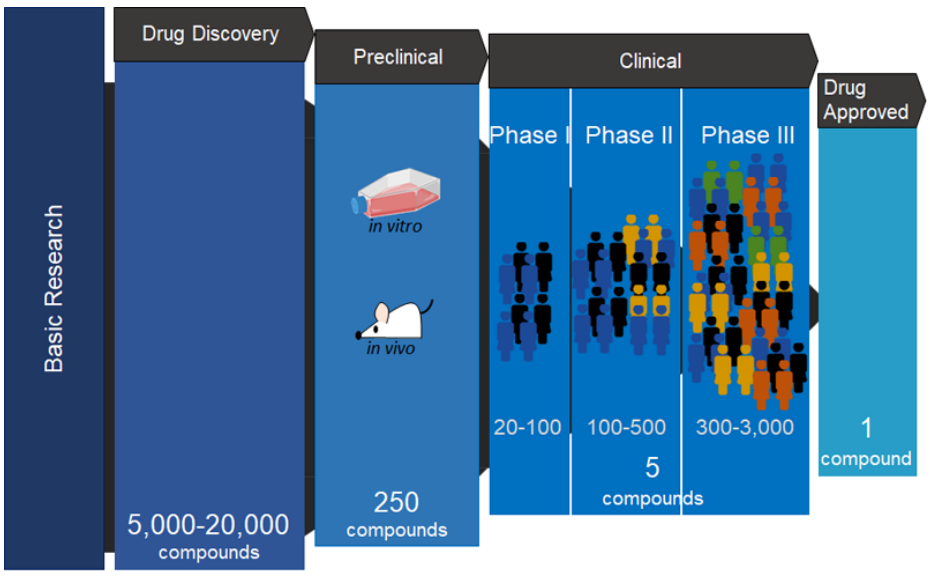

Figure I.5 - Workflow for the development of one drug candidate into the market. The information contained in the image was sourced from (FDA U.S Food & Drug Administration 2022).

For the discovery of a lead compound, pharmaceutical companies usually collaborate with academia to identify druggable disease targets and to design lead compounds that can interact and elicit an effect on the identified target. An important step of this process is the optimization of the pharmacokinetic properties of the drug, to improve the target and reduce the off-target interactions (affinity and specificity), employing structure-activity relationship-based approaches. At this stage, medicinal chemists have increasingly been working “hand-in-hand” with artificial intelligence systems to quickly accumulate extensive data on biology, structure, and chemistry of the lead compound (Lansdowne 2020), aiming to accelerate the process. After drug discovery and design, the drug development is mainly focused on the assessment of the efficacy and safety of the lead compound. In the preclinical development of the lead compounds, *in vitro* and *in vivo* models are employed before the translation into humans (Figure I.5). In the preclinical stage, the optimization of the lead pharmacokinetic and pharmacodynamic properties may continue towards improved potency, solubility and metabolic stability. Furthermore, the characterization of the interactions of the lead compound with other metabolites derived from the host response, or drug partners, is assessed both *in vitro* and *in vivo*. Data on the compound’s safety and efficacy generated by studies using *in vivo* models is required for the translation into clinical trials (FDA U.S Food & Drug Administration 2022).

The clinical trials aim to assess the drug’s efficacy and safety in humans. This stage is divided in phases that start from smaller and simpler populational groups to address safety and progress to larger

groups with increased complexity to assess efficacy (Figure I.5). Phase I clinical trials are the smallest studies with up to a maximum of 100 individuals (average of 20), usually healthy volunteers. It is mostly aimed at defining a safe dosage and administration regimen and identifying possible off-target effects in the human context. If a safe dose is found, the drug passes to the phase II clinical trials where a larger group of individuals (volunteers or patients) is tested, and efficacy and safety are assessed. The successful completion of phase II clinical trial leads to the most important phase that aims at demonstrating the beneficial effect of the drug under development. In phase III, a large and more diversified group is required (in the order of the thousands) and followed for a longer period of time that can go up to 4 years. Thus, it is also the phase providing most of the safety data, as in bigger populations and longer follow-ups, adverse effects undetected in the previous phases can be identified. The completion of the phase III clinical trials leads to review and approval (or not) of the drug by the regulatory agencies, prior to reaching the market. The drug is release to the market, being distributed and consumed by the patients a while a continuous process of drug safety surveillance is carried out (FDA U.S Food & Drug Administration 2022).

Due to the high morbidity and mortality of malaria, as well as the lack of knowledge on the parasite biology, most of the available therapies targeting this disease did not pass through the target-directed design process previously described. Most were selected based on their efficacy in inhibiting the growth of *Plasmodium* species, without the knowledge about their specific mode of action (reviewed by Rosenthal, 2003). The first anti-plasmodial drugs are good examples of that - quinine and artemisinin are natural compounds that showed anti-plasmodial activity when administered to alleviate the clinical symptoms of this disease. After that, most of the anti-plasmodial drugs developed

derived from chemical modifications of existing compounds (Rosenthal 2003), as it is the case of chloroquine, primaquine and mefloquine that were developed by chemical modifications of quinine. More recently, 4-aminoquinolines emerged, including pyronaridine used in this work, that are closely related to chloroquine, sharing the mode of action with the parental drug, but presenting efficacy against chloroquine-resistant *P. falciparum* strains (Chang et al. 1992; Rosenthal 2003). The lack of chemical diversity and shared mode of action of most of the available drugs, as well as the required wide distribution and frequent administration of such compounds, led to the fast-developing *Plasmodium* drug resistance. Strategies such as (i) optimization of the existing anti-plasmodial compounds (new dosing regimens or formulations) or (ii) combinations of novel and old anti-plasmodial agents, have alleviated this problem for a few years. However, currently, *Plasmodium* drug resistance has been reported for virtually all the anti-plasmodial drugs available (Antony and Parija 2016). Thus, new and target-directed approaches exploiting new mechanisms of action are required for anti-plasmodium drug development, a process that has been facilitated by the availability of the *P. falciparum* genome sequence, unveiled in 2002 (Gardner et al. 2002).

Together with the knowledge on the genome, public-private partnerships (PPP) such as the Medicines for Malaria Venture (MMV, started in 1999) and the Malaria Drug Accelerator (MalDA, consortium of 15 laboratories funded by the Bill & Melinda Gates Foundation since 2012) have contributed to the generation of several product development partnerships. Taking the expertise and knowledge of both the private and public sectors, and exploiting each of their strengths, these PPP aim to find the most efficient and effective solutions for neglected diseases, such as malaria. One of the anti-plasmodial drugs originated from these collaborations (within MMV), is M5717, currently

under clinical development, to which this thesis contributed. M5717 is discussed the section below.

Overall, the collaborations between private and public institutions are a strong and hopeful strategy to achieve the agenda of malaria eradication, however, due to the long time required and high attrition rates associated with the process of drug development, such contribution is still not reflected in the clinical approved malaria drug pipeline, but still under development.

The Malaria Pipeline: Pre-erythrocytic-targeted Therapeutics

The liver-stage of infection is the first step of the *Plasmodium* life cycle in the mammalian host. This is the stage when the lowest number of parasites are initially present, taking 7 to 10 days to proliferate and completely mature inside few infected hepatocytes (Prudêncio et al. 2011). Together with the persistence of latent forms of the parasite and the ability of hepatocytes to express antigens that can induce T-cell responses, the liver-stage of infection constitutes an attractive target for prophylactic intervention (Arora et al. 2021).

Vaccines

Pre-erythrocytic vaccines have been pursued since 1970. After decades of unsuccessful results, the first vaccine entering in Phase III clinical trials was RTS,S/AS01 (Cohen et al. 2010). RTS,S uses the hepatitis B virus (HBV) surface antigen (S protein) as a carrier matrix of repetitive epitope of the *P. falciparum* CSP (*Pf*CSP) and T-cell epitopes found in the C-terminal of *Pf*CSP sequence (Cohen et al. 2010). In its sequence, CSP contains repetitions of amino acids, responsible for immunogenicity (epitope) in the mammalian host. In *P. falciparum* the immunodominant epitope is contained within three repetitive sequences of NANP amino acids (Bumpus et al. 1984). Antibodies binding to this

repetitive epitope impair sporozoites infectivity and confer protection to immunized mice (Potocnjak et al. 1980). Hence, the fusion of this repetitive epitope, the T-cell epitopes and the HBV S proteins generated the winning vaccine construct that led to the regulatory approval of the new vaccine RTS,S/AS01 (Cohen et al. 2010). This vaccine has entered in 2016 in a pivotal study, reaching up to date 830 000 children in Ghana, Kenya and Malawi. The reduction of hospitalizations for 30% of severe malaria cases and the reduction of total malaria cases by 40% led to the recommendation on of this vaccine for children living in regions with moderate to high transmission on October 6th 2021 (WHO 2021).

Standard-of-care anti-plasmodial drugs

While a desirable effective vaccine against malaria remained unavailable, vector control measures and drug therapeutics were the cornerstone of disease control. Currently, the malaria drug pipeline is mainly constituted of anti-plasmodial drugs targeting the blood-stage of infection. However, the high parasitaemia levels present on this stage have shown to contribute to the vast *Plasmodium* drug resistance reported to most of the available therapies (Antony and Parija 2016).

The liver-stage of infection constitutes an alternative target, as low numbers of parasites are present at the beginning of this phase. However, the limited knowledge of this asymptomatic phase of infection has restricted the development of effective therapies. From the few clinically approved drugs targeting the pre-erythrocytic stage of infection, only two present anti-hypnozoidal activity, primaquine and tafenoquine. However, these cannot be widely distributed due to hemolytic effects reported on people carrying a deficiency on the glucose-6-phosphate dehydrogenase (G6PD) enzyme, a common trait in malaria-endemic areas (Ashley et al. 2014). Furthermore, liver-stage anti-plasmodial drugs did not escape to the appearance/development of resistant *P. falciparum* and *P. vivax* strains (Raphemot et al. 2016).

Drug resistance is often associated to patient non-compliance caused by, among other factors, the complexity and long-term duration of drug treatments available (Hafiz, A et al., 2020). An example is the combination of artesunate with sulfadoxine-pyrimethamine, recommended for uncomplicated *P. falciparum* infection, targeting both the liver- and blood-stages (Raphemot et al. 2016). This treatment is recommended in specific doses according to body weight and, it is prescribed as daily doses of artesunate for three days and one dose of sulfadoxine-pyrimethamine at day 1 of treatment. Fixed dose combinations and the administration in the same regimen of the different compounds could facilitate patient compliance (Hafiz, A et al., 2020). Primaquine, the preventive treatment of malaria relapses, is prescribed as a daily dose for 14 days or weekly doses for 8 weeks for people without or with G6PD deficiency, respectively (WHO 2015). These long-term treatments lead often to patient non-compliance, resulting in the exposure of parasites not eliminated to a suboptimal dose of the active compounds, inducing the development of drug resistance. Atovaquone (ATO), which presents potent anti-plasmodial activity against developing parasites of liver- and blood-stages of infection, is a mimetic of the parasite's mitochondrial protein ubiquinone, essential for the aerobic respiratory chain. The disruption of the membrane potential as a result of the inhibition of the parasite's respiratory chain leads to parasite's death (Baggish and Hill 2002). This drug surpasses the side effects and requirements for long-term administration, that cause patient non-compliance on the commonly used anti-plasmodial drugs (Baggish and Hill 2002). However, a single point mutation in the cytochrome b gene of *P. falciparum* was enough to confer drug resistance to this parasite species. Thus, ATO is now part of the wide drug pipeline to which *P. vivax* and *P. falciparum* have developed drug resistance (Antony and Parija 2016; Raphemot et al. 2016). Nevertheless, this drug is still used for travelers, as in short exposure time it is an effective

prophylactic in monotherapy or in combination with its partner of choice, proguanil, as reviewed by Baggish & Hill (Baggish and Hill 2002).

Drug candidates: The case study of M5717

As previously mentioned, in an attempt to overcome the widely acquired drug resistance observed throughout the last decades, it has been part of the malaria eradication agenda to develop new drug therapies that present: (i) novel modes of action, to avoid cross-resistance with the currently approved drugs; (ii) when in combination, a fixed formulation must be established with partner drug possessing different modes of action but similar pharmacokinetics, towards similar clearance times and delayed resistance acquisition; (iii) preferentially in single-dose cures to assure patient compliance, and (iv) cost-effective drugs with potential for transmission-blocking and relapse prevention, or at least compatible with primaquine, the currently standard-of-care targeting hypnozoites

Following these recommendations, Baragaña et al. presented M5717, a compound under clinical development that targets the parasitic translation elongation factor 2 (eEF2) (Baragaña et al. 2015). eEF2 catalyzes the GTP-dependent translocation of messenger RNA along the ribosome, crucial for protein synthesis (Redpath et al. 1996). The drug was discovered in 2015, by the Drug Discovery Unit of the University of Dundee. In a phenotypic screening of the protein kinase scaffold library against the 3D7 multi-drug-resistant *P. falciparum* strain, Baragaña and co-workers identified one compound with high potency but poor physicochemical properties (Baragaña et al. 2015). Optimization of the structure developed towards increased potency (in the range of nanomolar), solubility and good metabolic stability, led to the lead compound currently known as M5717 (Baragaña et al. 2015).

With the structure optimized, the compound's efficacy and safety were evaluated *in vitro,* against *P. falciparum* and *P. vivax* clinical

isolates from patients and, *in vivo,* in mouse models of *P. berghei* infection and in mice engrafted with human erythrocytes infected by *P. falciparum*. The inhibition of this eEF2 novel target was shown to prevent the development of blood-stage parasites and gametocytes, impairing the formation of female and male gametes (Baragaña et al. 2015). Additionally, M5717 showed potency in the nanomolar range inhibiting the liver-stage developing parasites of *P. berghei* and *P. yoelii*, in monolayer cultures of HepG2 cells. More recently, still in the preclinical phase, M5717 was employed in the advanced cell model developed under the scope of this thesis, in collaboration with Merck. The evaluation of its liver-stage activity *in vitro* was found concordantly in the nanomolar ranges in HepG2 spheroids and confirmed in a murine model of *P. berghei* infection **(chapter 2)**. These results were translated into phase I clinical trials by Merck (Khandelwal et al. 2022).

Due to its nanomolar range potency, its good pharmacokinetics profile and its long-lasting activity, this compound M5717 falls within the recommendations for the “next generation” of anti-plasmodial drugs, presenting a multi-stage effect from chemoprotection to transmission blocking (Baragaña et al. 2015).

Owing to general concerns about the emergence of *Plasmodium* drug resistance, it is important to evaluate this risk in all new anti-plasmodial drugs, both in preclinical and in clinical studies. By exposing *P. falciparum* strains to suboptimal doses of M5717, Baragaña et al., identified multiple independent gene mutations in the eEF2 sequence that conferred drug resistance to three *P. falciparum* strains (Baragaña et al. 2015). As a strategy to mitigate the development of drug resistance, combination therapies have shown efficiently to avoid or delay the fast rate of *Plasmodium* drug resistance. The rationale for this is that any parasite resisting the activity of one compound should be eliminated by the partner drug, if both have distinct modes of action. As

M5717 fulfils the criteria to be a long-duration partner to clear blood-stage parasites resistant to any fast-acting compound with the same pharmacological duration, the combination of M5717 with pyronaridine (pyro) was recently assessed against of erythrocytic stages of *P. falciparum* (Rottmann et al. 2020). Pyro, as previously mentioned briefly is a compound structure-related to chloroquine, acting as an inhibitor of hemozoin formation (Auparakkitanon et al. 2006), a process commonly occurring as part of heme detoxification in the erythrocytic parasite food vacuole. Pyro is a fast-acting compound contrarily to M5717, with matching half-lives and complementary mode of action. Importantly, no *P. falciparum* resistant strains to pyro were reported so far. The pharmacokinetic and pharmacodynamic drug-drug interactions of the combination of M5717 and pyro (M5717-pyro) targeting the blood-stage of infection were assessed by the isobologram methodology *in vitro* and employing a humanized mouse model of blood-stage *P. falciparum* infection (Rottmann et al. 2020). The isobologram methodology allows to address the effect resulting of combining two drug partners by employing different drug ratios. In this way, the antagonist, non-detrimental (or additive) and synergistic drug-drug interactions can be assessed (Fivelman et al. 2004). *In vivo*, M5717 showed non-detrimental drug-drug interactions with pyro (Rottmann et al. 2020). The authors assessed the pharmacokinetic properties, such as maximum blood concentration, showing that the half-life of pyro and M5717 and availability in the blood were comparable when applied in monotherapy or combination (Rottmann et al. 2020). Finally, not only the combination of M5717 and pyro showed additive parasitological properties, but the latter could suppress the emergence M5717-resistant parasites, even when pyro was employed at suboptimal doses (Rottmann et al. 2020). Thus, M5717-pyro showed to be a potentially effective, long-lasting anti-plasmodial drug combination with complementary pharmacodynamic profiles. Nevertheless, the drug-drug interactions on the M5717 liver-

stage activity remained unascertained until this thesis's work **(chapter 3)**. The HepG2 spheroids and the murine *P. berghei* model employed confirmed the benefit of this combination therapy, as it showed safety and enhanced efficacy against the liver-stage of *P. berghei* compared to the monotherapy.

Advanced cell culture models for drug discovery targeting *Plasmodium* liver-stage infection

Drug metabolism and toxicity studies are routinely performed in animal models but, due to metabolic interspecies differences they are not accurate in predicting the metabolic profile of a drug in humans. In fact, a study assessing the metabolism-derived toxicity of 150 compounds employing primate and rodent models demonstrated that rodent models alone were able to predict as much as 43% of the toxicity observed in humans, whereas a total of 71% prediction of hepatotoxicity was achieved when combining this information with that obtained from non-human primate models (Olson et al. 2000). Thus, this was the first study pointing out, with quantitative data (generated by 12 pharmaceutical companies), the need of employing models with higher predictive power of the human drug metabolism and hepatotoxicity in drug discovery.

Human hepatic cell sources widely employed for drug discovery purposes include hepatic cell lines and primary human hepatocytes (PHH) (Lauschke et al. 2016, 2019; Zeilinger et al. 2016).

Stem cell-derived hepatocyte-like cells

Stem cell-derived hepatocyte-like cells represent an advantageous cell source for disease modeling relatively to PHH and hepatic cell lines, due to their unlimited availability, patient-genetic background, and amenability for genetic manipulation (Saito et al.

2021). Recently, the liver stage development of rodent and human *Plasmodium species* was reported in hepatocyte-like cells derived from human induced pluripotent stem cells (Ng et al. 2015). The EEFs found in these cultures increased their size along 2 and 8 days after infection. Although the infectivity, or capacity to progress to the blood-stage infection was not assessed, the developed EEFs expressed merozoite surface protein 1 (MSP1), a marker of merozoite differentiation (Ng et al. 2015). Despite this, the differentiation protocols described so far are long, rendering rather immature metabolic phenotypes, thus not advantageous over hepatic cell lines for drug applications (Lauschke et al. 2016; Zeilinger et al. 2016). Hence, this cell source was not explored under the scope of this thesis.

Human hepatoma cell lines

Human hepatoma cell lines circumvent the inter-species differences of animal models and the limited availability of PHH, constituting an unlimited source of hepatic cells. However, hepatic cell lines are known to possess intrinsically lower metabolism capacity compared to PHH (Guo et al. 2011). Specifically, two of the hepatoma cell lines employed under the scope of this thesis, HepaRG and HepG2, have been widely used in drug toxicity studies (Gerets et al. 2012; Zeilinger et al. 2016). Hence, their metabolic profile is well described, being characterized by an overall lower basal expression of phase I metabolizing enzymes compared to PHH (Gerets et al. 2012). While the specific induction of CYP3A4, CYP1A2 and CYP2B6 led to closer expression levels of HepaRG metabolizing enzymes compared to the ones of PHH, in HepG2 cells, almost no changes were observed upon induction (Gerets et al. 2012). Nevertheless, their prediction of hepatotoxicity was comparable and in lower percentage relatively to PHH (Gerets et al. 2012). Important for the current malaria drug pipeline, HepG2 cells had no detectable levels of expression of the CYP2D6

gene, in a study comparing several cell lines with PHH (Guo et al. 2011). This isoform is responsible for the metabolism of 30% of marketed drugs, among them, the two currently approved drugs with hypnozoidal activity, primaquine and tafenoquine (Caridha et al. 2013; Marcsisin et al. 2014). The hepatoma cell line HC-04, and Huh7 (or derivatives e.g. Huh7.5) have not been as widely employed in drug metabolism assessments as HepG2 and HepaRG. In fact, there are few reports available on the characterization of the metabolic profile of these cell lines. Lim et al assessed the capacity of HC-04 cultured in monolayers to metabolize Midazolam, a substrate of CYP3A enzymes, for which HC-04 presented similar metabolism rates to PHH (Lim et al. 2007). Despite this, assessing the basal gene expression of phase I metabolizing enzymes of this cell line revealed that CYP2E1, CYP2A1 and CYP2C9 were not detectable, but up-regulated by specific inducers (e.g., ethanol for CYP2E1 and rifampicin to CYP3A4 and 2C9). However, the lack of further reports employing HC-04 in drug toxicity studies questions the ability of this cell line to reproduce the human drug metabolism capacity. Huh7 cells cultured in monolayers were assessed in monolayer cultures in DMSO- treated or untreated conditions (Choi et al. 2009). Although the DMSO-treated conditions improved the metabolic performance of CYP450 isoforms in this cell line, when compared with PHH, the activities and expression levels of most of the metabolizing enzymes were still significantly low, not being suitable for drug toxicity studies. Nevertheless, except for primaquine, most of the anti-plasmodial leads discovered in red blood cell screenings so far do not require metabolic activation (Gamo et al. 2010), making immortalized cell lines a viable cell source for their preclinical evaluation.

Another consideration in the selection of the cell source for the development of *in vitro* models of the hepatic infection, is the permissiveness to *Plasmodium* species. A wide range of hepatoma cell

lines are permissive to the rodent *P. berghei*, and *P. yoelli in vitro*, but the same does not translate to human infectious species, such as *P. falciparum* and *P. vivax* (Prudêncio et al. 2011). These *Plasmodia* present tropism for human mature hepatocytes and few hepatoma cell lines sustain the development of these parasites (Sattabongkot et al., 2006, and references therein). HepG2 cells (the subclone of HepG2-A16) and HC-04 have been reported to sustain *P. vivax* development (Sattabongkot et al. 2006; Chattopadhyay et al. 2010), whereas only HC-04 has been reported to sustain development of *P. falciparum* sporozoites into EEFs (Sattabongkot et al. 2006; Dumoulin et al. 2015). Huh7 and Huh7.5 have been widely employed for disease modeling, but more focused in hepatitis (reviewed in Arez et al. 2021), as this cell line does not sustain neither *P. falciparum* or *P. vivax* development (Prudêncio et al. 2011). Nevertheless, low infection rates of human *Plasmodium* species have been reported in cell lines, compared to the rodent (Sattabongkot et al. 2006; Chattopadhyay et al. 2010). This is a bottleneck that monolayer cultures of cell lines and PHH share, although improvements have been reported in bioengineered cell models of PHH (March et al. 2013) or monolayer cultures in a 384-well plate format (Roth et al. 2018).

Primary Human Hepatocytes (PHH)

Investigating the role of the biotransformation enzymes is critical to identify the generation of toxic metabolites and determine the pharmacokinetic properties of xenobiotics in humans. PHH, isolated from livers, can better reflect the functionality of the human organ than any other cell source. The inter-donor variability of PHH derived from different genetic backgrounds is especially important in pharmacological studies, to reflect different drug metabolism capacity and toxicity effects. These differences arise from distinct polymorphisms of metabolizing enzymes among the population, such as those reported between

genders and ethnicities (Wijnen et al. 2007). However, whether they are isolated from liver biopsies or from liver resections, these cells are of limited availability (Zeilinger et al. 2016), with time-consuming procedures and hard logistics between surgical and research teams (Zeilinger et al. 2016). PHH are highly variable, depending on donor demographics as well as surgical operating procedures, both reported to have an effect on the viability and yield of the isolated hepatocytes (Lee et al. 2014; Geerts et al. 2019; Solanas et al. 2022). This variability poses a challenge in the implementation of robust and reproducible platforms to be adopted by the pharmaceutical industry. Having a commercial source of cryopreserved hepatocytes circumvents some of the variability related with operating procedures (surgical, isolation and handling), and can provide a large batch of cells from a single donor, with assured quality. The high costs of cryopreserved PHH also limit their wide use in *in vitro* high-throughput platforms. Nonetheless, PHH are an important tool in drug discovery and development, being employed by the pharmaceutical industry for years now, in suspension or cultured as monolayers (2D cultures) (Shibata et al. 2002; Hallifax 2005; Brown et al. 2007). These culture formats are considered cost-effective and easy to handle, as most of the analytics and protocols are well established and validated, however, they induce a well reported decay in the hepatocyte phenotype (biosynthetic functions, as well as metabolic capacity) as early as 33 hours *in vitro* (Maurel 1996). Thus, their simplicity and short-term viability present limitations to the evaluation of complex toxic reactions. The phenotypic decay observed in these cultures is mostly associated by the poor recapitulation or absence of cues crucial in the maintenance of hepatocyte differentiation state and functionality - the three-dimensional microenvironment, including the hepatocyte interactions with neighboring cells and the ECM, as well as the gradients of soluble local and systemic cues (Berthiaume et al. 1996; Cunningham and Porat-Shliom 2021).

Therefore, aiming to improve the resemblance of such features *in vitro*, engineering approaches have been applied to liver cells in two mainly known formats: Scaffold-based monolayer approaches (commonly called quasi-3D cultures) and 3D cell spheroids.

Scaffold-based quasi-3D cultures

Engineering tools, such as biomaterials and biofabrication, as well as co-culture strategies, have contributed to improvements in 2D hepatic cell cultures (Figure I.6).

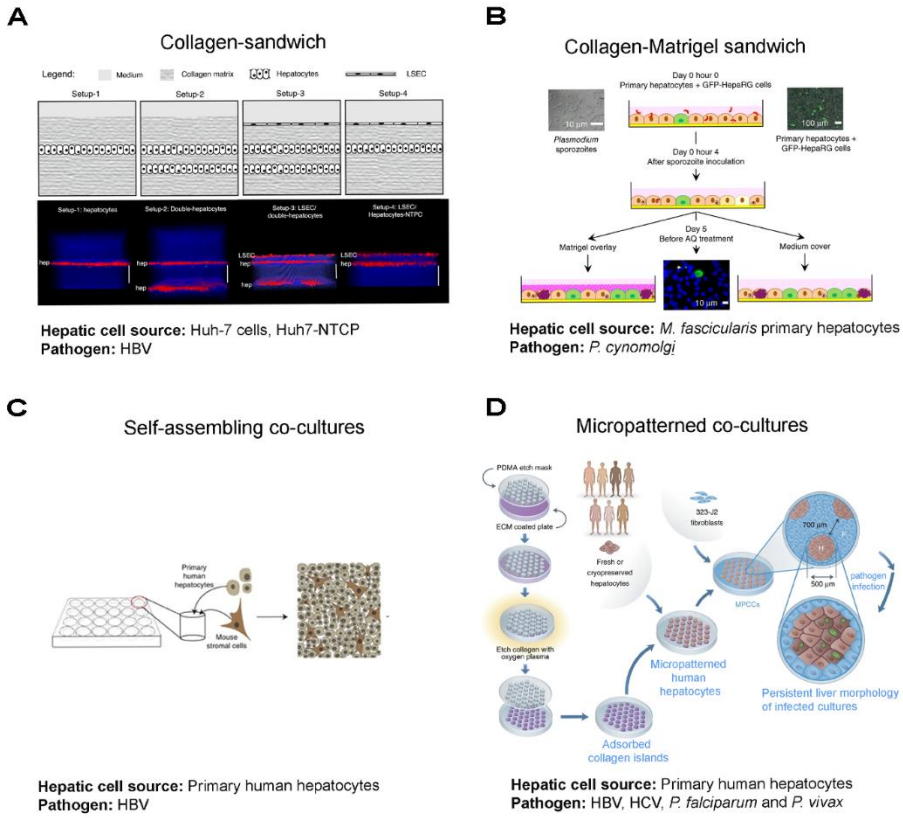

Figure I.6 - Engineered 2D human hepatic cell culture strategies. (A) Collagen-sandwich of a monolayer (setup-1) or double-layer (setup-2) of human hepatic cells without or together with a monolayer of liver sinusoidal

endothelial cells (LSECs) (setup 3 and 4, respectively). Image reproduced from (Petropolis et al. 2016). **(B)** Monolayer of primary human hepatocytes (PHH) co-cultured with HepaRG-GFP on top of a collagen-coated surface, with a top layer of MatrigelTM. Image reproduced with permission of (Dembélé et al. 2014). **(C)** Self-assembling co-culture of PHH and mouse embryonic fibroblast 3T3-J2 cells in a collagen-coated surface. Image reproduced from (Winer et al. 2017, 2020). **(D)** PHH cultured in islands pre-fabricated by lithographic methods, surrounded by mouse embryonic fibroblast 3T3-J2 cells. Image adapted with permission from (Arez et al. 2021).

Collagen-based sandwiches and co-culture with non-parenchymal cells have been shown to induce a better cell polarity and hepatic functions of PHH and hepatoma cell lines, while extending cell viability for up to 2 weeks (Bell et al. 2018; Gijbels et al. 2019). Briefly, the collagen sandwich method consists of PHH or hepatic cell lines cultured on top of a collagen layer and overlaid with another layer of either collagen (Petropolis et al. 2016) (Figure I.6A) or matrigel (Dembélé et al. 2014) (Figure I.6B). The hepatocyte-ECM interactions induce the reestablishment of cell polarity, namely the apical and basolateral domains and activate liver-specific gene expression, sustaining the transcriptional profile of differentiated hepatocytes (Dunn et al. 1992). Ultimately, a 2D multicellular network with functional BC is formed, which is reminiscent of the liver plate (Dunn et al. 1989; LeCluyse et al. 1994). In alternative configurations of the sandwich model, PHH are co-cultured with other cell types that can improve hepatocyte function, such as NPC (e.g., LSECs, Figure I.6A) or HepaRG cells (Figure I.6B). Such improvement occurs via cell-cell interactions and production, by the supportive cells, of ECM proteins and soluble factors that modulate the hepatocyte phenotype (Guguen-guillouzo et al. 1983; Loreal et al. 1993; Khetani et al. 2004). Additional co-culture strategies include self-assembling co-cultures (SACC, Figure I.6C) (Winer et al. 2017, 2020)

and micropatterned co-cultures (MPCC, Figure I.6D). MPCC were pioneered by Bhatia and co-workers (Khetani and Bhatia 2008), following the work of Khetani et al. 2004 that characterized 3T3-J2 murine fibroblasts as high inducers of a mature and functional phenotype of rat primary hepatocytes (Khetani et al. 2004). Bhatia and co-workers resourced to lithographic processes to fabricate collagen-coated islands in multi-well formats, for co-culture of PHH and mouse fibroblasts, thereby, providing the necessary homo- and heterotypic cell-cell interactions to preserve PHH viability and function for up to 6 weeks (Khetani and Bhatia 2008; March et al. 2013). The authors have shown that the spatial control over the two different cell types in a single culture, provided by micropatterning of collagen, rendered accelerated improvement in hepatocyte's biosynthetic functions (Bhatia, Sangeeta N., Martin L. Yarmush., Toner 1997) and higher infection rates by Hepatitis B virus (Shlomai et al. 2014) over randomly distributed co-cultures, respectively.

Both, sandwich and MPCC hepatic cultures have been applied to model hepatotropic infections, such as hepatitis viruses and *Plasmodium* parasites, as depicted in Figure I.6. For the latter, sandwich and MPCC cultures constitute the first *in vitro* models of hypnozoite formation and persistence *in vitro*, either from *P. cynomolgi* (sandwich, Dembélé et al., 2014) or *P. vivax* (MPCC, March et al., 2013). Hypnozoite activation *in vitro*, at 21 days of culture, was firstly reported in sandwich cultures, and confirmed through the specific action of primaquine *vs* ATO in the elimination of hypnozoites (Dembélé et al. 2014; Gural et al. 2018). Notably, MPCC cultures were further employed to characterize the transcriptional changes occurring throughout the *P. vivax* liver-stage infection (schizonts and hypnozoites) and could correlate such gene profile to the lack of hypnozoidal activity of anti-

plasmodial drugs, namely inhibitors of phosphatidylinositol 4-kinases (PI4K) and eEF2 (Gural et al. 2018).

The application of sandwich-based models and MPCC in drug discovery has been reported. These include studies on the prediction of hepatic responses to known hepatotoxicants (Xu et al. 2008; Khetani et al. 2013). Xu et al., employed PHH sandwich-cultured in a 96 multi-well format for 24 hours, and a high content screening approach with four endpoints of cell injury, to assess toxicity of 300 drugs with known clinical outcomes. The authors reported a prediction of hepatotoxicity of 50% and a false positive rate (FPR) of ~5% (Xu et al. 2008). Bhatia and co-workers hypothesized that longer treatments would better predict drug hepatotoxicity. Indeed, MPCC cultures treated for 9 days with known hepatotoxicants successfully predicted 66% of the 35 drugs known to have clinical hepatotoxicity, with a FPR of 10% for the 10 negative compounds tested. The predictive capacity of this co-culture increased to 100% when at least two different PHH donors were tested (Khetani et al. 2013). Importantly, in both studies the concentration of the drugs employed *in vitro* was 100-times higher than the C_{av} reported in humans. This concentration was the scaling factor that allowed better prediction of hepatotoxicity in these models. However, not accurately reflecting the availability of the drug in humans. In another study, the MPCC of PHH and KC mimicked the hepatic responses to inflammatory cues, such as lipopolysaccharide (LPS) and interleukin 6 (Nguyen et al. 2015). The co-culture of PHH with other liver cell types, such as LSEC (Ware et al. 2018) and HSC (Davidson et al. 2017), was also demonstrated in this culture format. Nevertheless, such cells were not able to replace murine fibroblasts in supporting PHH functionality in a MPCC configuration (Nguyen et al. 2015). Overall, the drawbacks of the abovementioned culture approaches for the application in drug development are the dependence on components of murine origin,

either matrigel, collagen or fibroblasts. These components may interfere with the prediction of the human drug response, in part due to possible pharmacokinetic alterations of the drugs traveling/contacting with Matrigel or biomolecules expressed by the murine fibroblasts. Furthermore, for the models in the pharmaceutical industry, the cellular components and process should be as robust as possible, which is impaired by the batch-to-batch variability associated to the use of collagen and matrigel, bottleneck that has been tackled by the application of synthetic biomaterials in sandwich cultures (Du et al. 2008; Foster et al. 2015; and references therein).

Furthermore, the response of cell lines cultured as spheroids to hepatotoxins was shown to be distinct from the response obtained by 2D monolayers (Leite et al. 2012; Gaskell et al. 2016), being closer to the one obtained with PHH rather than with their 2D counterparts (Ramaiahgari et al. 2017).

Spheroid cultures

Three-dimensional culture approaches, such as spheroids and organoids, are increasingly being recognized as alternative culture models capable of recapitulating the cell-cell and cell-ECM interactions happening *in vivo*.

A plethora of approaches have been proposed for the generation of cell spheroids that may or may not include scaffolds. The most common methodologies for scaffold-free approaches are based on gravity or low-adherence in microwells (hanging drop, low-adherence surfaces or AggreWell™) and agitation (orbital shaking or stirred-tank systems), whereas for scaffold-dependent the most common methodologies are the matrix-embedding methodologies, employing natural or synthetic scaffolds (Cox et al. 2020) (Figure I.7).

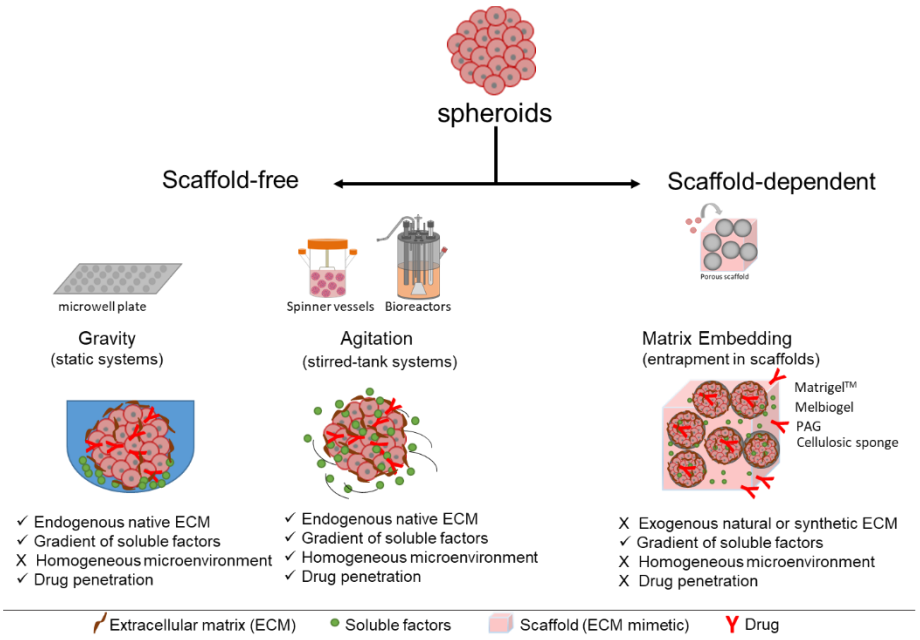

Figure I.7 - Approaches to generate hepatic spheroids. Description of the most common approaches and methodologies for the generation of cell spheroids. The advantages and disadvantages of the different approaches are highlighted.

In all these approaches cells undergo a process of spontaneous arrangement termed, self-assembly. The self-assembly results in numerous processes that happen *in vivo* including the formation of molecular gradients of (i) factors produced by cells during cellular organization (e.g. metabolites, paracrine factors) and (ii) components present in the culture medium (e.g., nutrients, oxygen, growth factors…) (Achilli et al. 2012). Additionally, spheroids form more complex cell-to-cell interactions and cell-to-ECM adhesions, which deliver additional signals (e.g. mechanical forces, biochemical signals and electrical coupling) that can influence cell shape, motility, proliferation, and differentiation, as well as gene expression (reviewed by Saji Joseph et

al. 2019). Therefore, they tend to present a more realistic organotypic phenotype of the living tissue.

The cellular aggregation is induced differently by the approaches mentioned above. In matrix embedding methodologies, the cell attachment and proliferation into a 3D architecture rely on the mechanical forces and chemical cues provided by the natural or synthetic scaffolds (reviewed by Saji Joseph et al. 2019). These may possess prominent ECM macromolecules that influence cell behavior via cell surface receptors (e.g., integrins) (Wang et al. 2016). Furthermore, the use of scaffolds can induce cells to establish a 3D structure with a particular architectural arrangement, advantageous for mimicking the tissue architecture for example, which can now be achieved with extraordinary precision using bioprinting techniques (reviewed by Kryou et al. 2019). The scaffold-free approaches include the hanging-drop method and the aggregation in low-attachment surfaces (Figure I.7), in which cells are devoided from anchorage surfaces or molecules, promoting self-assembly into spheroids (Achilli et al. 2012). The spheroid diameter in these approaches is controlled by adjusting the cell density and the volume of the drop (Chaicharoenaudomrung et al. 2019). These microwell-based methodologies are compatible with automation and high throughput screening platforms. On the contrary, the agitation-based approaches induce cell-cell contact by collision, leading to cellular aggregation into spheroids under more homogeneous physicochemical conditions than static systems (reviewed by Kryou et al. 2019). In this methodology, the control of spheroid diameter is attained by fine tuning parameters such as cell inoculum and agitation speed. Furthermore, agitation-based methodologies allow the non-destructive sampling of the cultures, an enormous advantage when dealing with long-term cultures and the spheroids generated under these conditions can feed higher throughput

platforms for parallel assays. Stirred-tank culture systems allow the generation of large spheroid numbers *per* batch, as these are scalable systems. Furthermore, the possibility of employing computer-controlled bioreactors, physicochemical parameters as pH, dissolved oxygen and temperature can be monitored and controlled more precisely than in an operator-based approach, increasing the robustness of spheroid cultures (Serra et al. 2012). With the aid of a perfusion operation mode, a stable flow of nutrients and oxygen can be obtained simultaneously to the clearing of toxic by-products, extending the cell viability of hepatic spheroids, allowing repeated drug induction studies and chronic toxicity applications (Tostões et al. 2012; Rebelo et al. 2017).

A multicenter study compared PHH cultured as spheroids (produced in ultra-low adherence plates) or in collagen - matrigel sandwich. The authors showed that hepatocytes in spheroids presented high metabolic performance and synthetic functions, which were stable for 5 weeks, whereas PHH in the sandwich format lost hepatic functionality after 2 weeks within that same period (Bell et al. 2018). Spheroid models also improved the hepatic phenotype and functions of hepatocarcinoma cell lines compared to monolayer cultures. HepaRG and HepG2 spheroids maintained the biosynthetic functions (e.g. albumin and urea secretion), the expression of hepatocyte-specific genes, such as the transcription factors involved in maturity and metabolic function of hepatocytes (HNF4-α and PXR), and *de novo* synthesis of phase I metabolizing enzymes up to 3 weeks, not possible by the 2D monolayers (e.g., by via rifampicin induction) (Leite et al. 2012; Rebelo et al. 2014; Gaskell et al. 2016).

Furthermore, Ingelman-Sundberg and co-workers also showed the suitability of PHH spheroids for disease modeling and drug toxicity studies, including chronic exposure to drugs, and viral transduction with recombinant adenovirus (Bell et al. 2016, 2020). The feasibility of

employing hepatic spheroids cultured in stirred-tank culture systems for repeated CYP induction assays and repeated dose toxicity assays, contrarily to their 2D counterparts, was shown for a diversity of hepatic cells (Tostões et al. 2012; Leite et al. 2012; Rebelo et al. 2015).

A plethora of spheroid models employing diverse hepatic cell sources and culture systems have been employed in drug metabolism and toxicity assays (Table I.1).

Table I.1- 3D human hepatic cell models for drug metabolism purposes. Published 3D models with applications in drug metabolism are presented and categorized by the aggregation approach and spheroid generating methodology.

3D system	Methodology	Hepatic cells	Compatability with Throughput	Biosynthetic function	Metabolic stability	Drug Metabolism	References
Scaffold-free microwells	Ultra-low attachment	HepG2	Medium (96-wp)	up to 5 weeks (urea and/or albumin)	-	APAP Diclofenac Trovafloxacin Fialuridine	Gaskel et al., 2016
		PHH	Medium (96-wp)	up to 5 weeks (urea and/or albumin)	<5 weeks (CYPs 1A2, 2D6, 3A4, 2C8, 2C9)	Amiodarone Bosentan Diclofenac Fialuridine Tolcapone	Bell et al., 2016
		ESC-derived hepatocytes	Medium (96-wp)	-	3 days spheroids (CYPs 1A2, 3A4)	APAP	Sengupta et al.,2014
		HepaRG	Medium-to high (384-wp)	-	3 weeks (CYP1A2 2B6 and 3A4)	APAP Diclofenac Cyclosporine A Isoniazid Rosigliatazone Troglitazone Aspirin Gemfibrozil Levofloxacin Trovafloxacin mesylate	Ramaiahgari et al., 2017
	Hanging drop	HepaRG:NPC	Medium (96-wp)	5 weeks (ATP and albumin)	-	APAP Diclofenac Trovafloxacin	Messner et al.,2013
Scaffold-free stirred tanks	Spinners	HepaRG	Compatible with high	1 week (albumin)	3 weeks (CYPs 1A1 1A2, 2B6, 2C9, 3A4)	APAP	Leite et al., 2012;
				2 weeks (albumin and urea)	2 weeks (CYPs 1A1 1A2, 2C9, 3A4)		Rebelo et al., 2014
		PHH		2 weeks (albumin)		Nevirapine	Pinheiro et al., 2017
	Computer controlled-bioreactors			4 weeks (albumin and urea)	>4 weeks (CYPs 1A1 1A2, 2C9, 3A4)	β-naphtoflavone Rifampicin	Tostões et al., 2012
		PHH:MSC		2 weeks (albumin and urea)	2 weeks (CYPs 1A2, 2C9, 3A4)	APAP	Rebelo et al., 2017
Scaffold-based	Matrigel	HepG2	Medium-to high (384-wp)	up to 4 weeks (albumin)	4 weeks (CYPs 1A2, 2E1, 2C9, 2C19, 2D6, 4F3)	APAP Bosentan Diclofenac Nimesulide Troglitazone Trovafloxacin Valproic acid Aspirin Dexamethasone Fluoxetine	Ramaiahgari et al., 2014

ESC- Embryonic stem cells, MSC – mesenchymal stem cells, wp – well plate, ATP- adenosine triphosphate, NPC – non parenchymal cells, PHH – primary human hepatocytes CYP-Cytochrome P450, APAP - Acetaminophen

The application of such advanced cell culture models in infectious diseases, more specifically targeting the *Plasmodium* liver-stage infection has been very limited, as recently reviewed by us (Arez et al. 2021). Currently, only two spheroid-based infection platforms have been reported to sustain the complete liver-stage of *Plasmodium* infection (one of them is the platform

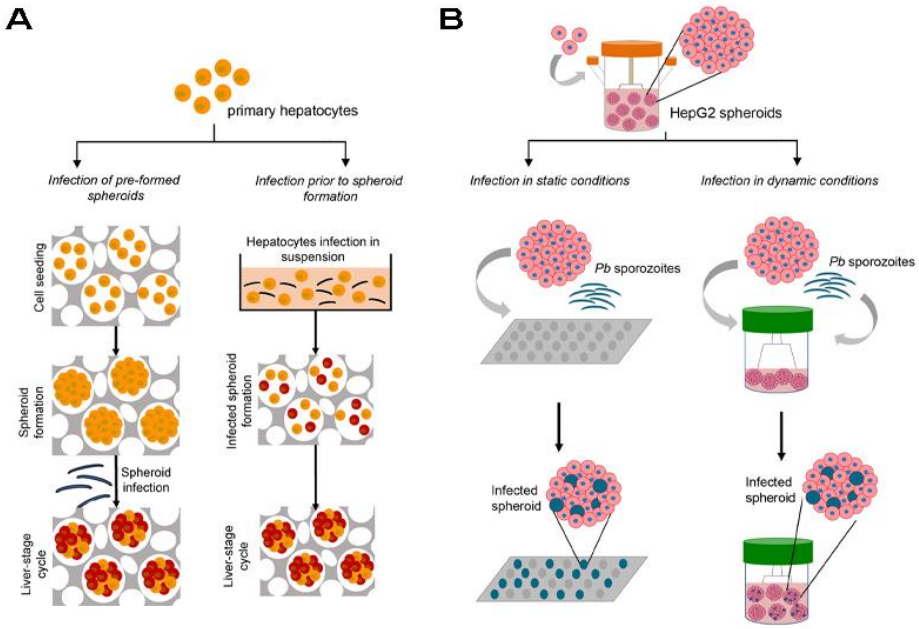

developed in this thesis) (Figure I.8).

Figure I.8- Engineered 3D models targeting *Plasmodium* infection. **(A)** Spheroid infection with *P. cynomolgi* (*Pc*) in cellulosic sponge scaffolds. Spheroids of primary simian hepatocytes generated in cellulosic sponges and infected with *Pc* sustained *Pc* invasion and development (left panel); single cells were infected with *Pc* sporozoites before spheroid formation and infected cultures were seeded in the cellulosic sponges for the generation of Pc-infected spheroids (right panel). Image adapted with permission of (Chua et al. 2019). **(B)** Scaffold-free spheroid infection with *P. berghei* (*Pb*). Spheroids generated in stirred-tank culture systems were transferred into 96-well plates (static, left panel) or into smaller scale stirred-tank culture systems (dynamic, right panel) and infected with *Pb* sporozoites, sustaining *Pb* invasion and development (Arez et al. 2019).

Chua et al. reported the first evidence of *Plasmodium* infection in a hepatic 3D model (Figure I.8A) (Chua et al. 2019). The authors employed a galactosylated cellulosic sponge for the generation of spheroids of simian hepatocytes, which has been previously described and employed to generate a model of HCV infection in hepatic cell lines (Nugraha et al. 2011). Simian hepatocytes were plated prior to or following *P. cynomolgi* infection (Figure I.8A), with the formation of hepatic spheroids that maintained structural integrity up to 60 days, when not infected, and up to 30 days when infected. Urea synthesis was measured as a surrogate of hepatocyte functionality, being detected and sustained for 22 days in the spheroids, at higher levels than in monolayers (Chua et al. 2019). Despite that, there was a clear decline in urea production in the spheroids after the first 8 days of culture. The conditions optimized for *Plasmodium* infection included a sporozoite to hepatocyte ratio of 2:1, the ratio leading to a higher infection rate while minimizing the risks of contamination derived from non-sterile sporozoites collected from mosquitoes. Hepatocytes exposed to the parasites before 3D culture had a 4-fold higher infection rate than hepatocytes infected as spheroids (Chua et al. 2019), possibly due to barrier limitations of the scaffold. The authors described the EEFs as punctuated parasites detected throughout the entire spheroid structure. Nonetheless, the development of the parasite was not characterized in full detail as the authors reported difficulties in characterizing EEFs in the 3D structures by microscopy-based techniques. Developing schizonts, both from primary infection and reactivated hypnozoites, fully matured into merozoites capable of infecting simian erythrocytes, confirming that the complete *Plasmodium* liver-stage infection could be reproduced in this model. As a proof-of-concept of the application of this system in drug assays, spheroid cultures were incubated with anti-plasmodial compounds, such as the standard-of-care atovaquone (targeting liver-stage schizonts but not hypnozoites) and primaquine (targets both liver-

stage schizonts and hypnozoites), as well as KDU691 (an exploratory drug with potential anti-relapse effects, previously reported to achieve radical cure in 2D monolayers but not *in vivo*). The assay readout was the detection of the *P. cynomolgi* HSP70 protein by immunofluorescence microscopy. Although this is not a convenient analytical method for high-throughput drug screening applications, the authors could detect the distinct anti-plasmodial effects of primaquine (near-complete infection clearance) and atovaquone (solely schizonts clearance). Interestingly, complete elimination with KD691 was not observed, consistent with *in vivo* data (Zeeman et al. 2016). The authors extended the impact of the model by demonstrating its applicability to PHH and the feasibility of infecting PHH spheroids with *P. vivax* infection (Chua et al. 2019). Overall, this was the first report that spheroid-based cultures support the invasion and complete liver-stage development of *P. cynomolgy* parasites in a system that could potentially be employed for anti-plasmodial drug screening.

Aim and scope of the thesis:

The liver-stage of infection is the first step of *Plasmodium* life cycle in the mammalian host, and when the initial number of parasites is the lowest. Thus, it is one of the most attractive therapeutic targets towards radical cure of malaria. Despite promising, the development of effective therapies against this stage of infection has been hampered by its asymptomatic character and by the lack of recapitulative and robust *in vitro* models of both *Plasmodium* hepatic infection and human drug response. Furthermore, to mitigate the *Plasmodium* drug resistance currently affecting the malaria drug pipeline, new anti-plasmodial drugs exploiting novel therapeutic targets and combination therapies of drug partners with complementary modes of action but similar pharmacokinetic properties are needed.

The aim of this thesis was the development of 3D human hepatic cell models for drug discovery targeting the liver-stage of *Plasmodium* infection.

More specifically, *in vitro* models, in which the complete liver-stage *Plasmodium* infection is replicated, from sporozoites into blood-infective merozoites, and novel drug therapies (monotherapies and combination therapies) can be evaluated against this stage of the *Plasmodium* life cycle.

In chapter 2, the objective was to combine (i) spheroids of immortalized human hepatic cell lines (HepG2, HC-04 and HepaRG), generated in stirred-tank culture systems and (ii) strains of the rodent infectious species *P. berghei* constitutively expressing luciferase (*Pb*-Luc) and/or green-fluorescent protein (*Pb*-GFP), to develop a human 3D infection platform. The infection conditions that led to higher infection rates were optimized by manipulating different parameters, such as cell and spheroid density, cell-to-sporozoite (cell:spz) ratio and the mode of cell:spz contact. *P. berghei* infection of HepG2 spheroids was established in static conditions, a medium throughput platform where several drug conditions can be tested (static infection). A stirred-tank scalable system, where one infected culture can be maintained for longer periods of time and followed longitudinally by non-destructive sampling (dynamic infection) was also developed. The infection dynamics of *Pb* parasites developing in the infected spheroids was extensively characterized by fluorescence microscopy and luciferase activity. In the static infection platform, the differentiation of sporozoites into blood-infective merozoites able to carry blood-stage infection in *P. berghei* mouse models was also assessed. In chapters 2 and 3 the aim was the application of the developed 3D infection platforms in drug discovery. The model was validated by assessment of safety and efficacy of standard-of-care anti-plasmodial drugs, such as atovaquone (chapter 2). We also tested a novel drug under clinical development by Merck, M5717. The compound was assessed in a dose- and time-dependent manner. The results obtained for the M5717 monotherapy were further validated by *in vivo* data. Moreover, the *in vitro* data fed a population pharmacokinetic model (Khandelwal et al. 2022) and simulations

to define meaningful effective dosages for a *Plasmodium* sporozoite-induced volunteer infection study (Phase I clinical trial NCT04250363).

In chapter 3, the objective was to assess a novel combination therapy of M5717 and pyronaridine, employing the static infection platform and comparing the results with *in vivo* data from a murine *P. berghei* infection model.

In chapter 4, the translation of the 3D human infection platform into human infectious *Plasmodium* species, such as *P. falciparum* and *P. vivax* was attempted, taking advantage of cryopreserved primary human hepatocytes (PHH) as hepatic cell source. In this context, the aggregation of cryopreserved PHH was described in a recently developed stirred-tank culture system of small scales (30 mL) to be compatible with *Plasmodium* sporozoites availability. The metabolism capacity of the cells was assessed in different PHH donors, demonstrating the potential application of this model for anti-plasmodial drugs that require metabolization into an active compound. Finally, the flexibility of the 3D platform to circumvent the PHH variability derived from different commercial sources and representing a broad range of genetic backgrounds was demonstrated by generating 3D cultures with similar aggregation profiles despite the different susceptibilities to *Pf* infection observed for such PHH donors in 2D monolayers

In chapter 5, results obtained along this work were further discussed, integrating thesis outcomes with state-of-the-art literature in the fields addressed throughout the previous chapters.

References

Achilli T-M, Meyer J, Morgan JR (2012) Advances in the formation, use and understanding of multi-cellular spheroids. Expert Opin Biol Ther 12:1347–1360. doi: 10.1517/14712598.2012.707181

Amino R, Thiberge S, Martin B, et al (2006) Quantitative imaging of Plasmodium transmission from mosquito to mammal. Nat Med 12:220–224. doi: 10.1038/nm1350

Antony H, Parija S (2016) Antimalarial drug resistance: An overview. Trop Parasitol 6:30. doi: 10.4103/2229-5070.175081

Arez F, Rebelo SP, Fontinha D, et al (2019) Flexible 3d cell-based platforms for the discovery and profiling of novel drugs targeting plasmodium hepatic infection. ACS Infect Dis 5:1831–1842. doi: 10.1021/acsinfecdis.9b00144

Arez F, Rodrigues AF, Brito C, Alves PM (2021) Review bioengineered liver cell models of hepatotropic infections. Viruses 13:1–25. doi: 10.3390/v13050773

Arora N, Anbalagan LC, Pannu AK (2021) Towards Eradication of Malaria: Is the WHO's RTS,S/AS01 Vaccination Effective Enough? Risk Manag Healthc Policy Volume 14:1033–1039. doi: 10.2147/RMHP.S219294

Ashley E a, Recht J, White NJ (2014) Primaquine: the risks and the benefits. Malar J 13:418. doi: 10.1186/1475-2875-13-418

Auparakkitanon S, Chapoomram S, Kuaha K, et al (2006) Targeting of Hematin by the Antimalarial Pyronaridine. Antimicrob Agents Chemother 50:2197–2200. doi: 10.1128/AAC.00119-06

Baggish AL, Hill DR (2002) Antiparasitic Agent Atovaquone. Antimicrob Agents Chemother 46:1163–1173. doi: 10.1128/AAC.46.5.1163-1173.2002

Bano N, Romano JD, Jayabalasingham B, Coppens I (2007) Cellular interactions of Plasmodium liver stage with its host mammalian cell. Int J Parasitol 37:1329–1341. doi: 10.1016/j.ijpara.2007.04.005

Baragaña B, Hallyburton I, Lee MCS, et al (2015) A novel multiple-stage antimalarial agent that inhibits protein synthesis. Nature 522:315–320. doi: 10.1038/nature14451

Bass CC, Johns FM (1912) The cultivation of malarial plasmodia (Plasmodium vivax and Plasmdoium falciparum) in vitro. J Exp Med 16:567–579. doi: 10.1084/jem.16.4.567

Bell CC, Chouhan B, Andersson LC, et al (2020) Functionality of primary hepatic non-parenchymal cells in a 3D spheroid model and contribution to acetaminophen hepatotoxicity. Arch Toxicol 94:1251–1263. doi: 10.1007/s00204-020-02682-w

Bell CC, Dankers ACA, Lauschke VM, et al (2018) Comparison of Hepatic 2D Sandwich Cultures and 3D Spheroids for Long-term Toxicity Applications: A Multicenter Study. Toxicol Sci 162:655–666. doi: 10.1093/toxsci/kfx289

Bell CC, Hendriks DFG, Moro SML, et al (2016) Characterization of primary human hepatocyte spheroids as a model system for drug-induced liver injury, liver function and disease. Sci Rep 6:25187. doi: 10.1038/srep25187

Berthiaume F, Moghe P V., Toner M, Yarmush ML (1996) Effect of extracellular matrix topology on cell structure, function, and physiological responsiveness: hepatocytes cultured in a sandwich configuration. FASEB J 10:1471–1484. doi: 10.1096/fasebj.10.13.8940293

Bhatia, Sangeeta N., Martin L. Yarmush., Toner M (1997) Engineered Substrates for Controlling Cell-Cell Interactions. ASME-PUBLICATIONS-HTD 355:99–104

Braeuning A, Ittrich C, Köhle C, et al (2006) Differential gene expression in periportal and perivenous mouse hepatocytes. FEBS J 273:5051–5061. doi: 10.1111/j.1742-4658.2006.05503.x

Brown HS, Griffin M, Houston JB (2007) Evaluation of Cryopreserved Human Hepatocytes as an Alternative in Vitro System to Microsomes for the Prediction of Metabolic Clearance. Drug Metab Dispos 35:293–301. doi: 10.1124/dmd.106.011569

Bumpus J a, Tien M, Wright D, Aust SD (1984) Center for the Study of Active Rationale for Development of a Synthetic Vaccine Against Plasmodium falciparum Malaria. 228:

Caridha D, Walker LA, Pybus BS, et al (2013) The metabolism of primaquine to its active metabolite is dependent on CYP 2D6. Malar J 12:1–7. doi: 10.1186/1475-2875-12-212

Cha S-J, Park K, Srinivasan P, et al (2015) CD68 acts as a major gateway for malaria sporozoite liver infection. J Exp Med 212:1391–1403. doi: 10.1084/jem.20110575

Cha SJ, Kim MS, Pandey A, Jacobs-Lorena M (2016) Identification of GAP DH on the surface of Plasmodium sporozoites as a new candidate for targeting malaria liver invasion. J Exp Med 213:2099–2112. doi: 10.1084/jem.20160059

Chaicharoenaudomrung N, Kunhorm P, Noisa P (2019) Three-dimensional cell culture systems as an in vitro platform for cancer and stem cell modeling. World J Stem Cells 11:1065–1083. doi: 10.4252/wjsc.v11.i12.1065

Chang C, Lin-Hua T, Jantanavivat C (1992) Studies on a new antimalarial compound: Pyronaridine. Trans R Soc Trop Med Hyg 86:7–10. doi: 10.1016/0035-9203(92)90414-8

Chattopadhyay R, Velmurugan S, Chakiath C, et al (2010) Establishment of an In vitro Assay for Assessing the Effects of Drugs on the Liver Stages of Plasmodium vivax Malaria. PLoS One 5:1–8. doi: 10.1371/journal.pone.0014275

Chiba H, Gotoh T, Kojima T, et al (2003) Hepatocyte nuclear factor (HNF)-4α triggers formation of functional tight junctions and establishment of polarized epithelial morphology in F9 embryonal carcinoma cells. Exp Cell Res 286:288–297. doi: 10.1016/S0014-4827(03)00116-2

Choi S, Sainz B, Corcoran P, et al (2009) Characterization of increased drug metabolism activity in dimethyl sulfoxide (DMSO)-treated Huh7 hepatoma cells. Xenobiotica 39:205–217. doi: 10.1080/00498250802613620

Chua ACY, Ong JJY, Malleret B, et al (2019) Robust continuous in vitro culture of the Plasmodium cynomolgi erythrocytic stages. Nat Commun 10:3635. doi: 10.1038/s41467-019-11332-4

Cohen J, Nussenzweig V, Nussenzweig R, et al (2010) From the circumsporozoite protein to the RTS, S/AS candidate vaccine. Hum Vaccin 6:90–96. doi: 10.4161/hv.6.1.9677

Coppi A, Tewari R, Bishop JR, et al (2007) Heparan Sulfate Proteoglycans Provide a Signal to Plasmodium Sporozoites to Stop Migrating and Productively Invade Host Cells. Cell Host Microbe 2:316–327. doi: 10.1016/j.chom.2007.10.002

Cox CR, Lynch S, Goldring C, Sharma P (2020) Current Perspective: 3D Spheroid Models Utilizing Human-Based Cells for Investigating Metabolism-Dependent Drug-Induced Liver Injury. Front Med Technol 2:. doi: 10.3389/fmedt.2020.611913

Cunningham RP, Porat-Shliom N (2021) Liver Zonation – Revisiting Old Questions With New Technologies. Front Physiol 12:. doi: 10.3389/fphys.2021.732929

Davidson MD, Kukla DA, Khetani SR (2017) Microengineered cultures containing human hepatic stellate cells and hepatocytes for drug development. Integr Biol 9:662–677. doi: 10.1039/C7IB00027H

Deloitte (2022) Nurturing growth - Measuring the return from pharmaceutical innovation 2021

Dembélé L, Franetich J-F, Lorthiois A, et al (2014) Persistence and activation of malaria hypnozoites in long-term primary hepatocyte cultures. Nat Med 20:307–312. doi: 10.1038/nm.3461

Dowden H, Munro J (2019) Trends in clinical success rates and therapeutic focus. Nat Rev Drug Discov 18:495–496. doi: 10.1038/d41573-019-00074-z

Du Y, Han R, Wen F, et al (2008) Synthetic sandwich culture of 3D hepatocyte monolayer. Biomaterials 29:290–301. doi: 10.1016/j.biomaterials.2007.09.016

Dumoulin PC, Trop S a., Ma J, et al (2015) Flow cytometry based detection and isolation of Plasmodium falciparum liver stages in vitro. PLoS One 10:1–24. doi: 10.1371/journal.pone.0129623

Dunn JC, Tompkins RG, Yarmush ML (1992) Hepatocytes in collagen sandwich: evidence for transcriptional and translational regulation. J Cell Biol 116:1043–1053. doi: 10.1083/jcb.116.4.1043

Dunn JCY, Yarmush ML, Koebe HG, Tompkins RG (1989) Hepatocyte function and extracellular matrix geometry: long-term culture in a sandwich configuration. FASEB J 3:174–177. doi: 10.1096/fasebj.3.2.2914628

Fanning AS, Jameson BJ, Jesaitis LA, Anderson JM (1998) The Tight Junction Protein ZO-1 Establishes a Link between the Transmembrane Protein Occludin and the Actin Cytoskeleton. J Biol Chem 273:29745–29753. doi: 10.1074/jbc.273.45.29745

FDA U.S Food & Drug Administration (2022) Learn About Drug and Device Approvals. FDA US Food Drug Adm

Fivelman QL, Adagu IS, Warhurst DC (2004) Modified fixed-ratio isobologram method for studying in vitro interactions between atovaquone and proguanil or dihydroartemisinin against drug-resistant strains of Plasmodium falciparum. Antimicrob Agents Chemother 48:4097–4102. doi: 10.1128/AAC.48.11.4097-4102.2004

Foquet L, Hermsen CC, Verhoye L, et al (2015) Anti-CD81 but not anti-SR-BI blocks Plasmodium falciparum liver infection in a humanized mouse model. J Antimicrob Chemother 70:1784–1787. doi: 10.1093/jac/dkv019

Foster E, You J, Siltanen C, et al (2015) Heparin hydrogel sandwich cultures of primary hepatocytes. Eur Polym J 72:726–735. doi: 10.1016/j.eurpolymj.2014.12.033

Gamo F-J, Sanz LM, Vidal J, et al (2010) Thousands of chemical starting points for antimalarial lead identification. Nature 465:305–310. doi: 10.1038/nature09107

Gardner MJ, Hall N, Fung E, et al (2002) Genome sequence of the human malaria parasite Plasmodium falciparum. Nature 419:498–511. doi: 10.1038/nature01097

Gaskell H, Sharma P, Colley HE, et al (2016) Characterization of a functional C3A liver spheroid model. Toxicol Res (Camb) 5:1053–1065. doi: 10.1039/C6TX00101G

Geerts S, Ozer S, Chu C, et al (2019) Exploring donor demographics effects on hepatocyte yield and viability: Results of whole human liver isolation from one center. Technology 07:1–11. doi: 10.1142/s2339547819500018

Gerets HHJ, Tilmant K, Gerin B, et al (2012) Characterization of primary human hepatocytes, HepG2 cells, and HepaRG cells at the mRNA level and CYP activity in response to inducers and their predictivity for the detection of human hepatotoxins. Cell Biol Toxicol 28:69–87. doi: 10.1007/s10565-011-9208-4

Gijbels E, Vanhaecke T, Vinken M (2019) Establishment of Sandwich Cultures of Primary Human Hepatocytes. pp 325–333

Gissen P, Arias IM (2015) Structural and functional hepatocyte polarity and liver disease. J Hepatol 63:1023–1037. doi: 10.1016/j.jhep.2015.06.015

Guguen-guillouzo C, Clement B, Baffet G, et al (1983) MAINTENANCE SECRETION WITH AND REVERSIBILITY BY ADULT LIVER OF ACTIVE ALBUMIN TYPE RAT HEPATOCYTES EPITHELIAL CO-CULTURE ANOTHER Adult rat hepatocytes can be easily pre- cellular matrix have been examined . Cell at- pared by liver perfusion methods [1 , . 143:47–54

Guo L, Dial S, Shi L, et al (2011) Similarities and Differences in the Expression of Drug-Metabolizing Enzymes between Human Hepatic Cell Lines and Primary Human Hepatocytes. Drug Metab Dispos 39:528–538. doi: 10.1124/dmd.110.035873

Gural N, Mancio-Silva L, Miller AB, et al (2018) In Vitro Culture, Drug Sensitivity, and Transcriptome of Plasmodium Vivax Hypnozoites. Cell Host Microbe 23:395-406.e4. doi: 10.1016/j.chom.2018.01.002

Hafiz, A, Alam, MA., Alghamdi, OA., Mohammed, A. (2020) Combination Therapy and multidrug resistance in malaria parasite. In: Wani MY, Ahmad A (eds) Combination Therapy Against Multidrug Resistance. Elsevier Inc., pp 141–153

Hallifax D (2005) Prediction of metabolic clearance using cryopreserved human hepatocytes kinetic characteristics for five benzodiazepines. Drug Metab Dispos. doi: 10.1124/dmd.105.005389

Hamilton GA, Jolley SL, Gilbert D, et al (2001) Regulation of cell morphology and cytochrome P450 expression in human hepatocytes by extracellular matrix and cell-cell interactions. Cell Tissue Res 306:85–99. doi: 10.1007/s004410100429

He L, Pu W, Liu X, et al (2021) Proliferation tracing reveals regional hepatocyte generation in liver homeostasis and repair. Science (80-) 371:. doi: 10.1126/science.abc4346

Imwong M, Snounou G, Pukrittayakamee S, et al (2007) Relapses of Plasmodium vivax Infection Usually Result from Activation of Heterologous Hypnozoites . J Infect Dis 195:927–933. doi: 10.1086/512241

Ishii M, Washioka H, Tonosaki A, Toyota T (1991) Regional orientation of actin filaments in the pericanalicular cytoplasm of rat hepatocytes. Gastroenterology 101:1663–1672. doi: 10.1016/0016-5085(91)90406-B

Joyner C, Barnwell JW, Galinski MR (2015) No more monkeying around: primate malaria model systems are key to understanding Plasmodium vivax liver-stage biology, hypnozoites, and relapses. Front Microbiol 6:. doi: 10.3389/fmicb.2015.00145

Jungermann K (1986) Functional heterogeneity of periportal and perivenous hepatocytes. Enzyme 35:161–180. doi: 10.1159/000469338

Kalra A, Yetiskul E, Wehrle CJ, Tuma F (2022) Physiology, Liver

Khandelwal A, Arez F, Alves PM, et al (2022) Translation of liver stage activity of M5717, a Plasmodium elongation factor 2 inhibitor: from bench to bedside. Malar J 21:151. doi: 10.1186/s12936-022-04171-0

Khetani SR, Bhatia SN (2008) Microscale culture of human liver cells for drug development. Nat Biotechnol 26:120–126. doi: 10.1038/nbt1361

Khetani SR, Kanchagar C, Ukairo O, et al (2013) Use of micropatterned cocultures to detect compounds that cause drug-induced liver injury in humans. Toxicol Sci 132:107–117. doi: 10.1093/toxsci/kfs326

Khetani SR, Szulgit G, Del Rio JA, et al (2004) Exploring interactions between rat hepatocytes and nonparenchymal cells using gene expression profiling. Hepatology 40:545–554. doi: 10.1002/hep.20351

King CA (1988) Cell motility of sporozoan protozoa. Parasitol Today 4:315–319. doi: 10.1016/0169-4758(88)90113-5

Kryou C, Leva V, Chatzipetrou M, Zergioti I (2019) Bioprinting for Liver Transplantation. Bioengineering 6:95. doi: 10.3390/bioengineering6040095

Langlois A-C, Manzoni G, Vincensini L, et al (2020) Molecular determinants of SR-B1-dependent Plasmodium sporozoite entry into hepatocytes. Sci Rep 10:13509. doi: 10.1038/s41598-020-70468-2

Lansdowne LE (2020) Exploring the Drug Development Process. Technol. Networks

Lauschke VM, Hendriks DFG, Bell CC, et al (2016) Novel 3D Culture Systems for Studies of Human Liver Function and Assessments of the Hepatotoxicity of Drugs and Drug Candidates. Chem Res Toxicol 29:1936–1955. doi: 10.1021/acs.chemrestox.6b00150

Lauschke VM, Shafagh RZ, Hendriks DFG, Ingelman-Sundberg M (2019) 3D Primary Hepatocyte Culture Systems for Analyses of Liver Diseases, Drug Metabolism, and Toxicity: Emerging Culture Paradigms and Applications. Biotechnol J 14:1800347. doi: 10.1002/biot.201800347

LeCluyse EL, Audus KL, Hochman JH (1994) Formation of extensive canalicular networks by rat hepatocytes cultured in collagen-sandwich configuration. Am J Physiol Physiol 266:C1764–C1774. doi: 10.1152/ajpcell.1994.266.6.C1764

Lee-Montiel FT, George SM, Gough AH, et al (2017) Control of oxygen tension recapitulates zone-specific functions in human liver microphysiology systems. Exp Biol Med 242:1617–1632. doi: 10.1177/1535370217703978

Lee SML, Schelcher C, Laubender RP, et al (2014) An algorithm that predicts the viability and the yield of human hepatocytes isolated from remnant liver pieces obtained from liver resections. PLoS One 9:. doi: 10.1371/journal.pone.0107567

Leite SB, Wilk-Zasadna I, Zaldivar JM, et al (2012) Three-Dimensional HepaRG Model As An Attractive Tool for Toxicity Testing. Toxicol Sci 130:106–116. doi: 10.1093/toxsci/kfs232

Li J, Ning G, Duncan SA (2000) Mammalian hepatocyte differentiation requires the transcription factor HNF-4α. Genes Dev 14:464–474. doi: 10.1101/gad.14.4.464

Lim PLK, Tan W, Latchoumycandane C, et al (2007) Molecular and functional characterization of drug-metabolizing enzymes and transporter expression in the

novel spontaneously immortalized human hepatocyte line HC-04. Toxicol Vitr 21:1390–1401. doi: 10.1016/j.tiv.2007.05.003

Loreal O, Levavasseur F, Fromaget C, et al (1993) Cooperation of Ito cells and hepatocytes in the deposition of an extracellular matrix in vitro. Am J Pathol 143:538–544

Loubens M, Vincensini L, Fernandes P, et al (2021) Plasmodium sporozoites on the move: Switching from cell traversal to productive invasion of hepatocytes. Mol Microbiol 115:870–881. doi: 10.1111/mmi.14645

Manikandan P, Nagini S (2018) Cytochrome P450 Structure, Function and Clinical Significance: A Review. Curr Drug Targets 19:38–54. doi: 10.2174/1389450118666170125144557

Manzoni G, Marinach C, Topçu S, et al (2017) Plasmodium P36 determines host cell receptor usage during sporozoite invasion. Elife 6:. doi: 10.7554/eLife.25903

March S, Ng S, Velmurugan S, et al (2013) A Microscale Human Liver Platform that Supports the Hepatic Stages of Plasmodium falciparum and vivax. Cell Host Microbe 14:104–115. doi: 10.1016/j.chom.2013.06.005

Marcsisin SR, Sousa JC, Reichard GA, et al (2014) Tafenoquine and NPC-1161B require CYP 2D.pdf. 1–9

Maurel P (1996) The use of adult human hepatocytes in primary culture and other in vitro systems to investigate drug metabolism in man. Adv Drug Deliv Rev 22:105–132. doi: 10.1016/S0169-409X(96)00417-6

McCutchan TF, Kissinger JC, Touray MG, et al (1996) Comparison of circumsporozoite proteins from avian and mammalian malarias: biological and phylogenetic implications. Proc Natl Acad Sci 93:11889–11894. doi: 10.1073/pnas.93.21.11889

Messner S, Agarkova I, Moritz W, Kelm JM (2013) Multi-cell type human liver microtissues for hepatotoxicity testing. Arch Toxicol 87:209–213. doi: 10.1007/s00204-012-0968-2

Mota MM, Hafalla JCR, Rodriguez A (2002) Migration through host cells activates Plasmodium sporozoites for infection. Nat Med 8:1318–1322. doi: 10.1038/nm785

Mueller A-K, Camargo N, Kaiser K, et al (2005) Plasmodium liver stage developmental arrest by depletion of a protein at the parasite–host interface. Proc Natl Acad Sci 102:3022–3027. doi: 10.1073/pnas.0408442102

Ng S, Schwartz RE, March S, et al (2015) Human iPSC-Derived Hepatocyte-like Cells Support Plasmodium Liver-Stage Infection In Vitro. Stem Cell Reports 4:348–359. doi: 10.1016/j.stemcr.2015.01.002

Nguyen-Dinh P, Gardner AL, Campbell CC, et al (1981) Cultivation in Vitro of the Vivax-Type Malaria Parasite Plasmodium cynomolgi. Science (80-) 212:1146–1148. doi: 10.1126/science.7233207

Nguyen T V., Ukairo O, Khetani SR, et al (2015) Establishment of a Hepatocyte-Kupffer Cell Coculture Model for Assessment of Proinflammatory Cytokine Effects on Metabolizing Enzymes and Drug Transporters. Drug Metab Dispos 43:774–785. doi: 10.1124/dmd.114.061317

Nugraha B, Hong X, Mo X, et al (2011) Galactosylated cellulosic sponge for multi-well drug safety testing. Biomaterials 32:6982–6994. doi: 10.1016/j.biomaterials.2011.05.087

Olson H, Betton G, Robinson D, et al (2000) Concordance of the Toxicity of Pharmaceuticals in Humans and in Animals. Regul Toxicol Pharmacol 32:56–67. doi: 10.1006/rtph.2000.1399

Pampaloni F, Reynaud EG, Stelzer EHK (2007) The third dimension bridges the gap between cell culture and live tissue. Nat Rev Mol Cell Biol 8:839–845. doi: 10.1038/nrm2236

Petropolis DB, Faust DM, Tolle M, et al (2016) Human Liver Infection in a Dish: Easy-To-Build 3D Liver Models for Studying Microbial Infection. PLoS One 11:e0148667. doi: 10.1371/journal.pone.0148667

Pinheiro PF, Pereira SA, Harjivan SG, et al (2017) Hepatocyte spheroids as a competent in vitro system for drug biotransformation studies: nevirapine as a bioactivation case study. Arch Toxicol 91:1199–1211. doi: 10.1007/s00204-016-1792-x

Portugal S, Drakesmith H, Mota MM (2011) Superinfection in malaria: Plasmodium shows its iron will. EMBO Rep 12:1233–1242. doi: 10.1038/embor.2011.213

Potocnjak P, Yoshida N, Nussenzweig RS, Nussenzweig V (1980) Monovalent fragments (Fab) of monoclonal antibodies to a sporozoite surface antigen (Pb44) protect mice against malarial infection. J Exp Med 151:1504–1513. doi: 10.1084/jem.151.6.1504

Prudêncio M, Mota MM, Mendes AM (2011) A toolbox to study liver stage malaria. Trends Parasitol 27:565–574. doi: 10.1016/j.pt.2011.09.004

Prudêncio M, Rodriguez A, Mota MM (2006) The silent path to thousands of merozoites: the Plasmodium liver stage. Nat Rev Microbiol 4:849–856. doi: 10.1038/nrmicro1529

Racanelli V, Rehermann B (2006) The liver as an immunological organ. Hepatology 43:. doi: 10.1002/hep.21060

Ramaiahgari SC, den Braver MW, Herpers B, et al (2014) A 3D in vitro model of differentiated HepG2 cell spheroids with improved liver-like properties for repeated dose high-throughput toxicity studies. Arch Toxicol. doi: 10.1007/s00204-014-1215-9

Ramaiahgari SC, Waidyanatha S, Dixon D, et al (2017) From the Cover: Three-Dimensional (3D) HepaRG Spheroid Model With Physiologically Relevant Xenobiotic Metabolism Competence and Hepatocyte Functionality for Liver Toxicity Screening. Toxicol Sci 159:124–136. doi: 10.1093/toxsci/kfx122

Raphemot R, Posfai D, Derbyshire ER (2016) Current therapies and future possibilities for drug development against liver-stage malaria. J Clin Invest 126:2013–2020. doi: 10.1172/JCI82981

Rebelo SP, Costa R, Estrada M, et al (2015) HepaRG microencapsulated spheroids in DMSO-free culture: novel culturing approaches for enhanced xenobiotic and biosynthetic metabolism. Arch Toxicol 89:1347–1358. doi: 10.1007/s00204-014-1320-9

Rebelo SP, Costa R, Silva MM, et al (2017) Three-dimensional co-culture of human hepatocytes and mesenchymal stem cells: improved functionality in long-term bioreactor cultures. J Tissue Eng Regen Med 11:2034–2045. doi: 10.1002/term.2099

Redpath NT, Foulstone EJ, Proud CG (1996) Regulation of translation elongation factor-2 by insulin via a rapamycin-sensitive signalling pathway. EMBO J 15:2291–2297. doi: 10.1002/j.1460-2075.1996.tb00582.x

Risco-Castillo V, Topçu S, Marinach C, et al (2015) Malaria sporozoites traverse host cells within transient vacuoles. Cell Host Microbe 18:593–603. doi: 10.1016/j.chom.2015.10.006

Rosenthal PJ (2003) Antimalarial drug discovery: Old and new approaches. J Exp Biol 206:3735–3744. doi: 10.1242/jeb.00589

Roth A, Maher SP, Conway AJ, et al (2018) A comprehensive model for assessment of liver stage therapies targeting Plasmodium vivax and Plasmodium falciparum. Nat Commun 9:. doi: 10.1038/s41467-018-04221-9

Rottmann M, Jonat B, Gumpp C, et al (2020) Preclinical antimalarial combination study of M5717, a Plasmodium falciparum elongation factor 2 inhibitor, and pyronaridine, a hemozoin formation inhibitor. Antimicrob Agents Chemother 64:1–9. doi: 10.1128/AAC.02181-19

Saito Y, Ikemoto T, Morine Y, Shimada M (2021) Current status of hepatocyte-like cell therapy from stem cells. Surg Today 51:340–349. doi: 10.1007/s00595-020-02092-6

Saji Joseph J, Tebogo Malindisa S, Ntwasa M (2019) Two-Dimensional (2D) and Three-Dimensional (3D) Cell Culturing in Drug Discovery. In: Cell Culture. IntechOpen

Sattabongkot J, Yimamnuaychoke N, Leelaudomlipi S, et al (2006) Establishment of a human hepatocyte line that supports in vitro development of the exo-erythrocytic stages of the malaria parasites Plasmodium falciparum and P. vivax. Am J Trop Med Hyg 74:708–15. doi: 74/5/708 [pii]

Schulze RJ, Schott MB, Casey CA, et al (2019) The cell biology of the hepatocyte: A membrane trafficking machine. J Cell Biol 218:2096–2112. doi: 10.1083/jcb.201903090

Sengupta S, Johnson BP, Swanson SA, et al (2014) Aggregate Culture of Human Embryonic Stem Cell-Derived Hepatocytes in Suspension Are an Improved In Vitro Model for Drug Metabolism and Toxicity Testing. Toxicol Sci 140:236–245. doi: 10.1093/toxsci/kfu069

Serra M, Brito C, Correia C, Alves PM (2012) Process engineering of human pluripotent stem cells for clinical application. Trends Biotechnol 30:350–359. doi: 10.1016/j.tibtech.2012.03.003

Sevior DK, Pelkonen O, Ahokas JT (2012) Hepatocytes: The powerhouse of biotransformation. Int J Biochem Cell Biol 44:257–261. doi: 10.1016/j.biocel.2011.11.011

Shibata Y, Takahashi H, Chiba M, Ishii Y (2002) Prediction of Hepatic Clearance and Availability by Cryopreserved Human Hepatocytes: An Application of Serum Incubation Method. Drug Metab Dispos 30:892–896. doi: 10.1124/dmd.30.8.892

Shlomai A, Schwartz RE, Ramanan V, et al (2014) Modeling host interactions with hepatitis B virus using primary and induced pluripotent stem cell-derived hepatocellular systems. Proc Natl Acad Sci 111:12193–12198. doi: 10.1073/pnas.1412631111

Silvie O, Greco C, Franetich JF, et al (2006) Expression of human CD81 differently affects host cell susceptibility to malaria sporozoites depending on the Plasmodium species. Cell Microbiol 8:1134–1146. doi: 10.1111/j.1462-5822.2006.00697.x

Silvie O, Rubinstein E, Franetich J-F, et al (2003) Hepatocyte CD81 is required for Plasmodium falciparum and Plasmodium yoelii sporozoite infectivity. Nat Med 9:93–96. doi: 10.1038/nm808

Solanas E, Sanchez-fuentes N, Serrablo A, Lue A (2022) How Donor and Surgical Factors Affect the Viability and Functionality of Human Hepatocytes Isolated From Liver Resections. 9:1–9. doi: 10.3389/fmed.2022.875147

Sultan AA, Thathy V, Frevert U, et al (1997) TRAP is necessary for gliding motility and infectivity of Plasmodium sporozoites. Cell 90:511–522. doi: 10.1016/S0092-8674(00)80511-5

Tachibana S-I, Sullivan SA, Kawai S, et al (2012) Plasmodium cynomolgi genome sequences provide insight into Plasmodium vivax and the monkey malaria clade. Nat Genet 44:1051–1055. doi: 10.1038/ng.2375

Tavares J, Costa DM, Teixeira AR, et al (2017) In vivo imaging of pathogen homing to the host tissues. Methods 127:37–44. doi: 10.1016/j.ymeth.2017.05.008

Tavares J, Formaglio P, Thiberge S, et al (2013) Role of host cell traversal by the malaria sporozoite during liver infection. J Exp Med 210:905–15. doi: 10.1084/jem.20121130

Templeton TJ, Kaslow DC (1997) Cloning and cross-species comparison of the thrombospondin-related anonymous protein (TRAP) gene from Plasmodium knowlesi, Plasmodium vivax and Plasmodium gallinaceum1Note: Nucleotide sequence data reported in this paper have been submitted to GenBankTM wi. Mol Biochem Parasitol 84:13–24. doi: 10.1016/S0166-6851(96)02775-2

Tesseromatis C, Alevizou A (2008) The role of the protein-binding on the mode of drug action as well the interactions with other drugs. Eur J Drug Metab Pharmacokinet 33:225–230. doi: 10.1007/BF03190876

Tostões RM, Leite SB, Serra M, et al (2012) Human liver cell spheroids in extended perfusion bioreactor culture for repeated-dose drug testing. Hepatology 55:1227–1236. doi: 10.1002/hep.24760

Trefts E, Gannon M, Wasserman DH (2018) The liver. 27:. doi: 10.1016/j.cub.2017.09.019.The

Treyer A, Müsch A (2013) Hepatocyte polarity. Compr Physiol 3:243–287. doi: 10.1002/cphy.c120009

Ueno T, Sata M, Tanikawa K (2003) Cells Responsible for Extracellular Matrix Production in the Liver. Extracell Matrix Liver Approach to Gene Ther 89–103. doi: 10.1016/B978-012525251-5/50007-5

Wang Y, Kim MH, Shirahama H, et al (2016) ECM proteins in a microporous scaffold influence hepatocyte morphology, function, and gene expression. Sci Rep 6:37427. doi: 10.1038/srep37427

Ware BR, Durham MJ, Monckton CP, Khetani SR (2018) A Cell Culture Platform to Maintain Long-term Phenotype of Primary Human Hepatocytes and Endothelial Cells. Cell Mol Gastroenterol Hepatol 5:187–207. doi: 10.1016/j.jcmgh.2017.11.007

Wei Y, Wang YG, Jia Y, et al (2021) Liver homeostasis is maintained by midlobular zone 2 hepatocytes. Science (80-) 371:1–25. doi: 10.1126/science.abb1625

WHO (2021) World malaria report 2021

WHO (2015) Guidelines for the treatment of Malaria - Third edition, 3rd edn. World Health Organization, Geneva

Wijnen PAHM, Op Den Buijsch RAM, Drent M, et al (2007) Review article: The prevalence and clinical relevance of cytochrome P450 polymorphisms. Aliment Pharmacol Ther 26:211–219. doi: 10.1111/j.1365-2036.2007.03490.x

Winer BY, Gaska JM, Lipkowitz G, et al (2020) Analysis of Host Responses to Hepatitis B and Delta Viral Infections in a Micro-scalable Hepatic Co-culture System. Hepatology 71:14–30. doi: 10.1002/hep.30815

Winer BY, Huang TS, Pludwinski E, et al (2017) Long-term hepatitis B infection in a scalable hepatic co-culture system. Nat Commun 8:. doi: 10.1038/s41467-017-00200-8

Xu JJ, Henstock P V., Dunn MC, et al (2008) Cellular imaging predictions of clinical drug-induced liver injury. Toxicol Sci 105:97–105. doi: 10.1093/toxsci/kfn109

Xu Q (2021) Human Three-Dimensional Hepatic Models: Cell Type Variety and Corresponding Applications. Front Bioeng Biotechnol 9:1–21. doi: 10.3389/fbioe.2021.730008

Yoshida N, Potocnjak P, Nussenzweig V, Nussenzweig RS (1981) Biosynthesis of Pb44, the protective antigen of sporozoites of Plasmodium berghei. J Exp Med 154:1225–1236. doi: 10.1084/jem.154.4.1225

Zeeman A-M, Lakshminarayana SB, van der Werff N, et al (2016) PI4 Kinase Is a Prophylactic but Not Radical Curative Target in Plasmodium vivax-Type Malaria Parasites. Antimicrob Agents Chemother 60:2858–2863. doi: 10.1128/AAC.03080-15

Zeilinger K, Freyer N, Damm G, et al (2016) Cell sources for in vitro human liver cell culture models. Exp Biol Med 241:1684–1698. doi: 10.1177/1535370216657448

Chapter II

Flexible 3D cell-based platforms for the discovery and profiling of novel drugs targeting *Plasmodium* hepatic infection

This chapter was adapted from:

Arez F.*, Rebelo SP.*, Fontinha D.*, Simão D., Martins TR., Machado M., Fischli C., Oeuvray C., Badolo L., Carrondo MJT., Rottmann M., Spangenberg T., Brito C., Greco B., Prudêncio M., Alves PM., (2019) Flexible 3D Cell-Based Platforms for the Discovery and Profiling of Novel Drugs Targeting Plasmodium Hepatic Infection. ACS Infectious Diseases. DOI: 10.1021/acsinfecdis.

F.A., S.P.R., and D.F. contributed equally
Conceptualization: S.R., M.J.T.C., T.S., C.B., B.G., M.P., P.M.A.
Methodology: F.A., S.R., D.F., D.S., M.M., T.S., C.B., M.R., M.P.
Formal analysis: F.A., S.R., D.F., L.B., C.F., M.R.
Investigation: F.A., S.R., D.F., D.S., T.R.M., M.M., C.F.
Writing – original draft: F.A., S.R., D.F.
Writing – review and editing: T.S., C.B., M.P., P.M.A.
Supervision: M.J.T.C., T.S., C.B., B.G., M.P., P.M.A.

Table of contents

Abstract

The restricted pipeline of drugs targeting the liver-stage of *Plasmodium* infection reflects the scarcity of cell models that mimic the human hepatic phenotype and drug metabolism, as well as *Plasmodium* hepatic infection. Using stirred-tank culture systems, spheroids of human hepatic cell lines were generated, sustaining a stable hepatic phenotype over four weeks of culture. Spheroids were employed in the establishment of 3D *P. berghei* infection platforms that relied on static or dynamic culture conditions. *P. berghei* invasion and development were recapitulated in the hepatic spheroids, yielding blood-infective merozoites. The translational potential of the 3D platforms was demonstrated by comparing the *in vitro* minimum inhibitory concentration of M5717, a compound under clinical development, with in vivo plasma concentrations that clear liver-stage *P. berghei* in mice. Our results show that the 3D platforms are flexible, scalable and can predict the efficacy of anti-plasmodial therapies, constituting a powerful tool for integration in drug discovery programs.

Keywords: 3D cell models, liver-stage infection, malaria, *Plasmodium*, drug discovery, *in vitro*.

Introduction

Malaria is one of the deadliest human infectious diseases worldwide, having caused an estimated total of 435 000 deaths in 2017 (WHO | World malaria report 2018 2018). The disease is caused by protozoan parasites of the *Plasmodium* genus, of which 5 species, *P. falciparum* (*Pf*), *P. vivax* (*Pv*), *P. ovale* (*Po*), *P. malariae* and *P. knowlesi*, are known to infect humans. The initial, obligatory phase of *Plasmodium* infection in the mammalian host occurs in the liver, where each sporozoite traverses several hepatocytes until productively invading one (Mota, Hafalla, and Rodriguez 2002). Inside the hepatocytes, sporozoites differentiate into exoerythrocytic forms (EEFs) that replicate into thousands of mature blood-infective merozoites. Once released into the blood stream merozoites infect erythrocytes, leading to the malaria-associated pathology (Prudêncio, Rodriguez, and Mota 2006). The clinically silent nature of *Plasmodium*'s initial and obligatory developmental phase in the liver makes this stage of infection an attractive target for prophylactic intervention. Furthermore, it is in the liver that *Pv* and *Po* parasites generate latent forms known as hypnozoites, that can remain dormant for months or years, until their activation leads to disease relapse (Wells, Burrows, and Baird 2010).

Due to the limitations inherent to addressing the liver-stage of *Plasmodium* infection experimentally, including the scarcity of liver-stage models and the limited access to hypnozoite-forming parasites, few anti-plasmodial therapies target this phase of the parasite's life cycle. Among these are 8-aminoquinolines (e.g.primaquine and tafenoquine), folate inhibitors sulfadoxine-pyrimethamine and atovaquone (ATO), a naphtoquinone inhibitor of the malaria parasite's cytochrome bc1 complex of the electron transport chain (reviewed by Raphemot et al 2016). The genetic diversity of *Plasmodium* parasites has led to the acquisition of resistance to the latter two of these drugs (Raphemot, Posfai, and Derbyshire 2016; Sridaran et al. 2010).

Therefore, to fulfill the current therapeutic gaps in the malaria eradication agenda, new candidates that can be employed in single-dose treatments are required (Burrows et al. 2017; Palmer, MJ. and Wells 2012). DDD107498 (M5717), a drug candidate targeting the *Plasmodium* eukaryotic translation elongation factor 2, may fulfil the single-dose requirement for cure, prophylaxis and transmission blocking activities against malaria. This compound has a long plasma half-life and displays potent activity against both liver and blood-stage parasites, as well as male and female gametocytes (Baragaña et al. 2015).

Despite the efforts to develop new drug candidates that target the liver stage of *Plasmodium* infection, the restricted pipeline of anti-plasmodial drugs acting on this phase of infection reflects the scarcity of preclinical *in vitro* models suitable for studying: (i) the complex biology of *Plasmodium* development; (ii) drug efficacy; (iii) drug metabolism and (iv) toxicology (Okombo and Chibale 2017). Preclinical *in vitro* models for discovery of anti-plasmodial drugs targeting the liver-stage of infection rely mostly on primary human hepatocytes (PHH), cultured in formats that sustain *Pv* and *Pf* infection (Dembélé et al. 2014; Gural et al. 2018; March et al. 2013; Roth et al. 2018). These platforms depend on extracellular matrix cues (e.g. collagen type I) or murine fibroblasts to sustain hepatocyte polarization and functionality, which are not attained in conventional 2D culture systems (Hoffmaster et al. 2004; Khetani and Bhatia 2008). However, the phenotypic stability of these culture formats is still limited (Dunn, Tompkins, and Yarmush 1992; Zeigerer et al. 2017). Moreover, the use of PHH is restricted by their high cost, limited availability and great variability between lots. Conversely, cell line-derived spheroids, in which cell–cell interactions are maximized, have been shown to promote the accumulation of native ECM and improve liver-specific features, such as the expression of polarity proteins and the membrane localization of phase III transporters (Chang and Hughes-Fulford 2009; Gaskell et al. 2016; Gunness et al.

2013; Rebelo et al. 2014), more closely resembling the *in vivo* architecture and functionality of the hepatic lobule. HepG2, a cell line with lower metabolic performance than HepaRG and PHH (Gerets et al. 2012) has been shown to present improved expression of metabolic enzymes when cultured as spheroids (Ramaiahgari et al. 2014). Both HepG2 and HepaRG spheroids have been used in drug testing platforms, displaying enhanced sensitivity for the determination of drug cytotoxicity, mainly for repeated drug dosing (Gaskell et al. 2016; Gunness et al. 2013; Leite et al. 2012; Ramaiahgari et al. 2014, 2017; Rebelo et al. 2014). The use of stirred-tank systems to generate spheroids provides a homogeneous physicochemical culture environment that maintains 3D hepatocyte cultures for longer periods of time, (Rebelo et al. 2017; Tostões et al. 2012) with the possibility of non-invasive sampling throughout culture time and upscaling (Santo et al. 2016; Serra et al. 2012), constituting a cost-effective alternative.

The present work focuses on the development of 3D cell-based *Plasmodium* hepatic infection platforms, relying on spheroids of human hepatic cell lines generated in stirred-tank culture systems, for the discovery of novel anti-plasmodial drugs. *Plasmodium* infection of the hepatic spheroids was optimized in both static and dynamic cell suspension conditions. The 3D infection platforms were used to assess the efficacy of two anti-plasmodial drugs with distinct modes of action, M5717 and ATO, throughout hepatic infection by rodent *P. berghei* (*Pb*) parasites. The translational potential of these platforms was assessed by comparing these results with those obtained in *in vivo* studies. Our results show the applicability of these novel platforms for drug discovery programs, given their scalability, flexibility and cost-effectiveness.

Methods

Animal and Cell sources

All animal experiments were performed in strict compliance with the guidelines of the animal ethics committee of Instituto de Medicina Molecular Joao Lobo Antunes (iMM, Lisboa, Portugal), which also approved the study, and the Federation of European Laboratory Animal Science Associations (FELASA). Male BALB/c mice (Charles River laboratories) with 6–8 weeks of age, were kept and manipulated in iMM's animal facility. The animal experiments carried out at the Swiss Tropical and Public Health Institute (Basel, Switzerland) adhered to local and national regulations of laboratory animal welfare in Switzerland (awarded permission no. 2693). Protocols are regularly reviewed and revised following approval by the local authority (Veterinäramt Basel Stadt). Female NMRI mice (Charles River laboratories) with 20-22 g of body weight were housed and manipulated in Swiss TPH's animal facility. The hepatic cell lines used in this study were HC-04, HepG2 and HepaRG. The HC-04 cell line was obtained from Sanaria Inc., while the HepG2 and HepaRG cell lines were purchased from ATCC and Thermo Fisher Scientific, respectively.

Two-dimensional (2D) Cell culture

2D cell cultures were maintained in static conditions. HepaRG cells were cultured as previously described (Gripon et al. 2002; Rebelo et al. 2014). HepG2 and HC-04 cells were cultured in low glucose DMEM and DMEM/F12 supplemented with HEPES, respectively (both from Thermo Fisher Scientific). The culture medium of both cell lines was supplemented with 1 % (v/v) pen/strep and 10 % (v/v) FBS. These cell lines were passaged twice every week at a cell inoculum of $5x10^4$ and $4x10^4$ cell/cm^2, respectively. All cell lines were routinely propagated in T-flasks under static conditions and maintained in an incubator with humidified environment, at 37 °C, 5 % CO_2.

Three-dimensional (3D) Cell culture (Spheroids)

Hepatic cell spheroids were generated and maintained up to 30 days in dynamic suspension, employing stirred vessels (125 mL or 30 mL spinner vessels from Corning®, Merck KGaA and ABLE Biott Corporation, respectively) placed on magnetic stirrers (2mag AG), kept in an incubator with humidified environment at 37 °C, 5 % CO_2. Single cell suspensions of $3x10^5$ cell/mL were inoculated into the spinners, in the culture medium employed for 2D cell culture, supplemented with 10-20 % (v/v) FBS. The agitation rate and the medium exchange regimen tailored for each cell line are described in the supplementary information (Table S1). Medium replacement was performed by centrifugation, followed by cell pellet resuspension in fresh culture medium supplemented with 5-10 % (v/v) FBS.

Production of *P. berghei* sporozoites

Green fluorescent protein (GFP)- or luciferase (Luc)-expressing *P. berghei* (*Pb*) ANKA sporozoites reared in iMM's insectary and *P. berghei* mCherry ANKA-Luci-GFP reared at Swiss TPH's insectarium were employed. *Anopheles stephensi* mosquitoes employed at iMM were infected by feeding on infected mice as previously described (Ploemen et al. 2009). At Swiss TPH's insectarium the mosquitoes were obtained by feeding on infected female NMRI mice after 12-24 h of starvation (without Glucose solution). Female *Anopheles stephensi* mosquitoes were allowed to feed on anaesthetized mice (Escornakon, pentobarbital in 15 % ethanol, 70 mg/kg, injected intraperitoneally (I.P.)) for 30 minutes and blood-fed mosquitoes were reared with 8 % fructose with 0.5 % PABA and H_2O solution.

Salivary glands of infected *Anopheles stephensi* mosquitoes were freshly isolated into RPMI 1640 medium (Thermo Fisher Scientific) or phosphate-buffered saline (PBS), macerated with a micro pistil and filtered through a 40 µm cell strainer to remove mosquito debris. The

free sporozoites were then counted in a Bürker-Türk or Neubauer chamber using phase-contrast microscopy).

Plasmodium infection of 2D cultures

2D cultures of HepG2, HC-04 and HepaRG cells were infected as previously described (Machado et al. 2017; Ploemen et al. 2009). Briefly, cells were plated at a density of $3.1x10^4$ cell/cm^2, in 96-well plates, the day before infection. The following day, the culture medium was replaced by infection medium (low glucose DMEM supplemented with 5 % (v/v) FBS, 1:300 Amphotericin B (250 µg/mL) and 1:1000 Gentamycin 50 mg/mL, all from Thermo Fisher Scientific) and $1x10^4$ sporozoites were added to each well, to achieve a cell:spz ratio of 1:1. In non-infected controls, medium was added in the place of sporozoites. Sporozoite addition was followed by a centrifugation step at 1800 xg for 5 min and plates were maintained in static conditions at 37 ºC and 5 % CO_2 for 2 h. After this period, an equal volume of fresh infection medium was added to the wells. The cultures were maintained in static conditions up to 48 h post-infection (hpi), at which time the infection rates were assessed either by detection of GFP by flow cytometry or by measurement of luciferase activity, as described below. For the assessment of parasite development throughout infection, 2D cultures were processed for flow cytometry, analysis at 24, 36, 48 and 60 hpi. HepaRG and HC-04 infection values were normalized by those obtained with HepG2.

Plasmodium infection of 3D cultures

Prior to infection, the cell density of each dynamic spheroid culture was determined, as described below.

For static infections, spheroids from day 9 of culture were plated in ultra-low attachment flat bottom 96-well plates (Corning®, Merck KGaA) at $1x10^4$, $2.5 x10^4$ and $5x10^4$ cell/well densities, in a total volume

of 100 µL. The infection procedure was performed as described for 2D cultures. The number of sporozoites was adjusted depending on the cell:spz ratio intended. For dynamic infection, a suspension spheroid culture was established at $5x10^5$ or $1x10^6$ cell/mL in 30 mL spinners from ABLE Biott Corporation. Sporozoite suspensions were added to attain cell:spz ratios of 1:1 and 2:1. The culture was maintained under constant stirring for 2 h after which a 1:4 to 1:8 dilution was performed, and the culture was maintained up to 84 hpi. The infection medium for static and dynamic infections was the same as that employed for 2D infection. A control condition of infection in 2D HepG2 cells was included in all experiments. For the assessment of parasite infection rate and development throughout infection, spheroids were collected at 24, 36, 48, 60 and 70 hpi for flow cytometry, bioluminescence, or immunofluorescence microscopy analysis, as described below.

Merozoite infectivity assessment *in vivo*

BALB/c mice were infected by intravenous (I.V.) injection of 200 µL of supernatants collected from *Pb*-Luc-infected cells, cultured in 2D and 3D static infection conditions. The supernatants from each condition were injected into 5 and 4 mice, respectively. A non-infected mouse was used as a negative control. Blood-stage infections were monitored by analysis of Giemsa-stained blood smears and detection of GFP by flow cytometry in tail blood, collected between days 4 and 11 post-injection.

Characterization of the spheroid cultures: cell viability, concentration, and spheroid diameter

Cell viability was determined by a fluorescence live/dead assay, as previously described (Estrada et al. 2015). Briefly, spheroids were incubated with fluorescein diacetate (Sigma-Aldrich, Merck) at 10 µg/mL for detection of viable cells and the DNA dye TO-PRO™-3 Iodide (Thermo Fisher Scientific) at 1 µM for detection of dead cells. FDA is a cell-permeant esterase substrate that measures both enzymatic activity,

which is required to activate its fluorescence, and cell membrane integrity, which is required for intracellular retention of their fluorescent product. TO-PRO® 3 is a DNA dye that stains cells with a compromised membrane. Spheroids were visualized in an inverted fluorescence microscope (Leica DMI6000). Cell concentration was determined by the Trypan blue exclusion method, as described previously (Rebelo et al. 2014). Spheroid size was determined by measuring Feret's diameter (Estrada et al. 2015) using the open-source ImageJ software (version 1.52b) (Rueden et al. 2017).

Fluorescence Microscopy

Fluorescence microscopy of spheroids and adherent cells was performed as previously reported (Rebelo et al. 2017). Briefly, cells were fixed in 4 % (w/v) paraformaldehyde with 4 % (w/v) sucrose in PBS for 20 min. For the generation of cryosections, spheroids were incubated in a solution of 30 % (w/v) sucrose overnight and frozen in optimum cutting temperature (O.C.T.™) compound Tissue-Tek (Sakura) at -80 °C. The frozen samples were sectioned in 10-40 µm slices using a Cryostat (Leica). For detection of intracellular epitopes, cryosections and adherent cells were processed for immunofluorescence: permeabilized with 0.1 % (v/v) Triton X-100 (TX-100) and blocked with 0.2 % (w/v) fish-skin gelatin (FSG) solution in PBS for 30 min. The incubation of primary antibodies was performed for 2 h in a solution containing 0.125 % (w/v) FSG followed by the incubation of secondary antibodies for 1 h in the same solution. For F-actin detection, following permeabilization, a single incubation step of 20 min with A488- or TRITC-conjugated Phalloidin (A12379, Thermo Fischer Scientific and P1951, Sigma-Aldrich, respectively) in PBS was performed. Finally, cryosections and adherent cells were mounted in DAPI-containing Prolong (P36935, Thermo Fisher Scientific). The primary antibodies used for immunodetection of hepatic phenotype included human serum albumin (Alb; Ab8940-1,

Abcam) and hepatocyte nuclear factor 4 alpha (HNF4α; Ab41898, Abcam). For the characterization of infection, antibodies against *P. berghei* UIS4 protein (AB0042, SICGEN), GFP (G6539, Merck), and mouse monoclonal antibody 2E6 against *Pb* heat shock protein 70 (PbHSP70) were used. The samples were visualized using point scanning (SP5, Leica), spinning disk microscopy (Andor revolution ×D, Andor Technology PLC) and LSM 710 confocal laser point-scanning (Zeiss) microscopes.

Assessment of *Plasmodium* Infection by flow cytometry

Pb-GFP-infected samples were washed with PBS, trypsinized for determination of cell density, and resuspended in 70-150 µL of 2 % (v/v) FBS in PBS. Blood from the tail of mice injected with the supernatants of infected cultures was collected to 2 % (v/v) FBS in PBS. Cells were analysed on a BD Accuri C6 or LSRFortessa (BD Biosciences) with the appropriate settings for the fluorophores used. Data acquisition and analysis were carried out using the Accuri C6 (version 1.0.264.21, BD), FACSDiva (version 6.2, BD) and FlowJo (version 10.0.8, FlowJo) software packages, respectively.

Assessment of *Plasmodium* infection by measurement of luciferase activity

Pb-Luc-infected cells were processed at time points ranging from 12 to 84 hpi, depending on the intended readout, for measurement of luciferase activity using the Firefly Luciferase Assay Kit (Biotium), following the manufacturer's instructions. Briefly, cells were washed twice with PBS, after which lysis buffer, diluted 1:4, was added. Cells were frozen and thawed alternating with agitation at 500 rpm until complete cell lysis. Bioluminescence was measured using a microplate reader (Infinite® 200 PRO, Tecan Trading AG) and the light reaction of each well was measured for 100 ms.

Drug Assays

M5717 was synthetized as described in (Baragaña et al. 2015) and supplied by Merck KGaA. Atovaquone (ATO) was bought from Merck (Sigma-Aldrich, A7986). Stock solutions of 10 mM were prepared in DMSO.

In vitro drug assays

Working solutions of compounds employed in drug assays were prepared fresh at concentrations ranging from 0.01 to 300 nM prior to incubation with cells. Infection of 2D HepG2 cell cultures with *Pb*-Luc was performed at $1x10^4$ cell/well with a cell:spz ratio of 1:1. Infection of HepG2 spheroids in static conditions was performed at $2.5x10^4$ cell/well at a cell:spz ratios of 1:1 and 1:2 and infection in dynamic conditions was performed at 5x106 and $1x10^6$ cell/mL at cell:spz ratios of 1:1 and 2:1, respectively. At 24 hpi, cells were exposed to the selected drug dilutions and cultured for an additional 24 h. For the construction of dose-dependency curves, infection rate and metabolic activity were assessed at 48 hpi, whereas for the time-dependent response studies infection rate and dsDNA concentration were assessed up to 84 hpi. Cell metabolic activity was determined by PrestoBlue (Thermo Fisher Scientific) following the manufacturer's instructions. Briefly, cells were incubated with Presto Blue 1X for 50 min at 37 ºC and the fluorescence of the culture supernatant was measured employing 560 nm and 590 nm excitation and emission wavelengths, respectively, using a microplate reader (Infinite® 200 PRO, Tecan Trading AG). dsDNA quantification was performed following manufacturer instructions for Quant-iT™ PicoGreen™ dsDNA Assay Kit (P7589, Thermo Fisher Scientific). Cell metabolic activity, which correlates to cell viability, was used as a normalization method of the infection rate in the IC50

determination assay, whereas DNA content was used to normalize infection rate in the time response assessment in vitro. Cells were then analyzed for bioluminescence as previously described.

Non-linear regression analysis was employed to fit the normalized results of the dose-response curves, and IC50 values were determined using GraphPad Prism version 6 for Windows (GraphPad software, La Jolla California USA). The lowest concentration of anti-plasmodial drug that inhibited infection by 99 % relative to DMSO-treated controls was considered the minimal inhibitory concentration (Russell et al. 2003).

In vivo drug assays (established liver infection)

Naïve mice were infected with $1x10^5$ sporozoites of *P. berghei* mCherry ANKA-Luci-GFP by I.V. injection in the tail vein. At -2 h or +24 hpi, single oral dose drug treatment with M5717 (0.3, 3 and 30 mg/kg as indicated in Figure II.5C) was given to groups of 3 mice. One mouse received 10 mg/kg ATO as positive control and three mice served as untreated controls (compounds were dissolved in a vehicle of 7 % Tween 80 and 3 % Ethanol). At 23 and 48 hpi, liver-stage *Plasmodium* infection was assessed *in vivo* in all mice. To this end, mice were anesthetized with isoflurane after an I.V. injection of D-Luciferin (30 mg/mL) with a volume of 5 mL/kg. To measure bioluminescence, which correlates with the degree of liver infection, anesthetized mice were placed in an IVIS Lumina II system and images were acquired with a highly sensitive CCD (charge-coupled device) camera using LivingImage 4.3 Software. The generated heat maps of mice represent intensity of bioluminescence with radiance (p/sec/cm2/sr) indicated by a pseudocolour scale (min= 1.20e4 and max= 1.00e6). At 7, 14, 17, 21, 24, 28, 31 and 35 days post-infection blood-stage parasitaemia was measured by light microscopy on Giemsa-stained blood smears, and positive mice were euthanized. Mice without detectable parasitaemia

until day 35 post-infection (33 days post-treatment) were considered as cured and were euthanized.

Blood-to-plasma ratio

M5717 was incubated at 1 µM for 30 minutes at 37 °C in mouse whole blood as well as in control plasma (i.e., surrogate for whole blood). Whole blood samples were centrifuged to obtain plasma. M5717 concentrations in plasma supernatant and control plasma were quantified by LC-MS/MS. The blood-to-plasma ratio (KB/P) was calculated based on M5717 / internal standard peak area ratios (PAR) according to the equation KB/P (CB/CP) = PARP (control)/ PARP. The Mouse CB/CP ratio for M5717 was found to be 3.27.

Data analysis and statistics

Statistical analysis was performed using GraphPad Prism version 6 for Windows (GraphPad software, La Jolla California USA). A parametric t-test was performed, considering paired conditions when subjected to the same batch of spz. For unpaired conditions, one-way ANOVA followed by Tukey's multicomparisons test was performed. P values are presented for statistically significant results (*, $P < 0.05$, **, $P<0.01$, *** $P<0.001$, ****$P<0.0001$).

Results

Production of 3D hepatic cell models in stirred-tank culture systems

For the generation of hepatic spheroids, three hepatic cell lines - HepG2, HC-04 and HepaRG - were selected based on their drug metabolic activities and/or susceptibility to *Plasmodium* infection (Dembélé et al. 2014; Gerets et al. 2012; Sattabongkot et al. 2006). All cell lines were inoculated as single cell suspensions in spinner vessels and their aggregation was optimized to attain high cell packing densities,

towards the formation of compact spheroids. The inoculum cell density, stirring rate and serum concentration were adjusted as previously described (Santo et al. 2016; Tostões et al. 2012). The parameters optimized for each cell line are presented in Table II.1.

Table II.1- Conditions for 3D culture of HepG2, HC-04 and HepaRG spheroids in stirred-tank systems.

Conditions	HepG2	HC-04	HepaRG
Cell inoculum (cell/mL)	$0.3x10^6$	$0.3x10^6$	$0.3x10^6$
Agitation rate (rpm)	40-100	50-90	40-60
Serum concentration (%, v/v)	10-5	20-5	10-5
Medium replacement (%, v/v)	50	50	20

By day 4, cultures of the three cell lines were mainly composed of compact spheroids (Figure II.1A). HepG2 and HC-04 spheroids presented high cell viability after 21 days of culture (Figure II.1A) and could be maintained for at least 30 days. At day 4 after inoculation, HepG2, HC-04 and HepaRG spheroids displayed average diameters of 70±22, 63±13 and 42±7 µm, respectively (Figure II.1B). While HepaRG spheroids maintained a similar average diameter throughout culture time, the diameter of HepG2 and HC-04 spheroids increased up to 169±45 and 179±56 µm by day 15 (Figure II.1B). The hepatic phenotype in the spheroids was analyzed by the characterization of cell polarization and hepatocyte-specific markers. F-actin filaments were detected adjacent to the cell membrane in the apical region of the cells from day 9 to day 15 of culture (Figure II.1C, D) forming bile canaliculi-like structures, typical of polarized hepatic cells (Gaskell et al. 2016; Rebelo et al. 2014, 2017). The membranar accumulation of E-cadherin corroborates the cell polarization observed at day 9 of culture (Figure II.S1).The hepatic identity and biosynthetic function of HepG2 and HC-04 spheroids were further corroborated by the presence of the

hepatocyte nuclear factor 4 alpha (HNF4α) and of the liver biosynthetic globular protein, albumin (Alb) by day 9 and 15 of culture (Figure II.1C, D).

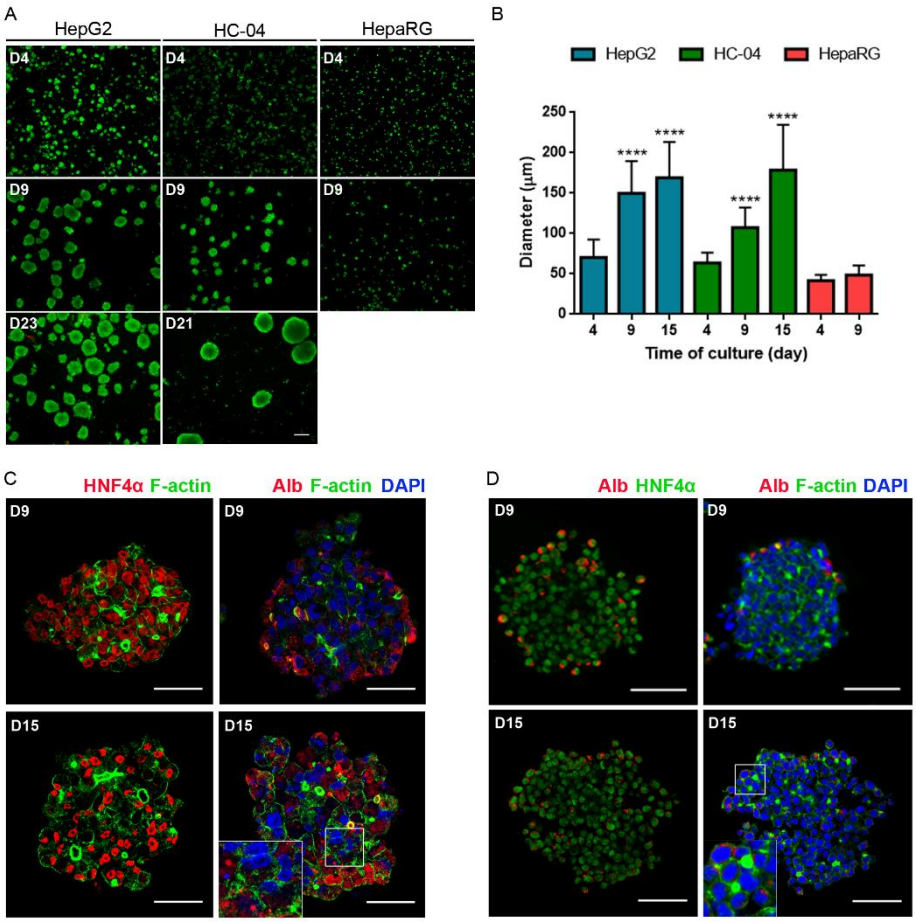

Figure II.1 - Characterization of HepG2, HC-04 and HepaRG cell lines in stirred culture systems. (A) Cell viability assay (fluorescein diacetate (FDA) - green; TOPRO-3 – red) at days 4, 9 and 21 (HC-04) or 23 (HepG2) of culture. Scale bar: 200 µm. **(B)** Spheroid diameter at days 4, 9 and 15 of culture. Data are represented as mean ± S.D. of at least 170 spheroids from 2 to 5 independent cultures for days 4, 9 and 15 of culture. Statistical analysis was performed by one-way ANOVA in comparison to day 4 of culture, followed by Tukey's multi-comparison test: ****, $p<0.0001$. **(C-D)** Phenotypic characterization by fluorescence microscopy of day 9 and day 15 spheroids:

HepG2 **(C)** and HC-04 **(D)**. Hepatic phenotypic markers detected include albumin (Alb), F-actin, and HNF4α. The insets in the bottom-right images of panels C and D highlight the membranar accumulation of F-actin, indicating cell polarization. Scale bars: 50 µm.

Infection of 3D hepatic spheroids with *Plasmodium berghei*

For the implementation and optimization of a 3D *Plasmodium* infection platform, the *Pb* infection procedure in 2D (described in Prudêncio, Mota, & Mendes, 2011) was adapted to infect spheroids in a 96-well plate format (static infection, Fig. II.S2A). Therefore, 2D HepG2 cells plated at $1x10^4$ cell/well and infected by *Pb* in 1:1 cell:spz ratio were used as an infection control in all experiments. Spheroids from days 4 and 9 were infected by *Pb*-Luc in different conditions (data not shown). Spheroids from day 9 were more homogeneous than those from day 4 and led to higher parasite loads, being therefore selected for optimization of infection parameters in 3D. Parameters influencing hepatic infection and spheroid morphology were evaluated employing HepG2 spheroids. To this end, cell densities of $1x10^4$, $2.5x10^4$ and $5x10^4$ cell/well and cell:spz ratios of 2:1, 1:1 and 1:2 were assessed using luciferase-expressing rodent *Pb* parasites (*Pb*-Luc, Figure II.S2B and S2C). Given the surface area covered, the morphology of spheroids observed under static conditions, and the parasite load estimated, cell concentrations of $2.5x10^4$ and $5x10^4$ cell/well and 1:1 and 1:2 cell:spz ratios were selected for further studies. Therefore, spheroids from day 9 of culture of the 3 cell lines were infected with *Pb*-Luc employing the 4 infection conditions selected (Figure II.2).

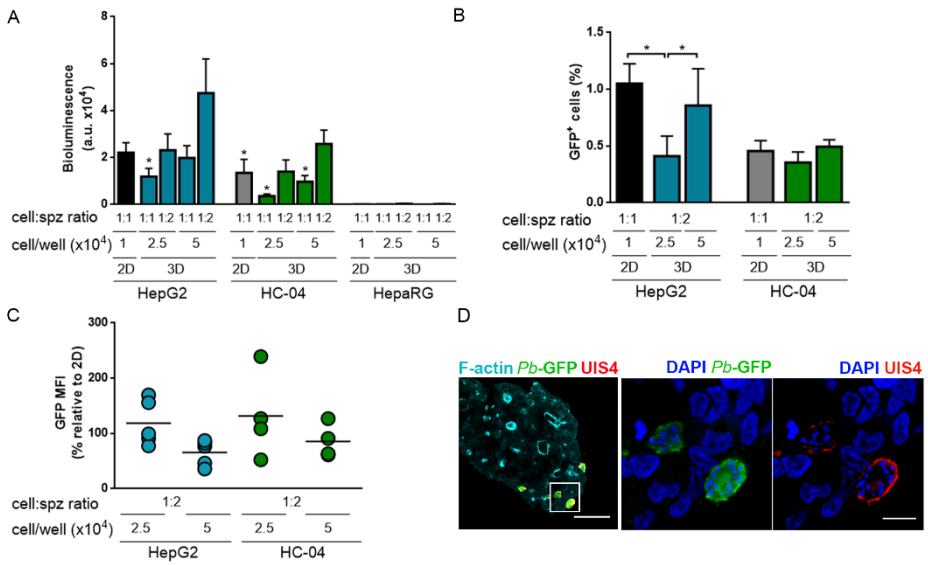

Figure II. 2 - Infection of hepatic cell lines with *Plasmodium berghei* (*Pb*). **(A)** Bioluminescence values expressed in arbitrary units (a.u.) of *Pb*-Luc-infected HepG2, HC-04 and HepaRG cells by measuring luciferase activity. Results are represented as mean ± S.E.M of at least 3 independent experiments. Statistical analysis of paired t-test was performed for both HepG2 and HC-04 relative to 2D HepG2: *, $p<0.05$. **(B)** % of infected cells by *Pb*-GFP for HepG2 and HC-04. Results show the percentage of GFP-positive cells quantified by flow cytometry, represented as the mean ± S.E.M. of at least 3 independent experiments. Statistical analysis by paired t-test was performed comparing all conditions: *, $p>0.05$. **(C)** *Pb* development in HepG2 and HC-04 cells, determined by measurement of the geometric mean of GFP fluorescence intensity (MFI). Data represent the mean ± S.E.M. of at least 3 independent cultures. Statistical analysis was performed by one-way ANOVA, followed by Tukey's multicomparison test. **(D)** Parasitophorous vacuole membrane detection shown by staining of the UIS4 membrane protein in *Pb* parasites developing inside HepG2 spheroids. Scale bar: 50 µm. The inset represents a zoom in of one stack of UIS4 staining. Scale bar: 10 µm

Forty-eight hours post-infection (hpi), the luciferase activity of HepG2 spheroids was similar to that of the 2D HepG2 cells for all the

conditions tested, except for 2.5x104 cell/well; cell:spz 1:1, which was significantly lower than the latter (41±13 % of 2D HepG2). HC-04 cells presented lower parasite loads than 2D HepG2 in 2D and 3D at cell:spz ratios of 1:1 (58±12 % for 2D and 21±3 % and 57±9 % for spheroids at $2.5x10^4$ cell/well and 5x104 cell/well). At a cell:spz ratio of 1:2, the parasite load was 72±26 % and 126±17 % of that observed in 2D HepG2 cells for $2.5x10^4$ and $5x10^4$ cell/well, respectively. In summary, both HepG2 and HC-04 spheroids sustained infection by *Pb* sporozoites in the four selected conditions, with higher amounts of spz and higher cell densities leading to higher parasite loads, suggesting that the conditions optimized for HepG2 can be translated to the HC-04 cell system. On the other hand, the HepaRG cell line was not infected by *Pb*, either in the 2D or in the 3D formats (Figure II.2A), suggesting that HepaRG does not sustain infection by rodent *Pb* parasites.

In order to further characterize *Pb* infection of 3D spheroids of HepG2 and HC-04 cells, a *Pb* strain constitutively expressing green fluorescent protein (*Pb*-GFP) was employed. This strain enables the quantification of GFP^+ cells and GFP intensity by flow cytometry, as surrogate measures of infection rate and parasite development, respectively (Prudêncio et al. 2007). *Pb*-GFP-infected 2D HepG2 cells employed as controls presented an average of 1.1±0.2 % infected cells, similar to the 0.9±0.3 % infection rate observed for the higher 3D cell density employed (Figure II.2B). No significant differences were observed between the different conditions employed for HC-04 cell infection, with a percentage of infected cells ranging from 0.4 to 0.5 % (Figure II.2B). Parasite development, as estimated from the GFP geometric mean fluorescence intensity (MFI) at 48 hpi, was also not statistically different between all experimental conditions (Figure II.2C). At this time point, the presence of the protein up-regulated in infective sporozoites 4 (UIS4), a constituent of the parasitophorous vacuole

membrane (PVM) (Mueller et al. 2005), was detected inside HepG2 cells in the inner layers of the spheroids (Figure II.2D). The parasite's hepatic development in HepG2 and HC-04 spheroids was further assessed throughout infection, at 24, 36, 48 and 60 hpi. *Pb* proliferated in the infected hepatocytes, as indicated by the increase in GFP MFI from 24 h onwards (Figure II.3A). These values peaked at 48 hpi in all cultures, only further increasing up to 60 hpi in adherent HepG2 cells (Figure II.3A). These results were corroborated by immunofluorescence microscopy analyses, which showed an increase in hepatic parasite size up to 60 hpi (Figure II.3B).

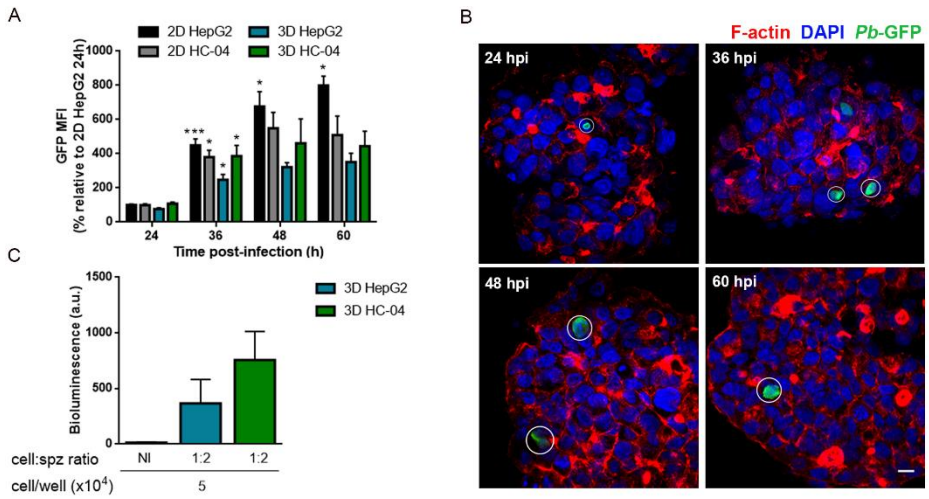

Figure II.3 - Characterization of *P. berghei* development in 3D cultures. (A) *Pb*-GFP development at 24, 36, 48 and 60 hpi analyzed by flow cytometry of 5.0x104 cell/well HepG2 and HC-04 spheroids infected at 1:2 cell:spz ratio. Results are represented as the mean ± S.E.M. of three independent replicates. Paired t-test was performed for each condition relative to previous time-point: *, p<0.05; ***, p>0.001. **(B)** *Pb*-GFP development at 24, 36, 48 and 60 hpi was assessed by confocal imaging. Scale bars: 10 µm. **(C)** Merozoite release as indicated by bioluminescence detection in supernatants of the conditions with spheroids at 5.0x10^4 cell/well infected by Pb-Luc at 1:2 cell:spz ratio. Non-infected (NI) 3D cultures were used as negative control. Results are

represented as bioluminescence arbitrary units (a.u.) measured by luciferase activity, mean ± S.E.M. from three independent experiments.

To evaluate the maturation of *Pb* parasites in HepG2 and HC-04 spheroids, merosome release was assessed at 70 hpi in supernatants of 3D cultures. In all conditions, luciferase activity was detected on culture supernatants (Figure II.3C), suggesting that parasites are able to mature into merozoites and be released from hepatic spheroids of both cell lines. To fully ascertain merozoite release and infectivity, HC-04 spheroid culture supernatants were then injected into Balb/c mice and the ensuing appearance of blood parasitaemia was monitored. The results show that mice developed parasitaemia from day 6 after supernatant injection onwards, with all mice becoming blood stage-positive at day 8 after injection (Table II.2).

Table II.2 - Merosome infectivity indicated by the number of blood-stage positive mice at different times post-injection of culture supernatants from HC-04 spheroids infected by *Pb*-GFP at 1:2 cell:spz ratio.

Time (day)	2D HepG2	3D HC-04
4	0/5	0/4
5	0/5	0/4
6	5/5	0/4
7	5/5	2/4
8	5/5	4/4
9	5/5	4/4
10	5/5	4/4
11	5/5	4/4

Altogether, these results show that the 3D cultures of HepG2 and HC-04 cells are able to sustain invasion by *Pb* sporozoites, as well as parasite replication and differentiation. Furthermore, merozoites derived

from HC-04 spheroids fully matured into blood-infective merozoites, leading to the onset of blood parasitaemia following injection into mice.

Next, an alternative approach to static *Pb* infection was established using HepG2 spheroids and *Pb*-Luc in stirred-tank vessels – dynamic 3D infection (Figure II.4A).

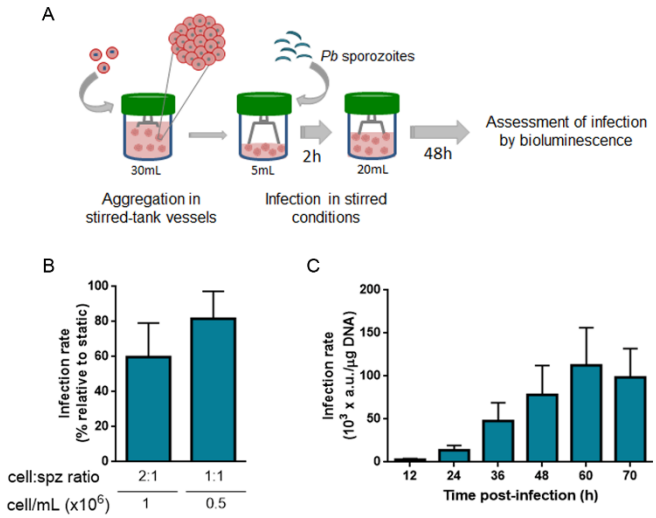

Figure II.4 - Characterization of *P. berghei* dynamic infection. **(A)** Schematic representation of the dynamic infection strategy (not at scale). **(B)** Infection rate of HepG2 spheroids infected with *Pb*-Luc in dynamic conditions at 2:1 and 1:1 cell:spz ratios. Infection rate is expressed as the percentage of bioluminescence normalized by µg DNA relative to infection in static conditions of $2.5x10^4$ cell/well in 1:1 cell:spz ratio. Data represent the mean ± S.E.M of at least two independent experiments. **(C)** *Pb*-Luc development in HepG2 spheroids infected by Pb-Luc in dynamic conditions at 2:1 cell:spz ratio. Data shown are bioluminescence values measured at 24, 36, 48, 60 and 70 hpi. Results are presented as mean ± S.E.M. of four independent experiments.

To promote the contact between spheroids and sporozoites, the former were cultured in suspension at high densities in a low culture volume, during the 2 h required for *Pb* invasion (cell:spz ratios of 2:1 and 1:1) (Prudêncio, Mota, and Mendes 2011). The infection of HepG2

spheroids in static conditions was used as a control ($2.5x10^4$ cell/well in 1:1 cell:spz ratio). Under stirring conditions, the infection rate observed at 48 hpi with 1:1 cell:spz ratio was 82±16 % that of the control (Figure II.4B). At 2:1 cell:spz, the infection rate was 60±19 % of that of the control. Bioluminescence values increased from 12 to 60 hpi, with a slight decrease at 70 hpi (Figure II.4C), suggesting that the parasites could develop in dynamic culture. Collectively, these results demonstrate that *Plasmodium* invasion and development in HepG2 spheroids occurs in both static and dynamic conditions.

3D infection platforms are suitable for evaluation of dose- and time-dependent responses to anti-plasmodial drugs

To correlate the *in vitro* hepatic spheroid infection platforms with the *in vivo* rodent *Pb* model, the activity and concentrations of M5717 were assessed and compared in a similar protocol. Addition of compounds occurred 24 h after *Pb* infection of 3D HepG2 spheroids and oral dosing was performed 24 h post-sporozoite injection into mice. ATO was used as positive control in these experiments (Figure II.5A).

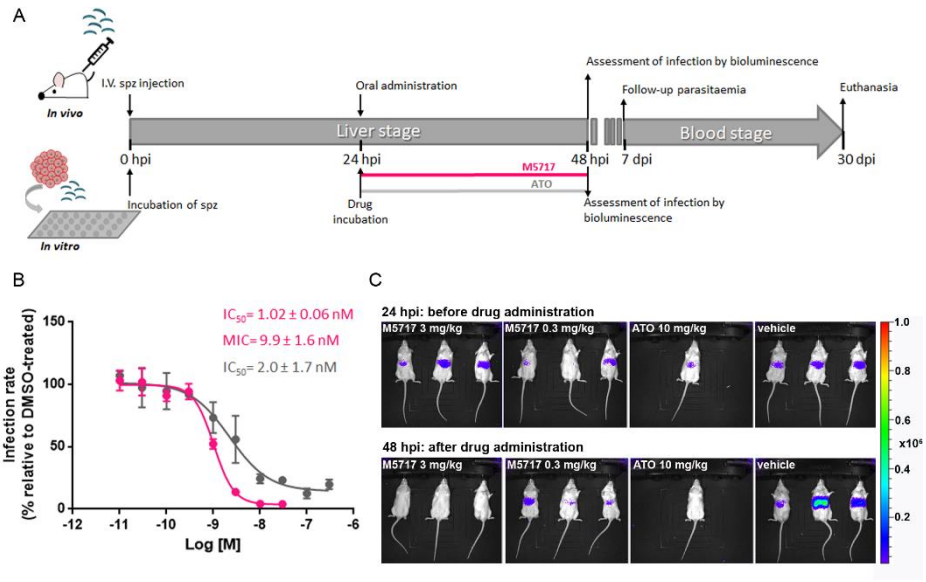

Figure II.*5* - Preclinical assessment of M5717 dose-response. (A) Schematic representation of drug administration in vivo and in vitro for IC50 determination (not at scale). **(B)** Dose-response curves and IC50 determination of M5717 (pink) and atovaquone (ATO, gray) in HepG2 spheroids infected by *Pb*-Luc under static conditions at 2.5x10^4 cell/well in 1:2 cell:spz ratio. The minimum inhibitory concentration (MIC) of M5717 was also determined. Results are presented as the mean ± S.D. of three independent experiments. **(C)** Ventral view images of NMRI mice infected with 100.000 luciferase-expressing sporozoites before (24 h) and after (48 h) treatment with 3 mg/kg of M5717, 0.3 mg/kg of M5717, 10 mg/kg ATO and vehicle. Heat maps of mice represent the intensity of bioluminescence, radiance (p/sec/cm2/sr) as indicated by pseudocolour scale. hpi – hours post-infection, dpi - days post-infection.

In vitro, the half maximal inhibitory concentration (IC50) was determined using the 3D static infection platform. The range of concentrations employed did not impact cell viability at 48 hpi (Figure II.S3A). IC50 values for M5717 and ATO in infected HepG2 spheroids analyzed at 48 hpi were 1.0±0.1 nM and 2.0±1.7 nM, respectively. Also the minimum inhibitory concentration (MIC) for M5717 was 9.9±0.1 nM, corresponding to approximately 10 times the drug's IC50 value (Figure

II.5B). These results are in agreement with the IC50 determined in the control 2D HepG2 cultures for M5717 and ATO (0.4±0.3 and 1.9±0.6 nM respectively) (Figure II.S3B).

In vivo, a single oral dose of 0.3 mg/kg failed to clear all liver stage parasites, while at 3 mg/kg M5717 was able to completely clear the *Pb* liver-stage infection, only 24 h after drug administration, with no recrudescence of parasites (monitored in the blood until day 33 post-treatment). As previously reported by (Baragaña et al. 2015) ATO was able to clear parasites at a single oral dose of 10 mg/kg (Figure II.5C).

To correlate the *in vivo* exposure with the 3D *in vitro* effective concentrations, the average plasma concentration (C_{av}) over 24 h was compared to the in vitro MIC. At 3 mg/kg the plasma C_{av}24h was 61 nM and corresponded to 6-fold the *in vitro* MIC (9.9 nM), whereas the non-curing dose of 0.3 mg/kg reached a Cav of 5 nM, which corresponded to only half of the MIC required *in vitro*.

To ascertain the platforms translational potential and take full advantage of the 3D dynamic infection platform, which allows long-term follow-up of the infected culture, the time-response of M5717 was assessed. Parasite inhibition in the dynamic 3D platform was assessed from 24 hpi with concentrations of M5717 above the MIC (25 nM) and below the MIC (1 nM). Both concentrations of M5717 showed an inhibitory effect immediately after drug exposure at 24 hpi (Figure II.6).

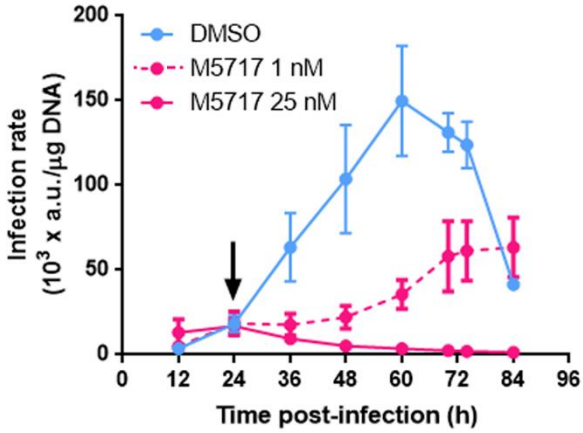

Figure II.6 - Time-response of M5717 in *Pb* infection. Time-response of M5717 determined under stirred conditions in *Pb* infection of HepG2 spheroids. Results are expressed as arbitrary units of bioluminescence (a.u.) measured by luciferase activity per µg DNA and represent the mean ± S.E.M. of three independent experiments. The arrow indicates the time at which the drug was administrated. M5717 was administrated at 1 nM (pink dashed line) and 25 nM (pink line). The drug vehicle, DMSO, was administered as a control (blue line).

Although *Pb* development was completely inhibited throughout the culture period at 25 nM of M5717, a concentration of M5717 below the MIC, i.e. 1 nM, only partially inhibited *Pb* infection up to 79±2 % at 48 hpi.

Discussion

The scarcity of accurate experimental models that adequately recapitulate the human hepatic phenotype, *Plasmodium* hepatic infection, and drug metabolism have hampered the development of drugs targeting the liver stages of the malaria parasite. We have previously shown that stirred-tank culture systems are suitable for generation of 3D hepatic cell models, which retain a stable hepatic phenotype up to several weeks of culture (Rebelo et al. 2017; Tostões et al. 2012). In the present work, spheroids of selected human hepatic

cell lines were employed in the establishment of static and dynamic 3D infection platforms, which sustain infection by, and the complete development of, *Plasmodium* parasites.

Two-dimensional cultures of hepatic cell lines have been extensively used as a model for the characterization of the liver stage of *Plasmodium* infection. More complex culture systems, relying on PHH cultured on natural matrixes (e.g. collagen I) and/or in co-culture with murine fibroblasts to provide signaling cues and confer spatial restriction to improve the hepatocyte phenotype, have also been employed for the assessment of *Plasmodium* infection and long-term parasite development (Hoffmaster et al. 2004; Khetani and Bhatia 2008). Three-dimensional cultures of hepatic cells resorting to the use of matrix components or microcarrier beads have been previously proposed for the study of another hepatotropic pathogen, the hepatitis C virus (HCV) (Aly, Shimotohno, and Hijikata 2009; Molina-Jimenez et al. 2012; Sainz, TenCate, and Uprichard 2009). Despite the advantages of these complex biological platforms over conventional 2D cultures, the presence of non-human and undefined components, the batch-to-batch variability of the materials and the donor variability and high cost associated with PHH are disadvantages for their routine application. Conversely, cell line-derived hepatic spheroids generated in stirred-tank vessels constitute a fully human cell model, which is robust and cost-effective for straightforward integration in screening platforms. In the present study, spheroids of three hepatic cell lines were generated in a stirred-tank culture system, by tuning critical parameters, such as cell inoculum, agitation rate, and serum concentration (Santo et al. 2016; Tostões et al. 2012). This process generated compact spheroids with an average diameter lower than 200 µm, which do to not generate necrotic centers in HepG2 spheroids (Gaskell et al. 2016). Furthermore, spheroids maintained cell viability for at least one month in culture.

Moreover, we show that hepatic spheroids of HepG2 and HC-04 cell lines kept a stable hepatic phenotype, characterized by the expression of liver-specific proteins, albumin and HNF4α, and cell polarity, a crucial feature for liver function (Zeigerer et al. 2017). Additionally, we have previously shown that hepatic spheroids secrete and accumulate extracellular matrix components that contribute to the long-term maintenance of hepatic phenotype (Leite et al. 2012; Rebelo et al. 2014). Therefore, hepatic spheroids recapitulate features of the liver architecture and metabolism.

Our results show that HepaRG cells could not be infected by *Pb*, similarly to what has been reported for the human-infective *Pf* and the monkey-infective *P. cynomolgi* parasite species, in which HepaRG cells were used as negative control of infection (Roth et al. 2018) or were not infected by *Pf/P. cynomolgi* in co-culture with PHH (Dembélé et al. 2014). Conversely, HepG2 and HC-04 spheroids sustained *Pb* infection, in according to what is reported for 2D cultures (Ploemen et al. 2009; Prudêncio, Mota, and Mendes 2011). *Pb* was able to infect cells in both the outer and inner layers of the spheroids, suggesting that the 3D architecture does not compromise the cell traversal process and subsequent productive invasion. Parasite development inside the invaded hepatocytes was observed by the continuous increase in parasite size up to 48 hpi, at which time the presence of UIS4, an essential protein for parasite maturation throughout the hepatic development (Mueller et al. 2005), showed full integrity of the PVM. The parasite maturation process, which, *in vivo*, culminates in the release of infectious merozoites to the bloodstream, was also replicated in the spheroid cultures, as shown by the detection of luminescence in the culture supernatant and the capability of the latter to initiate a blood stage infection in mice. Thus, besides displaying relevant hepatic architecture and polarization, hepatic spheroids sustain complete

Plasmodium hepatic infection. The 3D dynamic infection platform developed in this study took advantage of stirred-tank culture systems to maintain high cell densities, for longer periods of time. In the dynamic conditions, the infection rates obtained were within the same range of the ones obtained in static conditions. Therefore, the 3D dynamic infection platform developed sustains efficient *Pb* infection of hepatic spheroids in a system that supports homogenous distribution of all culture components, is scalable, and allows easy sampling and monitoring over time without compromising the continuity of the infected culture.

The newly generated static and dynamic platforms were further validated for drug testing. The determination of the IC50 values of both M5717 and ATO showed that M5717 displays higher inhibitory effect against *Plasmodium* hepatic infection than ATO, in agreement with a previous report by (Baragaña et al. 2015). Moreover, the translational potential of the 3D static platform was demonstrated by comparing effective concentrations of M5717 on *Pb* infection *in vitro* and *in vivo*. Using the 3D hepatic *in vitro* platform, we could show that concentrations as low as 10 nM, corresponding to the MIC, were efficient in clearing a patent liver infection. Furthermore, *in vivo* data demonstrated that average plasma concentrations over 24 h greater than the MIC (i.e. 61 nM) were able to clear the liver infection whereas doses of M5717 yielding to a C_{av} lower than the MIC (i.e. 0.5 nM) failed in clearing all parasites 48 hpi, resulting in detection of parasites in circulating blood. Due to the long-term maintenance and non-destructive, continuous sampling of the dynamic infection platform, we could follow-up infected cultures after the drug addition to ascertain its complete efficacy and exclude the possibility of remission. This was exemplified with M5717, which completely inhibited the progression of infection at a concentration greater than the MIC (i.e. 25 nM), while a

concentration below the MIC (i.e. 1 nM) only partially inhibited the *Pb* infection.

Beyond their translational potential from *in vitro* to *in vivo*, as well as drug screening purposes, these platforms may also constitute an invaluable tool to study the basic biology of *Plasmodium* hepatic infection in a physiologically relevant context, for instance, towards understanding the mechanisms of cell traversal by *Plasmodium* sporozoites, a process whose role in infection remains unclear (Mota, Hafalla, and Rodriguez 2002; Risco-Castillo et al. 2015). Moreover, the platforms described in this work can potentially be translated to human *Plasmodium* parasites, as stirred-tank culture systems are suitable for spheroid culture of HC-04 cells and PHH, which sustain infection by *Pv* and *Pf* (Dumoulin et al. 2015; Roth et al. 2018; Tostões et al. 2012). Moreover, the long-term maintenance of stable hepatic phenotypes can be especially useful when investigating hypnozoites, dormant forms generated by *Pv* and *Po* parasites that persist in hepatocytes (Dembélé et al. 2014; March et al. 2013).

Conclusion

To the extent of our knowledge, we hereby report for the first time that *P. berghei* can infect and develop inside hepatic spheroids, completely maturating into blood-infective parasites. This 3D culture platform constitutes a promising tool for drug discovery targeting liver stages of *Plasmodium* infection. Besides recapitulating key features of liver cell function, the system can be scaled up to feed medium to high throughput platforms for drug screening purposes or to sustain the *Plasmodium* infection in dynamic systems. With the possibility of long-term maintenance, medium culture exchange as well as non-destructive and continuous sampling, this technology allows the monitoring of

infected cultures subjected to various culture conditions (e.g. hypoxia) or drug-treatments, useful to support translational medicine purposes (e.g. pharmacokinetic/pharmacodynamic analysis). The feasibility of using cell sources that support infection by a range of rodent- and human-infective parasites, combined with the possibility of performing dose-response and time-response studies, emphasizes the flexibility of these platforms. Collectively, these features highlight the potential of hepatic spheroids for addressing particular issues of host-parasite interaction, with the ultimate goal of identifying novel compounds that can be used as prophylactic and/or therapeutic interventions.

Acknowledgments

We gratefully acknowledge Dr Ana Terrasso for the discussions on in vitro drug assays performed in this work. We acknowledge Ana Filipa Teixeira and Ana Parreira for mosquito production and infection. We acknowledge Merck for funding the work. M.P. is a recipient of an "Investigador FCT" award of Fundação para a Ciência e Tecnologia, Portugal (FCT). F.A. is recipient of a PhD fellowship PD/BD/128371/2017, funded by FCT.

Supplementary Material

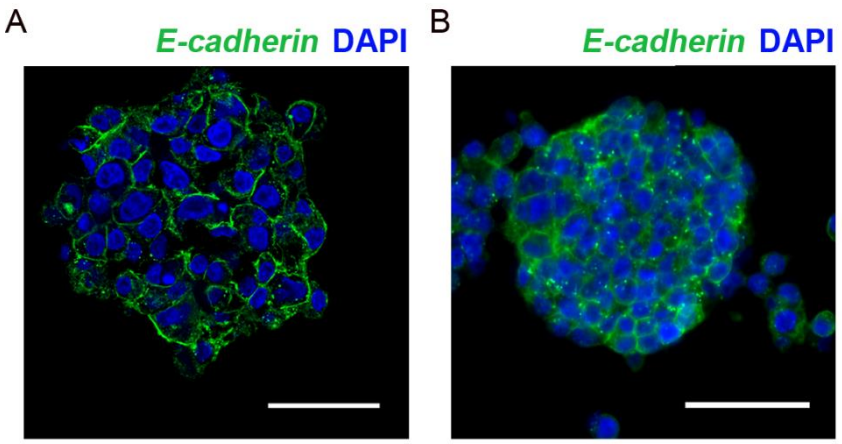

Figure II.S1 - Characterization of cellular polarization of spheroids. Detection of membranar E-cadherin at day 9 of culture. **(A)** HepG2 **(B)** HC-04. Scale bars: 50 µm

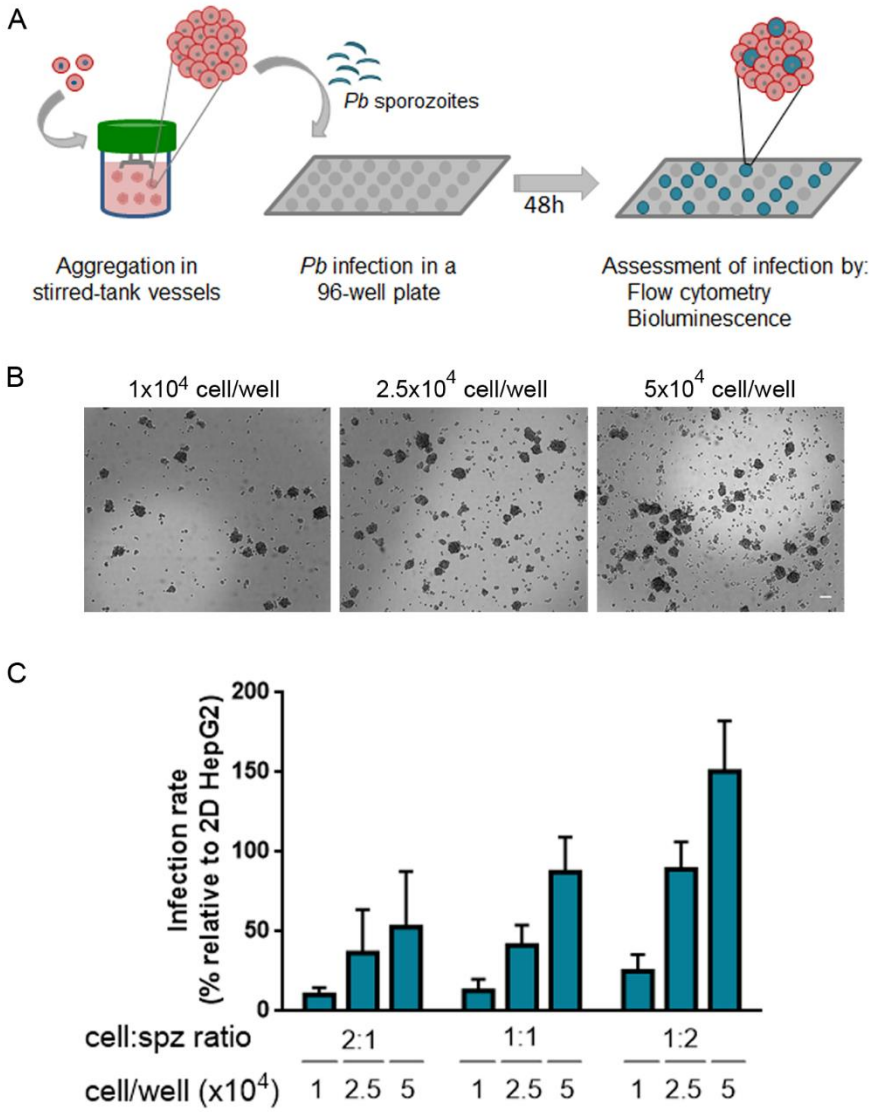

Figure II.S2 - Optimization of 3D infection conditions. (A) spheroid culture in stirred-tank vessels and infection in static conditions (not at scale). **(B)** Phase contrast microscopy images of HepG2 spheroids at different cell densities. Scale bar: 100 µm. **(C)** Bioluminescence measured by luciferase activity of HepG2 spheroids at different cell densities and cell:spz ratios. Results are presented as percentage or infection rate as mean ± S.E.M. relative to 2D HepG2 cells at 1:1 cell-to-spz ratio, of at least 3 independent experiments.

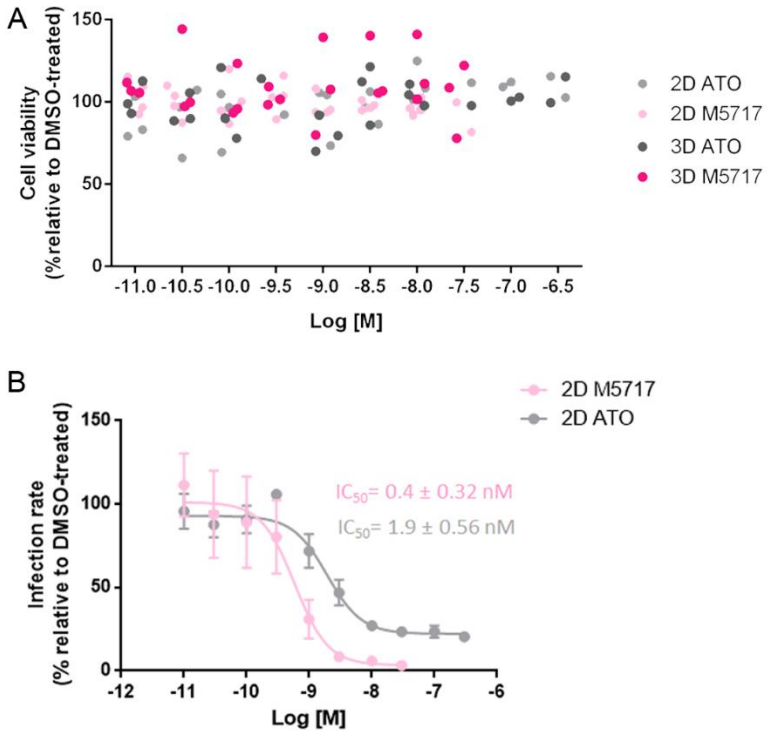

Figure II.S3 - Preclinical assessment of M5717 and ATO dose-response in vitro. (A) Cell viability response curves to the different doses of M5717 and ATO used for IC50 determination. **(B)** Dose-response curves and IC50 determinations of ATO and M5717 in adherent HepG2 cells. Data shown correspond to luciferase activity, measured as bioluminescence relative to DMSO-treated conditions. Data are presented as the mean ± S.D. of at least three independent experiments.

References

WHO | World malaria report 2018. WHO. 2018.

Mota MM, Hafalla JCR, Rodriguez A. Migration through host cells activates Plasmodium sporozoites for infection. Nat Med. 2002;8(11):1318-1322. doi:10.1038/nm785

Prudêncio M, Rodriguez A, Mota MM. The silent path to thousands of merozoites: the Plasmodium liver stage. Nat Rev Microbiol. 2006;4(11):849-856. doi:10.1038/nrmicro1529

Wells TNC, Burrows JN, Baird JK. Targeting the hypnozoite reservoir of Plasmodium vivax: the hidden obstacle to malaria elimination. Trends Parasitol. 2010;26(3):145-151. doi:10.1016/j.pt.2009.12.005

Raphemot R, Posfai D, Derbyshire ER. Current therapies and future possibilities for drug development against liver-stage malaria. J Clin Invest. 2016;126(6):2013-2020. doi:10.1172/JCI82981

Sridaran S, McClintock SK, Syphard LM, Herman KM, Barnwell JW, Udhayakumar V. Anti-folate drug resistance in Africa: Meta-analysis of reported dihydrofolate reductase (dhfr) and dihydropteroate synthase (dhps) mutant genotype frequencies in African Plasmodium falciparum parasite populations. Malar J. 2010;9(1):1-22. doi:10.1186/1475-2875-9-247

Burrows JN, Duparc S, Gutteridge WE, Hooft van Huijsduijnen R, Kaszubska W, Macintyre F, Mazzuri S, Möhrle JJ, Wells TNC. New developments in anti-malarial target candidate and product profiles. Malar J. 2017;16(1):26. doi:10.1186/s12936-016-1675-x

Palmer, MJ. and Wells T, ed. Neglected Disases and Drug Discovery. Cambridge, UK: Royal Society of Chmistry 2012; 2012.

Baragaña B, Hallyburton I, Lee MCS, Norcross NR, Grimaldi R, Otto TD, Proto WR, Blagborough AM, Meister S, Wirjanata G, Ruecker A, Upton LM, Abraham TS, Almeida MJ, Pradhan A, Porzelle A, Martínez MS, Bolscher

JM, Woodland A, Norval S, Zuccotto F, Thomas J, Simeons F, Stojanovski L, Osuna-Cabello M, Brock PM, Churcher TS, Sala KA, Zakutansky SE, Jiménez-Díaz MB, Sanz LM, Riley J, Basak R, Campbell M, Avery VM, Sauerwein RW, Dechering KJ, Noviyanti R, Campo B, Frearson JA, Angulo-Barturen I, Ferrer-Bazaga S, Gamo FJ, Wyatt PG, Leroy D, Siegl P, Delves MJ, Kyle DE, Wittlin S, Marfurt J, Price RN, Sinden RE, Winzeler EA, Charman SA, Bebrevska L, Gray DW, Campbell S, Fairlamb AH, Willis PA, Rayner JC, Fidock DA, Read KD, Gilbert IH. A novel multiple-stage antimalarial agent that inhibits protein synthesis. Nature. 2015;522(7556):315-320. doi:10.1038/nature14451

Okombo J, Chibale K. Insights into Integrated Lead Generation and Target Identification in Malaria and Tuberculosis Drug Discovery. Acc Chem Res. 2017;50(7):1606-1616. doi:10.1021/acs.accounts.6b00631

Dembélé L, Franetich J, Lorthiois A, Gego A, Zeeman A, Kocken CHM, Le Grand R, Dereuddre-Bosquet N, van Gemert G, Sauerwein R, Vaillant J, Hannoun L, Fuchter MJ, Diagana TT, Malmquist NA, Scherf A, Snounou G, Mazier D. Persistence and activation of malaria hypnozoites in long-term primary hepatocyte cultures. Nat Med. 2014;20(3):307-312. doi:10.1038/nm.3461

March S, Ng S, Velmurugan S, Galstian A, Shan J, Logan DJ, Carpenter AE, Thomas D, Sim BKL, Mota MM, Hoffman SL, Bhatia SN. A microscale human liver platform that supports the hepatic stages of plasmodium falciparum and vivax. Cell Host Microbe. 2013;14(1):104-115. doi:10.1016/j.chom.2013.06.005

Gural N, Mancio-Silva L, Miller AB, Galstian A, Butty VL, Levine SS, Patrapuvich R, Desai SP, Mikolajczak SA, Kappe SHI, Fleming HE, March S, Sattabongkot J, Bhatia SN. In Vitro Culture, Drug Sensitivity, and Transcriptome of Plasmodium Vivax Hypnozoites. Cell Host Microbe. 2018;23(3):395-406.e4. doi:10.1016/j.chom.2018.01.002

Roth A, Maher SP, Conway AJ, Ubalee R, Chaumeau V, Andolina C, Kaba SA, Vantaux A, Bakowski MA, Luque RT, Adapa SR, Singh N, Barnes SJ, Cooper CA, Rouillier M, McNamara CW, Mikolajczak SA, Sather N,

Witkowski B, Campo B, Kappe SHI, Lanar DE, Nosten F, Davidson S, Jiang RHY, Kyle DE, Adams JH. A comprehensive model for assessment of liver stage therapies targeting Plasmodium vivax and Plasmodium falciparum. Nat Commun. 2018;9(1). doi:10.1038/s41467-018-04221-9

Hoffmaster KA, Turncliff RZ, LeCluyse EL, Kim RB, Meier PJ, Brouwer KLR. P-glycoprotein expression, localization, and function in sandwich-cultured primary rat and human hepatocytes: relevance to the hepatobiliary disposition of a model opioid peptide. Pharm Res. 2004;21(7):1294-1302. http://www.ncbi.nlm.nih.gov/pubmed/15290872.

Khetani SR, Bhatia SN. Microscale culture of human liver cells for drug development. Nat Biotechnol. 2008;26(1):120-126. doi:10.1038/nbt1361

Dunn JCY, Tompkins RG, Yarmush ML. Hepatocytes in collagen sandwich: Evidence for transcriptional and translational regulation. J Cell Biol. 1992;116(4):1043-1053. doi:10.1083/jcb.116.4.1043

Zeigerer A, Wuttke A, Marsico G, Seifert S, Kalaidzidis Y, Zerial M. Functional properties of hepatocytes in vitro are correlated with cell polarity maintenance. Exp Cell Res. 2017;350(1):242-252. doi:10.1016/j.yexcr.2016.11.027

Rebelo SP, Costa R, Estrada M, Shevchenko V, Brito C, Alves PM. HepaRG microencapsulated spheroids in DMSO-free culture: novel culturing approaches for enhanced xenobiotic and biosynthetic metabolism. Arch Toxicol. 2014;89(July):1347-1358. doi:10.1007/s00204-014-1320-9

Gunness P, Mueller D, Shevchenko V, Heinzle E, Ingelman-Sundberg M, Noor F. 3D organotypic cultures of human heparg cells: A tool for in vitro toxicity studies. Toxicol Sci. 2013;133(1):67-78. doi:10.1093/toxsci/kft021

Chang TT, Hughes-Fulford M. Monolayer and Spheroid Culture of Human Liver Hepatocellular Carcinoma Cell Line Cells Demonstrate Distinct Global Gene Expression Patterns and Functional Phenotypes. Tissue Eng Part A. 2009;15(3):559-567. doi:10.1089/ten.tea.2007.0434

Gaskell H, Sharma P, Colley HE, Murdoch C, Williams DP, Webb SD. Characterization of a functional C3A liver spheroid model. Toxicol Res (Camb). 2016;5(4):1053-1065. doi:10.1039/c6tx00101g

Gerets HHJ, Tilmant K, Gerin B, Chanteux H, Depelchin BO, Dhalluin S, Atienzar FA. Characterization of primary human hepatocytes, HepG2 cells, and HepaRG cells at the mRNA level and CYP activity in response to inducers and their predictivity for the detection of human hepatotoxins. Cell Biol Toxicol. 2012;28(2):69-87. doi:10.1007/s10565-011-9208-4

Ramaiahgari SC, Den Braver MW, Herpers B, Terpstra V, Commandeur JNM, Van De Water B, Price LS. A 3D in vitro model of differentiated HepG2 cell spheroids with improved liver-like properties for repeated dose high-throughput toxicity studies. Arch Toxicol. 2014;88(5):1083-1095. doi:10.1007/s00204-014-1215-9

Leite SB, Wilk-Zasadna I, Zaldivar JM, Airola E, Reis-Fernandes MA, Mennecozzi M, Guguen-Guillouzo C, Chesne C, Guillou C, Alves PM, Coecke S. Three-dimensional HepaRG model as an attractive tool for toxicity testing. Toxicol Sci. 2012;130(1):106-116. doi:10.1093/toxsci/kfs232

Ramaiahgari SC, Waidyanatha S, Dixon D, DeVito MJ, Paules RS, Ferguson SS. Three-dimensional (3D) HepaRG spheroid model with physiologically relevant xenobiotic metabolism competence and hepatocyte functionality for liver toxicity screening. Toxicol Sci. 2017;159(1):124-136. doi:10.1093/toxsci/kfx122

Tostões RM, Leite SB, Serra M, Jensen J, Björquist P, Carrondo MJT, Brito C, Alves PM. Human liver cell spheroids in extended perfusion bioreactor culture for repeated-dose drug testing. Hepatology. 2012;55:1227-1236. doi:10.1002/hep.24760

Rebelo SP, Costa R, Silva MM, Marcelino P, Brito C, Alves PM. Three-dimensional co-culture of human hepatocytes and mesenchymal stem cells: improved functionality in long-term bioreactor cultures. J Tissue Eng Regen Med. 2017;11(7):2034-2045. doi:10.1002/term.2099

Serra M, Brito C, Correia C, Alves PM. Process engineering of human pluripotent stem cells for clinical application. Trends Biotechnol. 2012;30(6):350-359. doi:10.1016/j.tibtech.2012.03.003

Santo VE, Estrada MF, Rebelo SP, Abreu S, Silva I, Pinto C, Veloso SC, Serra AT, Boghaert E, Alves PM, Brito C. Adaptable stirred-tank culture strategies for large scale production of multicellular spheroid-based tumor cell models. J Biotechnol. 2016;221:118-129. doi:10.1016/j.jbiotec.2016.01.031

Sattabongkot J, Yimamnuaychoke N, Leelaudomlipi S, Rasameesoraj M, Jenwithisuk R, Coleman RE, Udomsangpetch R, Cui L, Brewer TG. Establishment of a human hepatocyte line that supports in vitro development of the exo-erythrocytic stages of the malaria parasites Plasmodium falciparum and P. vivax. Am J Trop Med Hyg. 2006;74(5):708-715. doi:74/5/708 [pii]

Prudêncio M, Mota MM, Mendes AM. A toolbox to study liver stage malaria. Trends Parasitol. 2011;27(12):565-574. doi:10.1016/j.pt.2011.09.004

Prudêncio M, Rodrigues CD, Ataíde R, Mota MM. Dissecting in vitro host cell infection by Plasmodium sporozoites using flow cytometry. Cell Microbiol. 2007;10(August 2007):070816152918001-??? doi:10.1111/j.1462-5822.2007.01032.x

Mueller A-K, Camargo N, Kaiser K, Andorfer C, Frevert U, Matuschewski K, Kappe SHI. Plasmodium liver stage developmental arrest by depletion of a protein at the parasite-host interface. Proc Natl Acad Sci U S A. 2005;102(8):3022-3027. doi:10.1073/pnas.0408442102

Aly HH, Shimotohno K, Hijikata M. 3D cultured immortalized human hepatocytes useful to develop drugs for blood-borne HCV. Biochem Biophys Res Commun. 2009;379(2):330-334. doi:10.1016/j.bbrc.2008.12.054

Molina-Jimenez F, Benedicto I, Dao Thi VL, Gondar V, Lavillette D, Marin JJ, Briz O, Moreno-Otero R, Aldabe R, Baumert TF, Cosset F, Lopez-Cabrera M, Majano P. Matrigel-embedded 3D culture of Huh-7 cells as a

hepatocyte-like polarized system to study hepatitis C virus cycle. Virology. 2012;425(1):31-39. doi:10.1016/J.VIROL.2011.12.021

Sainz B, TenCate V, Uprichard SL. Three-dimensional Huh7 cell culture system for the study of Hepatitis C virus infection. Virol J. 2009;6(1):103. doi:10.1186/1743-422X-6-103

Ploemen IHJ, Prudêncio M, Douradinha BG, Ramesar J, Fonager J, Van Gemert G, Jan L, Adrian JF, Hermsen CC, Sauerwein RW, Baptista FG, Mota MM, Waters AP, Que I, Lowik CWGM, Khan SM, Janse CJ, Franke-Fayard BMD. Visualisation and quantitative analysis of the rodent malaria liver stage by real time imaging. PLoS One. 2009;4(11):1-12. doi:10.1371/journal.pone.0007881

Risco-Castillo V, Topçu S, Marinach C, Manzoni G, Bigorgne AE, Briquet S, Baudin X, Lebrun M, Dubremetz J, Silvie O. Malaria sporozoites traverse host cells within transient vacuoles. Cell Host Microbe. 2015;18:593-603. doi:10.1016/j.chom.2015.10.006

Dumoulin PC, Trop S a., Ma J, Zhang H, Sherman M a., Levitskaya J. Flow cytometry based detection and isolation of Plasmodium falciparum liver stages in vitro. PLoS One. 2015;10:1-24. doi:10.1371/journal.pone.0129623

Gripon P, Rumin S, Urban S, Le Seyec J, Glaise D, Cannie I, Guyomard C, Lucas J, Trepo C, Guguen-Guillouzo C. Infection of a human hepatoma cell line by hepatitis B virus. Proc Natl Acad Sci U S A. 2002;99(24):15655-15660. doi:10.1073/pnas.232137699

Machado M, Sanches-Vaz M, Cruz JP, Mendes AM, Prudêncio M. Inhibition of Plasmodium Hepatic Infection by Antiretroviral Compounds. Front Cell Infect Microbiol. 2017;7(July):1-9. doi:10.3389/fcimb.2017.00329

Estrada MF, Rebelo SP, Davies EJ, Pinto MT, Pereira H, Santo VE, Smalley MJ, Barry ST, Gualda EJ, Alves PM, Anderson E, Brito C. Modelling the tumour microenvironment in long-term microencapsulated

3D co-cultures recapitulates phenotypic features of disease progression. Biomaterials. 2015;78:50-61. doi:10.1016/j.biomaterials.2015.11.030

Rueden CT, Schindelin J, Hiner MC, DeZonia BE, Walter AE, Arena ET, Eliceiri KW. ImageJ2: ImageJ for the next generation of scientific image data. BMC Bioinformatics. 2017;18(1):529. doi:10.1186/s12859-017-1934-z

Russell BM, Udomsangpetch R, Rieckmann KH, Kotecka BM, Coleman RE, Sattabongkot J. Simple In Vitro Assay for Determining the Sensitivity of. Antimicrob Agents Chemother. 2003;47(1):170-173. doi:10.1128/AAC.47.1.170

Chapter III

Pre-erythrocytic activity of M5717 in monotherapy and combination in preclinical *Plasmodium* infection models

This chapter was adapted from:

Fontinha D.*, Arez F.*, Ramella IG., Nogueira G., Moita D., Baeurle THH., Brito C., Spangenberg T., Alves PM., Prudêncio M., (2021) Pre-erythrocytic Activity of M5717 in Monotherapy and Combination in Preclinical Plasmodium Infection Models. ACS Infectious Diseases. DOI: 10.1021/acsinfecdis.1c00640 M,

Conceptualization: D.F., F.A., T.S., C.B., M.P., P.M.A.
Methodology: D.F., F.A., I.R.G., G.N., D.M., T.H.H.B.,
Formal analysis: D.F., F.A., I.R.G., T.H.H.B., C.B., M.P.
Writing – original draft: D.F., F.A.,
Writing – review and editing: T.S., C.B., M.P., P.M.A.
Funding acquisition: T.S., M.P., P.M.A.
Supervision: T.S., C.B., M.P., P.M.A.

Table of contents

Abstract

Combination therapies have emerged to mitigate *Plasmodium* drug resistance, which has hampered the combat against malaria. M5717 is a potent multi-stage anti-plasmodial drug under clinical development, which inhibits parasite protein synthesis. The combination of M5717 with pyronaridine, an inhibitor of hemozoin formation, displays potent activity against blood-stage *Plasmodium* infection. However, the impact of this therapy on liver *Plasmodium* infection remains unknown. Here, we employed a recently described 3D culture-based hepatic infection platform, to evaluate the activity of the M5717-pyronaridine combination against the hepatic infection by *P. berghei*. This effect was further confirmed *in vivo*, employing the C57BL/6J rodent *Plasmodium* infection model. Collectively, our data demonstrate that pyronaridine potentiates the activity of M5717 against *P. berghei* hepatic development. These preclinical results contribute to the validation of pyronaridine as a suitable partner drug for M5717, supporting the clinical evaluation of this novel anti-plasmodial combination therapy.

Keywords: Pyronaridine, M5717, combination therapy, liver stage infection, malaria, drug discovery.

Introduction

In 2020 alone, malaria was responsible for more than six hundred thousand deaths worldwide, resulting from over two hundred million infections by *Plasmodium* parasites, the causative agents of disease. The burden of malaria is mostly felt in the African region and primarily affects children under the age of 5 (WHO, 2021).

Plasmodium parasites, of which *P. falciparum* is the deadliest to humans, cycle between a mammalian host and an insect vector. An obligatory and clinically silent pre-erythrocytic stage of *Plasmodium* infection takes place in the host's liver cells (Lindner, Miller, & Kappe, 2012; Prudencio, Rodriguez, & Mota, 2006), where the parasite develops within a parasitophorous vacuole, giving rise to thousands of red blood cell-infectious merozoites (Lindner et al., 2012; Prudencio et al., 2006), leading to the erythrocytic stage of infection. The latter is responsible for the clinical manifestations of malaria (White et al., 2014), and for the transmission to the mosquito vector upon ingestion of gametocytes during a blood meal (Meibalan, Marti, & 2017).

Most pharmacological approaches against malaria focus on the clinically relevant erythrocytic stage of infection. However, the obligatorily nature of the pre-erythrocytic stage of the parasite's life cycle provides an appealing opportunity for prophylaxis (Prudencio et al., 2006). Only few drugs target the hepatic stage of infection, a scarcity that can be explained by the constraints in experimental access to sporozoites and the lack of drug screening models that faithfully recapitulate the liver microenvironment. We have recently established a 3D infection platform, employing spheroids of human hepatic cell lines that maintain a stable hepatic phenotype over the course of four weeks and enables the evaluation of drugs against hepatic infection by the rodent *P. berghei* parasite, in either static or dynamic culture conditions (Arez et al., 2019).

M5717, or DDD107498, a drug candidate under clinical development, was shown to inhibit protein synthesis by targeting *P. falciparum*'s translation elongation factor 2 (eEF2) (Baragaña et al., 2015). In preclinical studies, M5717 displayed nanomolar-ranged activity across the life cycle of *Plasmodium* parasites, including blocking of transmission. The anti-pre-erythrocytic activity of M5717 against *P. yoelii* and *P. berghei* infection was also demonstrated *in vitro* (Arez et al., 2019; Baragaña et al., 2015). Employing our *in vitro* platform, we estimated a 10 nM minimum inhibitory concentration of M5717, when administered during the hepatic development of *Plasmodium* (Arez et al., 2019). This observation correlated with the plasma concentration that cleared liver stage *P. berghei* infection *in vivo* when M5717 was administrated as radical cure (Arez et al., 2019) or as prophylactic treatment, prior to infection (Baragaña et al., 2015). M5717's novel mechanism of action, potent multistage anti-plasmodial activity and long plasma half-life make it a promising candidate for the treatment and prevention of malaria (McCarthy et al., 2021). Since generation of resistance to M5717 was identified in preclinical studies (Baragaña et al., 2015), suitable partner drugs have been sought. Pyronaridine, a hemozoin formation inhibitor (Croft et al., 2012; Zheng, Chen, Gao, Zhu, & Guo, 1982; Zheng, Xia, Gao, & Chen, 1979), was identified as a suitable combination partner for M5717 in a mouse model of human malaria (Rottmann et al., 2020). No detrimental pharmacokinetic interactions were observed between the two drugs, and M5717 did not impact the killing rate of pyronaridine. Moreover, the latter cleared M5717-related resistance and delayed parasite recrudescence (Rottmann et al., 2020). The effectiveness of the combination of M5717 and pyronaridine against pre-erythrocytic stage parasites remains unknown.

In this work, we assessed the impact of M5717 combination with pyronaridine on the pre-erythrocytic stage of the malaria parasite's life cycle, employing preclinical models of *Plasmodium berghei* infection. We show that pyronaridine is not detrimental to the pre-erythrocytic activity of M5717, rather potentiating its activity against *P. berghei* hepatic infection *in vitro* and *in vivo*. Altogether, our results support the selection of pyronaridine as a suitable partner drug for M5717.

Materials and Methods

Ethics statement

Animal experiments carried out at Instituto de Medicina Molecular João Lobo Antunes (iMM JLA, Lisbon, Portugal) were performed in strict compliance with the guidelines of the institute's animal ethics committee (ORBEA), which also approved the study, and the Federation of European Laboratory Animal Science Associations (FELASA). Animal experiments carried out at the Swiss Tropical and Public Health Institute (Swiss TPH, Basel, Switzerland) were in agreement with local and national regulations of laboratory animal welfare in Switzerland (awarded permission no. 2693). Protocols were regularly reviewed and revised following approval by the local authority (Veterinäramt Basel Stadt).

Mice, cell sources and parasites

Male C57BL/6J mice (Charles River Laboratories), 7 to 12 weeks old, were housed in specific pathogen-free (SPF) conditions at iMM JLA's rodent facility. Female NMRI mice (Charles River laboratories), with 20-22 g of body weight were housed and manipulated in Swiss TPH's animal facility. The in vitro studies were performed employing the HepG2 cell line purchased from ATCC (CRL/10741). Infection procedures were performed employing sporozoites recovered from infected *Anopheles stephensi* mosquitoes, reared and maintained in the

insectarium facilities of iMM JLA and of Swiss TPH. Uninfected mosquitoes were allowed to feed on mice infected by *P. berghei* (*Pb*) ANKA expressing luciferase (Luc). Sporozoites were freshly isolated from mosquito's salivary glands into RPMI 1640 medium (Thermo Fisher Scientific) or phosphate-buffered saline (PBS), macerated and filtered through a 40 µm cell strainer prior to infection experiments.

Two-dimensional (2D) cell culture

HepG2 2D cultures were maintained in T-flasks in static conditions, as previously described (Arez et al., 2019). Briefly, HepG2 cells were cultured in low glucose DMEM (Thermo Fisher Scientific) supplemented with 1 % (v/v) pen/strep and 10 % (v/v) FBS. Cells were passaged twice every week at a cell inoculum of $5x10^4$ cell/cm^2. Cells were maintained in an incubator with humidified environment, at 37 °C and 5 % CO_2.

Three-dimensional (3D) Cell culture (Spheroids)

Hepatic cell spheroids were generated and maintained in dynamic suspensions agitated by magnetic stirrers (2mag AG) in an incubator with humidified environment at 37 °C and 5 % CO_2. HepG2 cells were inoculated as monocultures in 125 mL spinners (Corning®, Merck KGaA, Darmstadt, Germany). Single cell suspensions of $3x10^5$ cell/mL were inoculated into the spinners, in the culture medium employed for the 2D cell culture. HepG2 3D cultures started at an agitation rate of 40 rpm, and reached up to 120 rpm by the end of culture time. Medium replacement was performed in order to attain 100 % medium renovation *per* week. Therefore, 50 % of the culture medium was replaced every three days. To this end, spheroids were sedimented by centrifugation, followed by pellet resuspension in the adequate proportion of pre-existent and fresh culture medium supplemented with 5 % (v/v) FBS.

Determination of cell viability and concentration

Cell viability of spheroid cultures was assessed as previously described (Arez et al. 2019). Briefly, spheroids were incubated with a cell permeant dye (fluorescein diacetate, Sigma-Aldrich, Merck KGaA, Darmstadt, Germany) at 10 µg/mL and a DNA dye (TO-PRO™-3 Iodide,Thermo Fisher Scientific) at 1 µM for detection of viable and dead cells, respectively. Spheroids visual inspection was performed using an inverted fluorescence microscope (Leica DMI6000). Cell density of 2D and 3D cultures was determined by the Trypan blue exclusion method, as previously described (Rebelo et al., 2014).

***In vitro Plasmodium* infection**

Spheroids were inoculated at $5x10^5$ cell/mL in infection medium (basal culture medium supplemented with 5 % (v/v) FBS, 1:300 Amphotericin B (250 µg/mL) and 1:1000 Gentamycin 50 mg/mL, all from Thermo Fisher Scientific), on the day of infection, in ultra-low attachment flat bottom 96-well plates (Corning®, Merck KGaA, Darmstadt, Germany). Sporozoites were added to 3D cultures at a 1:2 cell:spz ratio. Sporozoite addition in microplates was followed by a centrifugation step at 1800 *xg* for 5 min, after which plates were maintained in static conditions at 37 ºC and 5 % CO_2 for 48 h. The infection rates were assessed by bioluminescence, as a measurement of luciferase activity.

***In vitro* assessment of *Plasmodium* infection by bioluminescence**

Infection load of *Pb*-Luc-infected cells was assessed employing a commercially available Firefly Luciferase Assay Kit from Biotium, following the manufacturer's instructions. Briefly, cells and spheroids were washed twice with PBS, and later incubated in lysis buffer diluted 1:4 in Milli-Q water. Samples underwent several freeze-thaw cycles, alternated with agitation steps at 500 rpm, until complete cell lysis was

confirmed by visual inspection. Bioluminescence was measured using a microplate reader (Infinite® 200 PRO, Tecan Trading AG) and the light reaction of each well was measured for 100 ms.

Drug assays

M5717 and pyronaridine (pyro) were synthetized and supplied by Merck KGaA, Darmstadt, Germany.

In vitro drug assays

Stock solutions of 10 mM were prepared in DMSO. Working solutions of compounds employed in drug assays were prepared freshly at concentrations ranging from 0.01 to 30 nM for M5717 or at a fixed concentration of 1 µM for pyro. *Pb*-infected cells were exposed to the aforementioned drug dilutions at 24 hpi and cultured for an additional 24 h. For the dose-response analysis, cell viability and infection rate were assessed at the end of the drug incubation period (48 hpi), as previously described (Arez, et al., 2019). Briefly, cell metabolic activity was determined by incubation of adherent cells and spheroids for 50 min at 37 ºC, protected from light, with PrestoBlue™ Cell Viability Reagent (A-13262, Thermo Fisher Scientific) 1X. The fluorescence of the culture supernatant was measured at 560 nm and 590 nm excitation and emission wavelengths, respectively. Cell metabolic activity was used as a measurement of cell viability and employed in the normalization of the infection rates. Samples were further analyzed for bioluminescence as described above.

In vivo drug assays

Male C57BL/6J mice were infected by intravenous injection (I.V.) of $3x10^4$ firefly luciferase-expressing *P. berghei* sporozoites. Hepatic infection was confirmed at 24 hpi by live bioluminescence, prior to

compound administration, as previously described (Ploemen et al., 2009). Briefly, mice were anesthetized with isofluorane and subcutaneously injected with 200 µL of D-Luciferin (PerkinElmer) dissolved in PBS (10 mg/mL). After 5 min, mice were anesthetized by intraperitoneal injection of a Ketamine/Xylazine solution. Image acquisition took place at approximately 10 min after D-Luciferin injection, employing the in vivo IVIS Lumina Imaging System (Caliper LifeSciences, Waltham, MA, USA). *P. berghei* bioluminescence was measured as total flux (photons/s) and analyzed with the Living Image software (version 3.0, PerkinElmer, Waltham, MA, USA). Compounds were solubilized in a solution of 70% Tween-80 and 30% ethanol, followed by a ten-fold dilution in water, and administered by oral gavage at 24 hpi. M5717 was administered at 0.4 or 0.3 mg/kg of mouse weight, whereas pyronaridine was administered at 12 mg/kg. An equivalent amount of drug vehicle was administered as a control. At 48 hpi, mice were sacrificed and livers were collected to denaturing solution (4 M guanidine thiocyanate, 25 mM sodium citrate pH 7.0, 0.5% (w/v) sarcosyl and 0.7% (v/v) ß-mercaptoethanol in DEPC-treated water) for parasite load quantification by quantitative real-time PCR (RT-qPCR). Liver samples were then mechanically homogenized and RNA was extracted using the TripleXtractor directRNA Kit (GRiSP), according to the manufacturer's recommendations. Complementary DNA (cDNA) was synthesized from 1 µg of RNA, using the NZY First-strand cDNA Synthesis Kit (NZYTech). *P. berghei* load was quantified by RT-qPCR, employing primers specific for *Pb* 18S RNA (5′-AAGCATTAAATAAAGCGAATACATCCTTAC-3′ and 5′-GGAGATTGGTTTTGACGTTTATGTG-3′). Gene expression levels were normalized to the endogenous mouse housekeeping gene hypoxanthine-guanine phosphoribosyltransferase (Hprt) (primers 5′-TTTGCTGACCTGCTGGATTAC-3′ and 5′-CAAGACATTCTTTCCAGTTAAAGTTG-3′). The RT-qPCR reaction

was performed in a total volume of 10 µL using the NZYSpeedy qPCR Green, ROX (NZYtech), employing the ViiA 7 System (Applied Biosystems). The comparative ΔΔCT method was used for analysis of RT-qPCR.

Data analysis and statistics

Non-linear regression analysis of the normalized results for the determination of IC50 values and statistical analysis were performed employing GraphPad Prism version 6 for Windows (GraphPad software, La Jolla California USA). Outliers were identified by the ROUT method. Normality was assessed by the Shapiro-Wilk normality test. Significant differences were determined using a parametric or non-parametric t-test, considering paired conditions when subjected to the same batch of spz, or using one-way ANOVA. P values are presented for statistically significant results (*, $P < 0.05$, **, $P<0.01$, *** $P<0.001$, ****$P<0.0001$), as indicated in each figure legend.

Results

Pre-erythrocytic activity of the M5717-pyronaridine combination

As an hemozoin inhibitor, pyronaridine is not expected to possess liver stage anti-plasmodial activity. However, drug-drug interactions are an important aspect in the development of new combination therapies. Therefore, the effect of the M5717-Pyro combination against the pre-erythrocytic stage of *Plasmodium* infection was compared to that of M5717 in monotherapy, employing luciferase-expressing *P. berghei* (*Pb*-Luc).

In vitro drug activity was assessed in HepG2 spheroids, as previously established and validated for drug evaluation purposes (Figure III.1A) (Arez et al., 2019).

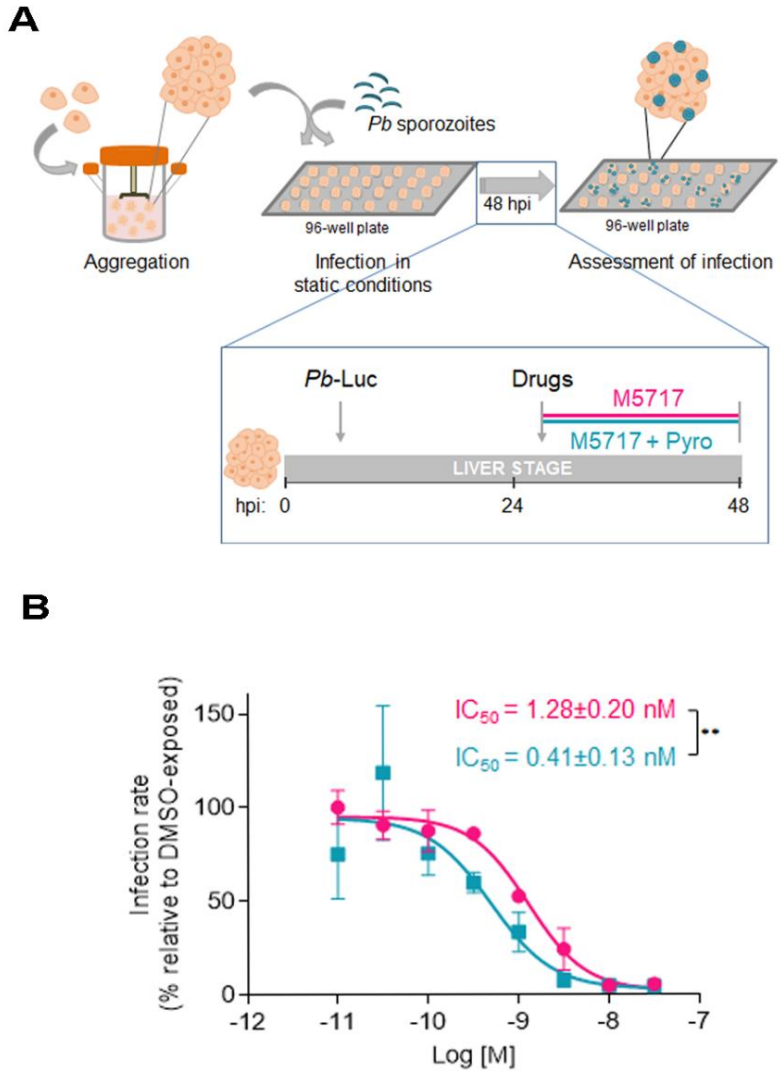

Figure III. 1- *In vitro* assessment of the pre-erythrocytic activity of M5717-Pyro combination in *Pb*-infected HepG2 spheroids. **A)** Schematic representation of the static infection platform employing HepG2 spheroids and *Pb*-Luc sporozoites (not at scale) and the drug exposure mode used for IC50 determination. **B)** Dose-response curves and IC50 determination of M5717 (pink) and M5717-pyro combination (M5717 + Pyro, blue). Cells were plated at a density of $2.5x10^4$ cell/well and infected at a cell:spz ratio of 1:2. Infection rate was normalized to that of DMSO-exposed spheroids and results are

represented as the mean ± SD of at least three independent experiments. Statistical analysis was performed using an unpaired t-test. ** P ≤ 0.01

A range of eight concentrations of M5717, employed in monotherapy or combined with a fixed dose of 1 µM of Pyro, was added to *Pb*-Luc-infected HepG2 spheroids at 24 h post infection (hpi) (Figure III.1A). Twenty-four h later, at 48 hpi, the impact of each drug concentration on the infection rate was assessed by bioluminescence and the half-maximal inhibitory concentration (IC50) of M5717 alone or in combination with Pyro was determined (Figure III.1B). The IC50 of M5717 (1.3±0.2 nM) was in agreement to what had been previously determined in this platform (Arez et al., 2019). The addition of 1 µM of Pyro resulted in a statistically significant 3-fold reduction of the IC50 of M5717 (0.4±0.1 nM). Importantly, no dose-dependent toxicity towards the host cell was noted, as observed by the percentage of cell viability, which was relatively constant across the experimental conditions tested (Figure III.S1).

Next, the difference between the impact of the administration of M5717 alone or in combination with Pyro observed *in vitro* was confirmed *in vivo*, in a rodent model of *P. berghei* infection (Figure III.2).

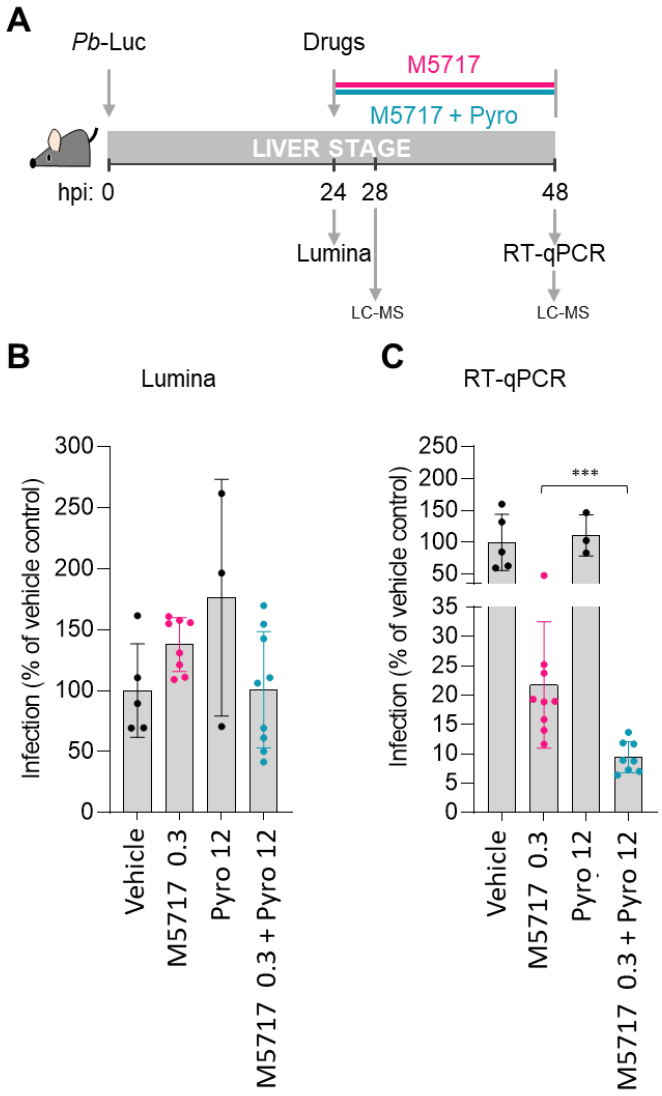

Figure III. 2 - *In vivo* assessment of the pre-erythrocytic activity of M5717-pyronaridine combination. A) Schematic representation of *in vivo* drug administration and analysis of liver infection. C57BL/6J mice were infected with $3x10^4$ *Pb*-Luc sporozoites. At 24 hours post-infection (hpi), the liver load was assessed by live bioluminescence and the drugs of interest were administered. At 48 hpi the impact of M5717 (pink) or M5717-pyronaridine combination (blue) on the liver load of the same mice was evaluated by RT-qPCR analysis. At 28 and 48 hpi, a blood sample was collected for LC-MS analysis. **B)** Assessment of the liver load at 24 hpi by live bioluminescence. **(C)** Assessment of the

infection rate at 48hpi by gene expression analysis (RT-qPCR). Infection (B,C) was normalized to the vehicle-treated control group and results are represented as mean ± SD of three to seven mice from one independent experiment. Statistical analysis of luminescence data was performed by one-way ANOVA, whereas analysis of RT-qPCR data was performed using a Mann-Whitney test. *** $P \leq 0.001$

Mice were injected with *Pb* sporozoites and the success of the liver infection was confirmed by live bioluminescence (Lumina) after 24 h. Drugs were then administered by oral gavage and their impact on the liver load was determined by real time quantitative PCR (RT-qPCR) 24 h later, at 48 hpi (Figure III.2A). A dose of 0.3 mg/kg of M5717 *per* mouse body weight was selected, as it has previously been shown to not abolish infection completely (Arez et al., 2019). Pyro was employed at 12 mg/kg of mouse body weight, a dose previously assessed *in vivo* in combination with M5717, in the context of erythrocytic activity (Rottmann et al., 2020). Mice treated with drug vehicle alone were splayed as controls. Our results show that mice from all experimental groups were similarly infected prior to drug administration (Figure III. 2B and Figure III.S2A). Pharmacokinetic analysis of the blood of the treated mice by liquid chromatography (LC)-mass spectrometry (MS)/MS showed that the plasma concentrations of pyronaridine in monotherapy and in combination with M5717 remained stable throughout the duration of parasite exposure to the drugs, i.e., from 28 to 48 hpi (Table III.S1). Unfortunately, we were unable to quantify M5717 at the selected concentration using this methodology (Table III.S1). Nevertheless, 0.3 mg/kg M5717 drastically reduced infection at 48 hpi to 22 % of that of vehicle-treated mice, while Pyro administered in monotherapy had no impact on the *P. berghei* liver load (Figure III.2C). Importantly, the combination of Pyro with M5717 further reduced infection to 9 %, a 2.3-fold reduction relative to that observed upon administration of M5717

alone (Figure III.2C). A similar decrease was observed when the same dose of Pyro was combined with a slightly higher dose of 0.4 mg/kg of M5717, resulting in a 2.2-fold reduction of infection upon administration of the combination, when compared to administration of M5717 alone (Figure III.S2B).

Collectively, the *in vitro* and *in vivo* assessment of Pyro as a possible drug partner of M5717 against the hepatic stage of infection by *P. berghei* shows not only that the former is not detrimental to the latter, but also that addition of pyronaridine consistently potentiates M5717's anti-plasmodial effect during this phase of the parasite's life cycle.

Discussion

Between 2010 and 2018, the global incidence rate and the number of malaria deaths have declined. However, despite the long lasting struggle to end this infectious disease, this progress is coming to a halt (WHO, 2021). New anti-plasmodial strategies are, therefore, required to accelerate the progress towards the goal of malaria eradication. In a context where a highly desirable effective vaccine against malaria remains unavailable, vector control measures and therapeutics persist as the cornerstone of disease control.

As for other infectious diseases, such as tuberculosis, the treatment of malaria resorts to combination therapies as a means of decreasing the risk of emergence of drug resistance (Nosten & Brasseur, 2002). In the search of a suitable combination partner for a given drug, several aspects need to be taken into consideration, including each drug's mode of action, pharmacokinetic properties, and toxicity (Nosten & Brasseur, 2002). Crucially, combinations should be assessed for drug-drug interactions that may compromise the efficacy of either drug. M5717-resistant *Plasmodium* parasites have been

identified *in vitro* during the preclinical characterization of this drug, highlighting the need to combine it with a suitable partner drug (Baragaña et al., 2015). A second study identified Pyro as an appropriate candidate for combination with M5717, given its different target, faster action, matching half-life, and ability to suppress the selection of M5717-resistant mutants when tested against the asexual erythrocytic stage of the *Plasmodium* life cycle (Rottmann et al., 2020). Importantly, *in vitro* isobologram studies and *in vivo* testing revealed a non-detrimental interaction between both drugs (Rottmann et al., 2020).

Besides its efficacy against asexual blood-stage *Plasmodium* parasites, M5717 is also active against exoerythrocytic parasite forms. Thus, it was important to ensure that its combination with Pyro would not hamper these relevant prophylactic and transmission-blocking activities. Our *in vitro* and *in vivo* observations demonstrate that the combination of M5717 with Pyro does not impair its pre-erythrocytic activity. Interestingly, our results point to a potentiation of this activity, both *in vitro* and *in vivo*. As an inhibitor of hemozoin formation, pyronaridine is not expected to possess liver stage activity. This has been formally demonstrated in an *in vitro* model of *P. yoelii* infection of mouse primary hepatocytes, where infected cells were exposed to pyronaridine throughout the 48 h of hepatic infection (Basco, Ringwald, Franetich, & Mazier, 1999). At nanomolar-range doses (100, 10 and 1 nM), Pyro did not display activity against the parasite's hepatic stages. At higher doses, which included the 1 µM dose employed in this study, Pyro was hepatotoxic, which did not allow the assessment of its impact on the infection rate (Baragaña et al., 2015). In our *in vitro* 3D model, 1 µM pyronaridine did not show hepatotoxicity, as confirmed by different analytical methods (Figure III.S3). Rather, the viability of cell spheroids that were exposed to the M5717-Pyro combination was comparable to that of spheroids that were exposed solely to M5717. The absence of

pre-erythrocytic activity of pyronaridine was further supported by our *in vivo* observations, which show that the administration of this drug to *Pb*-Luc-infected mice has no impact on the ongoing liver infection. Thus, the enhanced pre-erythrocytic activity of the combination is not justified by the addition of the activities of the individual drugs. This type of interaction is not unprecedented, as chloroquine, an anti-plasmodial drug structurally and target related to pyronaridine, has been described to potentiate primaquine's activity against the pre-erythrocytic stage of infection, even though chloroquine has no inhibitory activity of its own (Dembélé et al., 2020). This effect was shown to be specific to this combination, as it was not observed when chloroquine was combined with atovaquone (Dembélé et al., 2020). Interestingly, this potentiation effect was only noted in primary hepatocytes, but not in HepG2-A16 cells, which have reduced cytochrome P450 activities (Dembélé et al., 2020). The fact that we observed the potentiation of M5717's activity *in vitro* using the HepG2 cell line may be related to the enhanced physiological relevance of the 3D hepatic system employed (Gaskell et al., 2016; Leite et al., 2012; Rebelo et al., 2015). Similar to the enhancement of primaquine's activity by chloroquine (Dembélé et al., 2020), the identification of the molecular mechanism underlying the potentiation of M5717's activity by Pyro described in this study requires further experimental work.

An assessment of the effect of a drug combination against the pre-erythrocytic stage of *Plasmodium* infection was first carried out in 2016 for Malarone™ (Barata et al., 2016). This combination of atovaquone and proguanil, employed both for the chemoprevention and the treatment of malaria, was already known to display a synergistic effect against the erythrocytic stage of infection (Canfield, Pudney, & Gutteridge, 1995), and was next demonstrated to also be synergistic against developing hepatic *P. yoelii* parasites, providing a

pharmacological basis for its success in chemoprevention (Barata et al., 2016). Although this study highlighted the importance of widening the evaluation of anti-plasmodial drug combinations against the pre-erythrocytic stage of the parasite's life cycle, the literature on this subject remains rather limited. Other drug combinations have since been evaluated in the pre-erythrocytic context, such as the combination of several antiretroviral drugs (Machado, Sanches-Vaz, Cruz, Mendes, & Prudêncio, 2017) or of metformin with primaquine (Vera et al., 2019) against rodent *Plasmodium* infection, and of ivermectin and chloroquine against *P. cynomolgi* in rhesus macaques (Vanachayangkul et al., 2020). Our study now adds to the scarce information available on the pre-erythrocytic activity of anti-plasmodial drug combinations, and further validates the physiologically relevant 3D *in vitro* hepatic platform to provide data that correlates with the outcome of drug evaluation *in vivo*.

This study identifies Pyro not only as a suitable partner drug for M5717 but also as an enhancer of this drug's activity against the pre-erythrocytic stage of *Plasmodium* infection. Our results demonstrate the added value of this drug combination for malaria chemoprevention, informing the clinical development of this compound, and paving the way for its deployment in the field.

Acknowledgments

We acknowledge Ana Filipa Teixeira and Ana Parreira for mosquito production and infection. This work was funded by the healthcare business of Merck KGaA, Darmstadt, Germany (CrossRef Funder ID: 10.13039/100009945). M.P. is a recipient of a "Concurso de Estímulo ao Emprego Científico" Principal Investigator award of Fundação para a Ciência e Tecnologia, Portugal (FCT), with Ref. N.

CEECIND/03539/2017. D.F. is funded by FCT project CRCNA/BRB/0281/2019. F.A. is recipient of PhD fellowship PD/BD/128371/2017, funded by FCT.

Supplementary Material

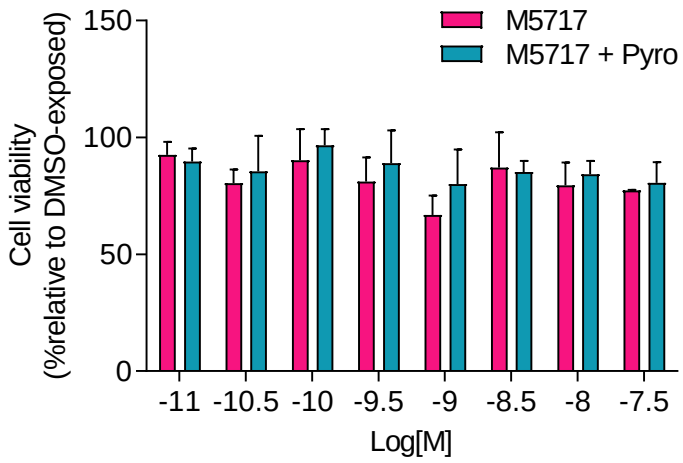

Figure III.S1 - Cell viability of *Pb*-infected HepG2 spheroids exposed to the M5717-pyronaridine combination.

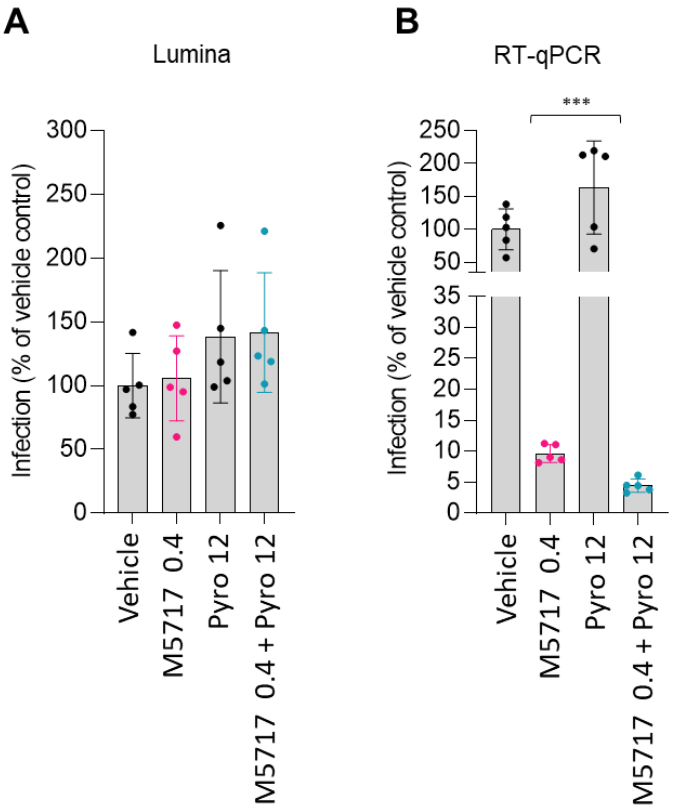

Figure III.S2 - *In vivo* assessment of the pre-erythrocytic activity of M5717-pyronaridine combination.

Table III.S1 - Pharmacokinetic analysis of *P. berghei* blood samples.

Conditions	Time **(hpi)**	M5717 Concentration **(µM)**	Pyr Concentration **(µM)**
Vehicle (n=5)	28	<LLOQ	<LLOQ
Vehicle (n=5)	48	<LLOQ	<LLOQ
M5717 0.3 mg/kg (n=9)	28	<LLOQ	<LLOQ
M5717 0.3 mg/kg (n=9)	48	<LLOQ	<LLOQ
Pyronaridine 12 mg/kg	28	<LLOQ	0.0455 (n=3)
Pyronaridine 12 mg/kg	48	<LLOQ	0.0658±0.0518 (n=3)
M5717 0.3 mg/kg + Pyronaridine 12 mg/kg	28	<LLOQ	0.107±0.11 (n=5) 0.0700±0.09 (n=4)
M5717 0.3 mg/kg + Pyronaridine 12 mg/kg	48	<LLOQ	0.0902±0.08 (n=5) 0.0741±0.08 (n=4)

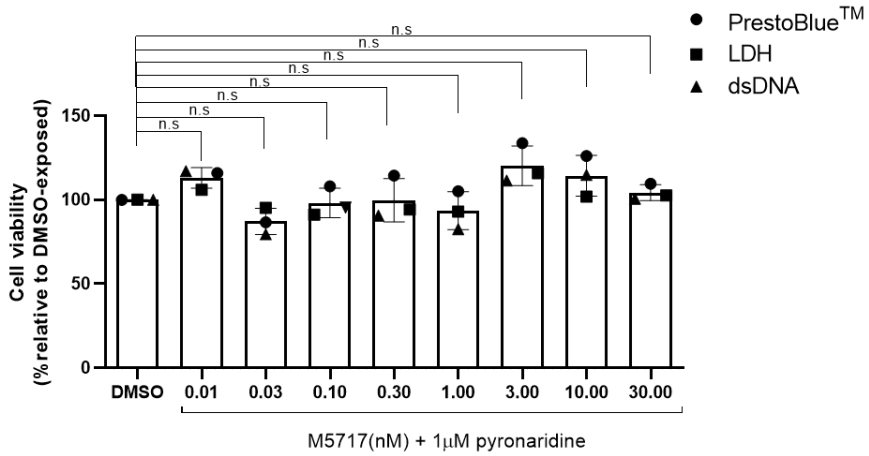

Figure III.S3 - *In vitro* assessment of the hepatotoxicity of pyronaridine 1µM in combination by different analytical methods.

References

Arez, F., Rebelo, S. P., Fontinha, D., Simao, D., Martins, T. R., Machado, M., . . . Alves, P. M. (2019). Flexible 3D Cell-Based Platforms for the Discovery and Profiling of Novel Drugs Targeting Plasmodium Hepatic Infection. ACS Infect Dis, 5(11), 1831-1842. doi:10.1021/acsinfecdis.9b00144

Baragaña, B., Hallyburton, I., Lee, M. C. S., Norcross, N. R., Grimaldi, R., Otto, T. D., . . . Gilbert, I. H. (2015). A novel multiple-stage antimalarial agent that inhibits protein synthesis. Nature, 522(7556), 315-320. doi:10.1038/nature14451

Barata, L., Houzé, P., Boutbibe, K., Zanghi, G., Franetich, J. F., Mazier, D., & Clain, J. (2016). In Vitro Analysis of the Interaction between Atovaquone and Proguanil against Liver Stage Malaria Parasites. Antimicrobial agents and chemotherapy, 60(7), 4333-4335. doi:10.1128/aac.01685-15

Basco, L. K., Ringwald, P., Franetich, J. F., & Mazier, D. (1999). Assessment of pyronaridine activity in vivo and in vitro against the hepatic stages of malaria in laboratory mice. Trans R Soc Trop Med Hyg, 93(6), 651-652. doi:10.1016/s0035-9203(99)90085-8

Canfield, C. J., Pudney, M., & Gutteridge, W. E. (1995). Interactions of Atovaquone with Other Antimalarial Drugs against Plasmodium falciparum in Vitro. Experimental Parasitology, 80(3), 373-381. doi:https://doi.org/10.1006/expr.1995.1049

Croft, S. L., Duparc, S., Arbe-Barnes, S. J., Craft, J. C., Shin, C.-S., Fleckenstein, L., . . . Rim, H.-J. (2012). Review of pyronaridine anti-malarial properties and product characteristics. Malaria journal, 11, 270-270. doi:10.1186/1475-2875-11-270

Dembélé, L., Franetich, J. F., Soulard, V., Amanzougaghene, N., Tajeri, S., Bousema, T., . . . Snounou, G. (2020). Chloroquine Potentiates Primaquine Activity against Active and Latent Hepatic Plasmodia Ex Vivo: Potentials and Pitfalls. Antimicrobial agents and chemotherapy, 65(1). doi:10.1128/aac.01416-20

Gaskell, H., Sharma, P., Colley, H. E., Murdoch, C., Williams, D. P., & Webb, S. D. (2016). Characterization of a functional C3A liver spheroid model. Toxicol Res (Camb), 5(4), 1053-1065. doi:10.1039/c6tx00101g

Leite, S. B., Wilk-Zasadna, I., Zaldivar, J. M., Airola, E., Reis-Fernandes, M. A., Mennecozzi, M., . . . Coecke, S. (2012). Three-dimensional HepaRG model as an attractive tool for toxicity testing. Toxicol Sci, 130(1), 106-116. doi:10.1093/toxsci/kfs232

Lindner, S. E., Miller, J. L., & Kappe, S. H. (2012). Malaria parasite pre-erythrocytic infection: preparation meets opportunity. Cell Microbiol, 14(3), 316-324. doi:10.1111/j.1462-5822.2011.01734.x

Machado, M., Sanches-Vaz, M., Cruz, J. P., Mendes, A. M., & Prudêncio, M. (2017). Inhibition of Plasmodium Hepatic Infection by Antiretroviral Compounds. Frontiers in cellular and infection microbiology, 7, 329-329. doi:10.3389/fcimb.2017.00329

McCarthy, J. S., Yalkinoglu, O., Odedra, A., Webster, R., Oeuvray, C., Tappert, A., . . . Bagchus, W. M. (2021). Safety, pharmacokinetics, and antimalarial activity of the novel plasmodium eukaryotic translation elongation factor 2 inhibitor M5717: a first-in-human, randomised, placebo-controlled, double-blind, single ascending dose study and volunteer infection study. Lancet Infect Dis, 21(12), 1713-1724. doi:10.1016/S1473-3099(21)00252-8

Meibalan, E., Marti, M., & (2017). Biology of malaria transmission. Cold Spring Harb Perspect Med, 7(3), a025452.

Nosten, F., & Brasseur, P. (2002). Combination therapy for malaria: the way forward? Drugs, 62(9), 1315-1329. doi:10.2165/00003495-200262090-00003

Ploemen, I. H., Prudêncio, M., Douradinha, B. G., Ramesar, J., Fonager, J., van Gemert, G. J., . . . Franke-Fayard, B. M. (2009). Visualisation and quantitative analysis of the rodent malaria liver stage by real time imaging. PLoS One, 4(11), e7881. doi:10.1371/journal.pone.0007881

Prudencio, M., Rodriguez, A., & Mota, M. M. (2006). The silent path to thousands of merozoites: the Plasmodium liver stage. Nat Rev Microbiol, 4(11), 849-856. doi:10.1038/nrmicro1529

Rebelo, S. P., Costa, R., Estrada, M., Shevchenko, V., Brito, C., & Alves, P. M. (2015). HepaRG microencapsulated spheroids in DMSO-free culture: novel culturing approaches for enhanced xenobiotic and biosynthetic metabolism. Arch Toxicol, 89(8), 1347-1358. doi:10.1007/s00204-014-1320-9

Rottmann, M., Jonat, B., Gumpp, C., Dhingra, S. K., Giddins, M. J., Yin, X., . . . Spangenberg, T. (2020). Preclinical Antimalarial Combination Study of M5717, a Plasmodium falciparum Elongation Factor 2 Inhibitor, and Pyronaridine, a Hemozoin Formation Inhibitor. Antimicrobial agents and chemotherapy, 64(4), e02181-02119. doi:10.1128/AAC.02181-19

Vanachayangkul, P., Im-Erbsin, R., Tungtaeng, A., Kodchakorn, C., Roth, A., Adams, J., . . . Kobylinski, K. C. (2020). Safety, Pharmacokinetics, and Activity of High-Dose Ivermectin and Chloroquine against the Liver Stage of Plasmodium cynomolgi Infection in Rhesus Macaques. Antimicrobial agents and chemotherapy, 64(9). doi:10.1128/aac.00741-20

Vera, I. M., Grilo Ruivo, M. T., Lemos Rocha, L. F., Marques, S., Bhatia, S. N., Mota, M. M., & Mancio-Silva, L. (2019). Targeting liver stage malaria with metformin. JCI insight, 4(24), e127441. doi:10.1172/jci.insight.127441

White, N. J., Pukrittayakamee, S., Hien, T. T., Faiz, M. A., Mokuolu, O. A., & Dondorp, A. M. (2014). Malaria. Lancet, 383(9918), 723–735.

WHO. (2021). World Malaria Report 2021. Geneva, Switzerland: World Health Organization.

Zheng, X. Y., Chen, C., Gao, F. H., Zhu, P. E., & Guo, H. Z. (1982). [Synthesis of new antimalarial drug pyronaridine and its analogues (author's transl)]. Yao Xue Xue Bao, 17(2), 118-125.

Zheng, X. Y., Xia, Y., Gao, F. H., & Chen, C. (1979). [Synthesis of 7351, a new antimalarial drug (author's transl)]. Yao Xue Xue Bao, 14(12), 736-737.

Chapter IV

Towards a cryopreserved primary human hepatocyte-based 3D infection platform to address hepatotropic pathogens

Author contributions:

The author was involved in the conceptualization and experimental design; was responsible for methodology and analysis of the data generated with primary human hepatocytes and the 3D in vitro cell model (generation, optimization of culture conditions and characterization). The author wrote the original draft, which was reviewed and edited by: Dr Catarina Brito, Dr Thomas Spangenberg, Dr Miguel Prudêncio and Prof Paula M Alves.

Table of contents

Abstract

The species-specific tropism of human *Plasmodium* parasites and the limited metabolic capacity of human hepatic cell lines are the current main hurdles of *in vitro* models for drug discovery targeting the liver-stage of *Plasmodium* infection. Primary human hepatocytes (PHH) are permissive to *P. falciparum* (*Pf*) and *P. vivax (Pv)*, the parasite species more commonly causing malaria, and are the best cell source to predict the human drug response. Nevertheless, PHH are of limited availability and present large variability among donors and commercial sources, which is reflected in PHH yield, viability and plating efficiency. The access to cryopreserved PHH mitigates some of this variability, by extending the availability of cells derived from a single donor and standardizing the operation procedures across several PHH lots.

Our group has previously developed a platform for long-term culture of human and murine hepatocytes in 500 mL stirred-tank bioreactors. In this work, we downscaled to 30 mL stirred-tank vessels and translated to cryopreserved PHH, aiming to reduce the inter-donor variability of this cell source.

The spheroids generated preserved PHH polarization and expression of hepatic-specific proteins, such as the transcription factor HNF-4α, and promoted the deposition of components of the liver microenvironment, such as collagen type I, over the course of 4 weeks of culture. Importantly, in PHH spheroids we detected activity of at least 5 of the 6 isoforms of cytochrome P450, the phase I metabolizing enzymes that are responsible for 90% of xenobiotic metabolism. The capacity to metabolize M5717, an anti-plasmodial drug candidate under clinical development, was also confirmed.

Cryopreserved PHH representing different genetic backgrounds and from different commercial sources were successfully cultured employing the same strategy. The several donors presented similar aggregation profiles, showing the potential of the developed platform to circumvent

some of the inter-donor variability and represent diverse metabolic profiles across the human population. The long-term maintenance of PHH spheroid cultures in a system allowing non-destructive sampling has the potential to assess drug repeated toxicity of anti-plasmodial drugs, and sustain infection of parasites with longer intra-hepatic life cycle, such as of *Pf* and *Pv* schizonts and activation of *Pv* latent forms in the liver, the hypnozoites, that take weeks to months to be activated after the primary infection.

Keywords: primary human hepatocytes, 3D cell models, hepatic spheroids, *in vitro* assays for drug discovery, drug metabolism, liver-stage *Plasmodium* infection, malaria.

Introduction

The liver-stage of the *Plasmodium* infection is considered a promising target to achieve malaria radical cure (Prudêncio et al. 2011). This is the first stage of *Plasmodium* life cycle in the mammalian host, which is obligatory and precedes the blood stage associated to the clinical symptoms. The liver is also the reservoir of hypnozoites, latent forms of the parasite (Prudêncio et al. 2011). Nevertheless, few available therapies are effective against the liver-stage of the *Plasmodium* infection, hypnozoites evade the therapeutic action of most anti-plasmodial drugs, and *P. falciparum* (*Pf*) and *P. vivax* (*Pv*) resistant strains have been reported for most of the drugs (reviewed by Raphemot et al. 2016).

The species-specific tropism of human *Plasmodium* parasites and the scarcity of human *in vitro* models of the liver-stage of the infection are the current main hurdles in drug discovery targeting the liver-stage of the infection. To mitigate these bottlenecks, we and others have proposed micropatterned cultures of PHH and stromal cells (March et al. 2013), spheroid-based cultures of human hepatic cell lines (Arez et al. 2019), and scaffold-based spheroids of primary monkey hepatocytes (Chua et al. 2019). These platforms showed predictive potential in the assessment of the pre-erythrocytic activity against liver-stage developing parasites, using standard-of-care drugs as a proof-of-concept. The platforms were employed to study exploratory drugs (Chua et al. 2019), as well as drug candidates under clinical development (Arez et al. 2019; Fontinha et al. 2022). Despite promising, all infection spheroid models proposed so far employed *Plasmodium* surrogate species, which may differ from the human infectious *Plasmodium* species in their response to drug candidates with novel modes of action and metabolization requirements. Importantly, the hepatic cell sources explored are not fully recapitulative of the human drug response. The

poor drug metabolism capacity of hepatic cell lines restricts their use in drug discovery (Gerets et al. 2012; Ramaiahgari et al. 2017), and even for PHH, the expression and activity of the phase I Cytochrome P450 (CYP450) are down-regulated during *in vitro* monolayer cultures (2D cultures). An additional limitation of hepatic cell lines is their restricted permissiveness to infectious pathogens, as it is the case of the human infectious *Plasmodium* species *Pf* and *Pv* (Prudêncio et al. 2011). These *Plasmodium* species present tropism for mature human primary hepatocytes *in vitro*, with few human hepatoma derived cell lines supporting the development of human infectious *Plasmodium* sporozoites beyond the uninucleate stage (Sattabongkot et al. 2006; Dumoulin et al. 2015). The few cell lines that sustain the complete development of sporozoites into blood-infective merozoites present very low infection rates, ranging from approximately 0.009 to 0.06% (Karnasuta et al. 1995; Sattabongkot et al. 2006; Chattopadhyay et al. 2010; Dumoulin et al. 2015). These low infection rates are a bottleneck shared with 2D *in vitro* cultures of PHH (Smith et al. 1984). Bioengineered hepatic cell cultures can increase the longevity and phenotype of PHH, and have been applied to mimic *Plasmodium* hepatic development and to test anti-plasmodium drugs targeting the liver-stage of infection. Specifically, micropatterned co-cultures of PHH plated on collagen-coated islands surrounded by murine fibroblasts have been reported to sustain both *Pv* and *Pf* liver-stages (March et al. 2013; Gural et al. 2018). More recently, Roth et al. published a platform based on commercially available collagen-treated 384-well plates that could support long-term viability of PHH (up to a month) and liver-stage infection of *Pf* and *Pv* (Roth et al. 2018). However, the authors have not addressed the factors that contributed to the extended fitness of hepatocytes.

PHH are thus the best available cell source to reproduce the *Plasmodium* liver-stage infection while reflecting the complete liver functionality and providing predictive results in pharmacological and toxicological *in vitro* research. Nevertheless, PHH are normally isolated from liver biopsies or from liver resections, being a limited cell source. Furthermore, the viability of the hepatocytes isolated depend on a plethora of factors which include the background of the donor (genetics, physical characteristics, and lifestyle), cool ischemia of the tissue between collection and processing, isolation procedure, cryopreservation method and further handling of the isolated hepatocytes (Lee et al. 2014). Albeit at high cost, commercially available cryopreserved PHH circumvent some of these challenges, as bioprocessing parameters can be standardized and applied to a panel of donors, generating a reasonable number of cells from each single donor. Currently, PHH suppliers are characterizing the hepatocyte phenotype and functionality of each lot, and pre-validating features required for different applications, such as self-aggregation ability for 3D culture, metabolism competence for drug metabolism assays, susceptibility to infection, among others. However, variability between donors and vendors is still reported, e.g., in cell self-aggregation, highlighting the need for standardized culture platforms that can be applied to a broad range of donors, from different vendors.

Herein, we present a robust platform to generate and culture spheroids of cryopreserved PHH from different donors and suppliers. We took advantage of a culture strategy previously described by our team, based on stirred-tank bioreactors (Tostões et al. 2012; Rebelo et al. 2017). Recently, we have downscaled the culture system, employing 30 mL spinners, to develop a *Plasmodium* infection model based on hepatic cell lines (Arez et al. 2019). Using these small-scale vessels, we optimized the aggregation strategy and culture conditions (*e.g.,*

inoculum cell density, agitation rate, and co-culture strategy), and characterized the long-term maintenance of cell polarization, hepatic identity and metabolism of PHH in spheroids (up to 4 weeks). For the metabolism characterization, we (i) assessed the activity of 5 from the 6 most relevant CYP isoforms, and (ii) evaluated the capacity to metabolize M5717, a novel anti-plasmodial drug under development by Merck. The aggregation and culture conditions were successfully employed to a total of 12 PHH lots, from different donors, with distinct genetic backgrounds, and from several vendors.

Overall, the PHH spheroid culture platform developed in this work showed potential to be applied in drug discovery targeting infections by higher incidence pathogens that present species-specific tropism, such as *Pv* and *Pf*, as well as hepatitis viruses (e.g., hepatitis C virus, HCV). The long-term fitness of PHH spheroids can be particularly useful for *Pv* hypnozoites.

Material and Methods

Cell sources and two-dimensional cultures

Cryopreserved primary human hepatocytes (PHH) lots presenting different individual features (age, gender, ethnicity, drug dependency and cause of death- Table IVS.1) were purchased from Thermo Fisher Scientific (HU1955, HU8287, HU8295, HU1955, HU8340, HU8360 and HU8373), Lonza (HUM182411, HUM183121, HUM182351, HUM182701 and HUM182851), Yecuris (HHM01008) and BioIVT (M00995-P). PHH were thawed according to the vendor's instructions. Briefly, vials were thawed at 37ºC and diluted in cryopreserved hepatocytes recovery medium (CM7000, Thermo). Following a sedimentation step at 100 *xg* for 10 min, PHH were resuspended in hepatocyte maintenance medium (Williams' Medium E supplemented with Hepatocyte Maintenance Supplement Pack (Serum-free) and 10%

(v/v) Fetal bovine serum (FBS), all acquired from Thermo Fisher Scientific). The hepatocyte suspension was employed for the generation of 2D or 3D cultures. To achieve confluent monolayers (2D cultures) PHH were seeded in collagen type I-coated plates of 24- or 96-wells, at $4x10^5$ or $6.4x10^4$ cell/well, respectively. Plates were maintained in culture at 37ºC and 5% CO_2, for up to 10 days. The HepaRG cell line was purchased from Thermo Fisher Scientific. These cells were thawed in a 37ºC water bath, for approximately 2 minutes. The vial content was diluted 1:10 in William's E medium, supplemented with 1 % (v/v) Glutamine, 1 % (v/v) penicillin/streptomycin, 10 % (v/v) FBS (all from Thermo Fisher Scientific), 5 µg/ml bovine insulin and 50 µM hydrocortisone hemissuccinate (both from Merck). The cell concentration was adjusted to plate $2.6x10^4$ cell/cm^2 in T-flasks. Medium replacement was performed 24h after thawing and then twice a week, until day 14 of culture, when cells were split. HepaRG cells were passaged every 14 days at least twice before co-culture with PHH.

Three-dimensional culture of primary human hepatocytes

Hepatic cell spheroids were generated in 30 mL spinner vessels from ABLE Biott Corporation. Single cell suspensions with PHH densities of $3x10^5$ or $5x10^5$ cell/mL were used for monocultures or PHH:HepaRG co-cultures with cell ratios of 9:1 or 4:1, according to the aggregation strategy. Following cell inoculum, spinner vessels were maintained under different agitation rates ranging from 50-110 rpm, for up to 25 days. Cells were inoculated in the culture medium previously described for PHH. From day 3 until the end of the culture, a medium exchange regimen with serum-free medium was implemented, to achieve full medium replacement every week.

Live/Dead Assay: assessment of cell viability

Hepatic cell spheroids were generated in 30 mL spinner vessels from ABLE Biott Corporation. Single cell suspensions with PHH densities of $3x10^5$ or $5x10^5$ cell/mL were used for monocultures or PHH:HepaRG co-cultures with cell ratios of 9:1 or 4:1, according to the aggregation strategy. Following cell inoculum, spinner vessels were maintained under different agitation rates ranging from 50-110 rpm, for up to 25 days. Cells were inoculated in the culture medium previously described for PHH. From day 3 until the end of the culture, a medium exchange regimen with serum-free medium was implemented, to achieve full medium replacement every week.

Spheroid cryosectioning and confocal microscopy: characterization of hepatocyte

Characterization of the phenotype of PHH in spheroids was performed by confocal microscopy, as previously described (Arez et al. 2019). Spheroids were fixed in 4% (w/v) paraformaldehyde with 4% (w/v) sucrose in PBS, for 20 min. For cryosections, spheroids were dehydrated with 30 % (w/v) sucrose, overnight and frozen at -80 °C, in the optimum cutting temperature (O.C.T.TM) compound Tissue-Tek (Sakura). The frozen samples were sectioned in 20 µm slices using a Cryostat (Leica). For the immunofluorescence microscopy, samples were permeabilized and blocked with 0.1 % (v/v) Triton X-100 (TX-100) and 0.2 % (w/v) fish-skin gelatin (FSG) solution in PBS, for 30 min. The incubation of primary antibody hepatocyte nuclear factor 4 alpha (HNF4α; Ab41898, Abcam) was performed for 2 h and the incubation of the secondary antibody for 1h in a solution containing 0.125 % (w/v) FSG. F-actin detection was attained by an incubation with A488-conjugated Phalloidin (A12379, Thermo Fischer Scientific) 1:100 in PBS, for 20 min. This step was performed following antibody

incubations. Samples were analyzed by point scanning confocal microscopy (SP5, Leica).

Drug Metabolism Assays: characterization of CYP450 metabolic activity in PHH spheroids

At day 5 or 7, the spheroid cultures were split 1:3, generating three 10 mL cultures at approximately $1x10^5$ cell/mL. Cultures were incubated with (i) a drug cocktail - 10 µM midazolam (CYP3A4), 10 µM amodiaquine (CYP2C8), 100 µM phenacetin (CYP1A2), 10 µM diclofenac (CYP2C9) and 5 µM dextrometorphan (CYP2D6), substrates of the specific CYP450 isoforms, as indicated in brackets; (ii) 1 µM M5717, a compound under clinical development; and (iii) DMSO drug vehicle. Drugs were kindly provided by Merck KGaA, and the stock solutions prepared at concentrations higher than 1000-fold the working concentration, so that DMSO was not higher than 0.1% of the culture medium. The cultures were maintained at 37ºC and 5% CO_2 under stirring rates between 55 and 75 rpms. Ten time-points were collected along 48 to 72 hours, in duplicates, for determination of cell viability, quantification of total cell protein and metabolite concentration in the supernatants. Briefly, 250 µL of samples were collected and the supernatant was separated from the cell pellet by a sedimentation step (centrifugation at 1000 *xg*, 5 min). The metabolism reactions were halted by incubation of the supernatant with an ice cold stop solution (99% acetonitrile, 1% formic acid and 3 µM pruvanserin, used in this solution as an internal control for the LC-MS analysis). In parallel, the cell pellet was washed with PBS (-/-), snap frozen in liquid N_2 and stored at -80 ºC until protein quantification. DMSO-treated spheroids were evaluated as controls of cell viability - spheroids were incubated with FDA/PI as described above.

LC-MS analysis was performed at Merck KGaA. Briefly, a LC-MS/MS calibration curve was generated for each compound and respective specific metabolite. The concentration of metabolites in the culture supernatants was determined based on the calibration curve. All values were normalized by dividing the analytes' peak area by the internal standard (pruvanserin) peak area. The metabolite concentrations were plotted against the incubation time. A non-linear fit was performed to determine substrate depletion rates, whereas for the metabolite synthesis a linear regression was performed. The metabolite formation rate was retrieved from the slope of the linear regression, which was normalized by the average of total protein concentration at the incubation time, quantified by the bicinchoninic acid (BCA from Thermo Fisher Scientific) assay, according to the manufacturer's instructions.

Pf Infection of PHH monolayer cultures

P. falciparum Pf-NF54-infected mosquitoes were reared at Instituto de Medicina Molecular João Lobo Antunes (iMM|JLA, Lisboa, Portugal) or kindly provided by Prof. Robert Sauerwein, Radboud University Medical Centre, Nijmegen. PHH were plated in collagen I-coated plates as described above and inoculated with $1x10^5$ sporozoites per well (spz/well) or $6.4x10^4$ spz/well, for cell-to-sporozoite ratios of 4:1 and 1:1, in 24-well and 96-well plates, respectively. At day 5 post-infection (dpi), the detection of the exoerythrocytic forms (EEFs) was performed by immunofluorescence. For this, cells were fixed by incubation with a solution of 4% PFA, for 20 min. After fixation, cells were permeabilized and blocked with a solution of 0.1% TX-100 and 1% BSA in PBS, for 30 min. The incubation of primary antibodies - mouse monoclonal antibody 2E6 against *Plasmodium* heat shock protein 70 (HSP70) and mouse monoclonal antibody 2A10 against *P. falciparum* circumsporozoite protein (*Pf*CSP), as well as with secondary antibodies for 1h, was

performed in the previous solution containing both permeabilization and blocking agents. Nuclei were stained with DAPI or Hoechst. The acquisition of the images was performed in a Zeiss wide-field Fluorescence Axiovert 200M microscope and image analysis was performed on ImageJ.

Results

Cryopreserved primary human hepatocytes aggregate in a 30 mL stirred-tank culture system

Aggregation and long-term maintenance of PHH spheroids, with high cell viability and functional, have been successfully reported by our team in stirred-tank bioreactors of 200 mL, employing freshly isolated cells (Tostões et al. 2012; Rebelo et al. 2017). The limited access to fresh primary material and the high cost of cryopreserved PHH, as well as the limited access to *Plasmodium* sporozoites, restricts the use of such large scales in a routine manner. Hence, we established the bioprocess in a novel configuration of spinner vessels, with a maximum working volume of 30 mL, recently developed by Able Biott Corporation®. This is a newly developed system, not yet characterized for the parameters defining the hydrodynamic conditions (e.g., impeller number, power input). As such, the culture conditions leading to cellular aggregation of the cryopreserved PHH were empirically optimized by fine tuning three main parameters that influence cellular aggregation and hepatocyte longevity: (i) cell inoculum and (ii) agitation rate, reported to influence aggregation efficiency and spheroid diameter in stirred-tank culture systems (Miranda et al. 2010; Serra et al. 2012; Santo et al. 2016); and (iii) co-culture with HepaRG, a bipotent hepatic cell line previously reported to improve the longevity of primary hepatocytes from non-human primates in a sandwich *in vitro* culture

format (Dembélé et al. 2014). The 3D cultures generated were monitored for spheroid morphology and cell viability (Figure IV.1).

Culture conditions	Strategy 1	Strategy 2	Strategy 3	Strategy 4
Inoculum concentration (x10^6 cell/mL)	0.5	0.3	0.3	0.3
Agitation rate (rpm)	50-100	80-110	80-110	80-110
Ratio PHH:HepaRG	n.a	n.a	9:1	4:1

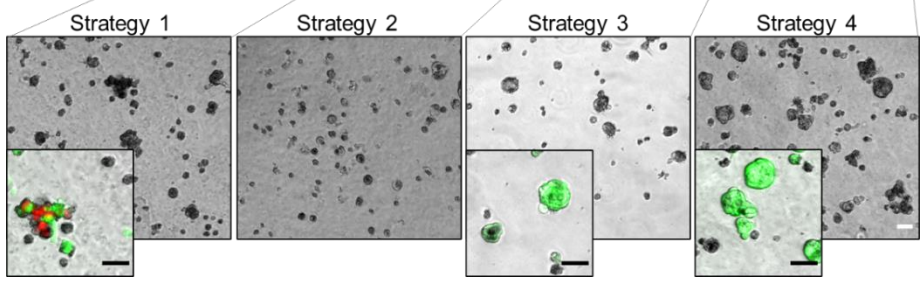

Figure IV.1 - Optimization of cryopreserved primary human hepatocytes (PHH) (lot HU8287) aggregation, in 30 mL stirred-tank culture vessels. Optimization was performed with PHH lot HU8287 (Thermo). Upper panel: culture conditions employed in each aggregation strategy. Strategy 1 and 2 are PHH monocultures (Ratio PHH:HepaRG non-applicable - n.a). Lower panel: phase contrast images of the spheroids generated with each strategy at day 7 of culture. Insets are a merge of phase contrast and fluorescence images of live/dead assay (fluorescein – green, live cells; propidium iodide – red, dead cells). Scale bars: 50 µm.

At day 7 of culture, PHH monocultures presented mostly cells that clustered together but failed to further compact into round-shaped spheroids and lost viability (Figure IV.1, strategy 1), or cells that did not aggregate (Figure IV.1, strategy 2). The co-culture with the HepaRG cell line improved considerably the PHH aggregation, leading to the generation of small and highly compact round-shaped spheroids (Figure

IV.1, strategies 3 and 4), as typically described for primary hepatocytes from murine and human origin (Landry et al. 1985; Tostões et al. 2012).

Cells started interacting soon after inoculation, forming clusters of irregular shape; as early as day three of co-culture cells in clusters rearranged to form small compact spheroids (Figure IV.2A). In both co-culture conditions tested, HepaRG cells were incorporated in heterotypic spheroids mainly composed of PHH; no monotypic spheroids of HepaRG cells were detected (Figure IV.2A). Heterotypic spheroids showed high cell viability (Figure IV.1) and an average diameter of approximately 50 µm (Figure IV.2B). This value is within the range reported for spheroids of primary murine hepatocytes and PHH at one week of culture (Landry et al. 1985; Tostões et al. 2012). Increasing the HepaRG proportion from 1 in 10 to 1 in 5 total cells (strategies 3 and 4, respectively), demonstrated a higher number of spheroids obtained at day 7 of culture. (Figure IV.1 and Figure IV.2A). However, further quantification is needed to validate this observation. Culture longevity was also increased, with high cell viability and spheroid integrity maintained for at least 15 days.

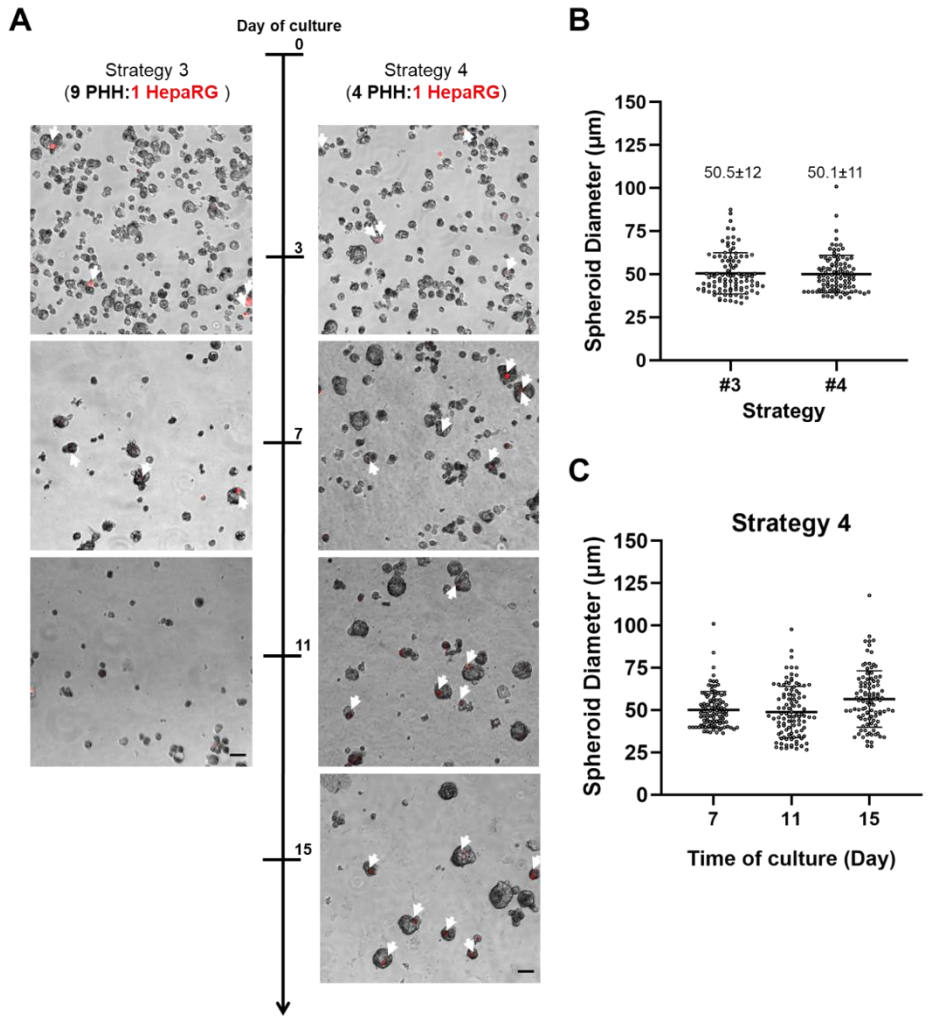

Figure IV.2 - Characterization of 3D co-cultures of cryopreserved primary human hepatocytes (PHH) and HepaRG, at different cell ratios. (A) Representative images of the co-cultures with PHH:HepaRG ratios of 9:1 (strategy 3, left) and 4:1 (strategy 4, right), at days 3, 7, 11 and 15 (only for strategy 4). Prior to cell inoculation, HepaRG cells were incubated with the cell tracker deep red dye (red). Images of phase contrast and fluorescence microscopy were merged to assess HepaRG (red) distribution in the spheroids along culture time. Arrowheads depict examples of HepaRG cells withing the spheroids. Scale bars: 50 µm. **(B-C)** Spheroid diameter distribution of strategy 3 and 4, at day 7 of culture **(C)** and of strategy 4 at days 7, 11, and 15 of culture

(C). Results are the mean and S.D of an average of 100 spheroids from one single experiment.

Altogether, these results indicate that strategy 4 (the co-culture of PHH and HepaRG cells at a 4:1 ratio, with a cell inoculum of 0.3 x10^6 total cells *per* mL, and an initial agitation rate of 80 rpm *per* minute) was more efficient in generating long-term 3D cultures of cryopreserved PHH. The potential of this strategy to be extended further than 15 days and applied in drug discovery was assessed employing the lot used for the previous optimizations (HU8287 lot).

Cryopreserved primary human hepatocytes preserve polarity, phenotype and functionality for at least 4 weeks, in 3D co-cultures with HepaRG cells, in stirred-tank culture vessels

To benchmark the 3D co-cultures of cryopreserved primary human hepatocytes (PHH) and HepaRG for drug discovery applications, culture time was extended further, until day 25, and hepatocyte polarity, phenotype (Figure IV.3) and drug metabolism capacity (Figure IV.4) were characterized.

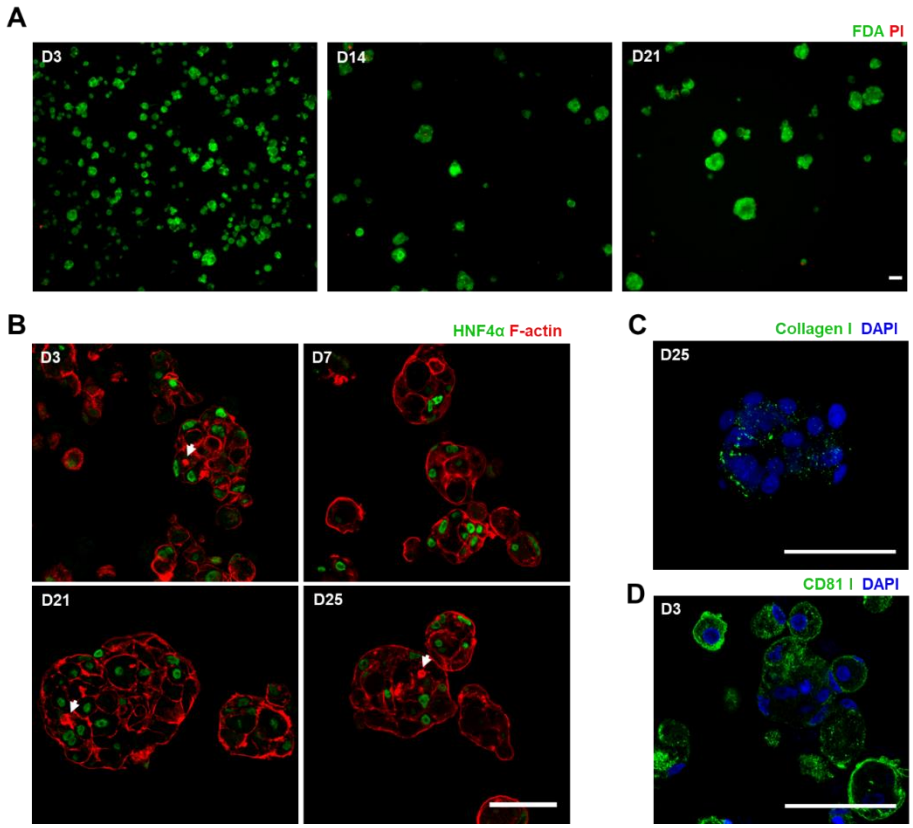

Figure IV.3 - Characterization of 3D co-cultures of cryopreserved primary human hepatocytes (PHH) lot HU8287 and HepaRG by fluorescence microscopy. (A) Representative images of cell viability, evaluated by a live/dead assay (Fluorescein – green, live cells; Propidium iodide – red, dead cells) at day (D) 4, 14 and 21 of culture. **(B)** Representative images of hepatic phenotype, by the detection of F-actin (phalloidin, green) and hepatocyte nuclear factor 4 alpha (HNF4α, green), at D3, 7, 21 and 25 of culture. White arrowheads indicate bile canaliculi-like structures (BC). **(C-D)** Representative images of other hepatic proteins, such as collagen type I (collagen I, green, C) and CD81 receptor (green, D), at D25 and D3 of culture, respectively. Nuclei were stained with DAPI (blue). Images from 20 µm thick cryosections. Scale bars: 50 µm.

Spheroids retained their compact morphology and high cell viability along the four weeks of culture (Figure IV.3), with very rare dead cells

labeled by propidium iodide (PI). The hepatic phenotype focused on two main hepatic features: cellular polarization and hepatic-specific proteins (Treyer and Müsch 2013). F-actin enrichment in the intercellular regions throughout the spheroids depth indicates cellular polarization and delineates bile canaliculi-like structures (identified by arrowheads, Figure IV.3B), typically formed in polarized hepatocyte cultures (Tostões et al. 2012; Rebelo et al. 2017). The hepatocyte identity was confirmed by the presence of the hepatic-specific protein hepatic nuclear factor 4 alpha (HNF4α) (Li et al. 2000) in the cells constituting the spheroids (Figure IV.3B). Collagen type I, one of the major components of the extracellular matrix of the liver (Aycock and Seyer 1989), was detected intra- and inter-cellularly (Figure IV.3C), highlighting the built-up of a liver-like microenvironment in these co-cultures. The receptor CD81, expressed in hepatocytes and essential for the invasion by *Pf* sporozoites (Silvie et al. 2003), was detected as early as day 3 of culture, with the typical plasma membrane localization (Figure IV.3D).

The 3D co-cultures of PHH and HepaRG were further assessed for their phase I metabolizing capacity. At day 5 or 7, each 30 mL parental culture was split into three 10 mL cultures and maintained under agitation (Figure IV.4A). In parallel, hepatocytes were cultured as monolayers, in collagen-I-coated plates, as control. The 3D and 2D cultures were exposed to (i) a cocktail of substrates specific for five of the CYP450 isoforms - 10 µM midazolam (CYP3A4), 10 µM diclofenac (CYP2C9), 5 µM dextrometorphan (CYP2D6), 100 µM phenacetin (CYP1A2) and 10 µM amodiaquine (CYP2C8); and (ii) 1 µM M5717, an anti-plasmodial drug candidate under clinical development. Samples were collected at ten different time-points, during 72h, for assessment of cell viability and metabolite formation (Figure IV.4A).

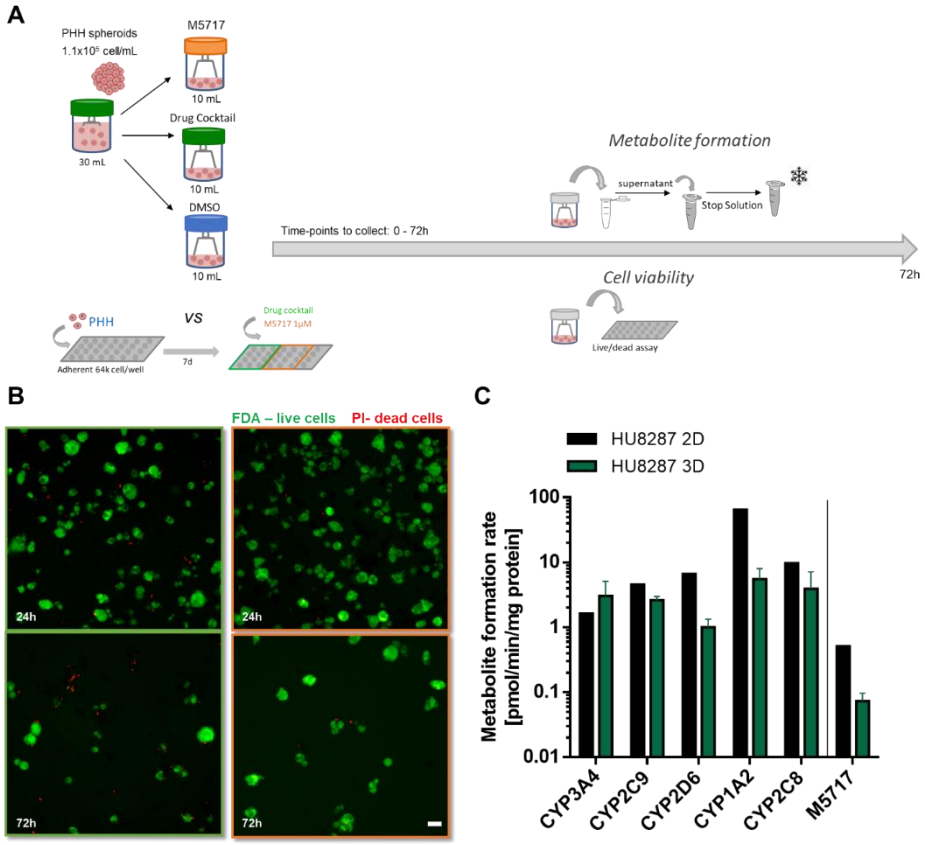

Figure IV.4 - Assessment of drug metabolism capacity of 3D co-cultures of cryopreserved primary human hepatocytes (PHH) lot HU8287 and HepaRG. (A) Schematic representation of the experimental layout. Briefly, spheroid co-cultures of PHH and HepaRG (3D, 5 or 7 days of culture) and PHH monolayers on collagen I (2D, 7 days of culture) were incubated with: a drug cocktail composed of 10 µM midazolam (CYP3A4), 10 µM diclofenac (CYP2C9), 5 µM dextromethorphan (CYP2D6), 100 µM phenacetin (CYP1A2) and 10 µM amodiaquine (CYP2C8); 1µM M5717; or 0.1% DMSO (vehicle control). The assay was performed in spinner cultures of 10 mL (3D) or in 96-well plates (2D). Cell and supernatant samples were collected at ten time-points, along 72h, to assess: cell viability by fluorescence microscopy, intermediate metabolite formation in the culture supernatants by LC-MS and total cell protein quantification. **(B)** Fluorescence microscopy images representative of cell viability in spheroids, at 24 and 72 hours of incubation

with the drug cocktail (green border) and M5717 (orange border), determined by a live/dead assay (fluorescein – live cells, green; propidium iodide – dead cells, red). Scale bar: 50 µm. **(C)** Metabolite formation rate determined by LC-MS. Results are represented as the mean±S.D of 2 (drug cocktail, 3D) or 3 (drug cocktail, 3D) independent experiments; for 2D, bars represent mean±S.D. of 2 technical replicates.

The concentrations of the parental compounds and intermediate metabolites in the culture supernatants were determined by LC-MS/MS (Figure IV.4C). In 3D cultures, the metabolism capacity of hepatic cells was similar to that of HU8287 PHH in 2D. Furthermore, intermediate metabolite of M5717 was detected in the 3D culture supernatants, indicating the ability of these cultures to address the metabolization of this anti-plasmodial compound. Cryopreserved PHH from a different donor, the HU1955 lot, were also assessed for metabolic functionality (Figure IV.5).

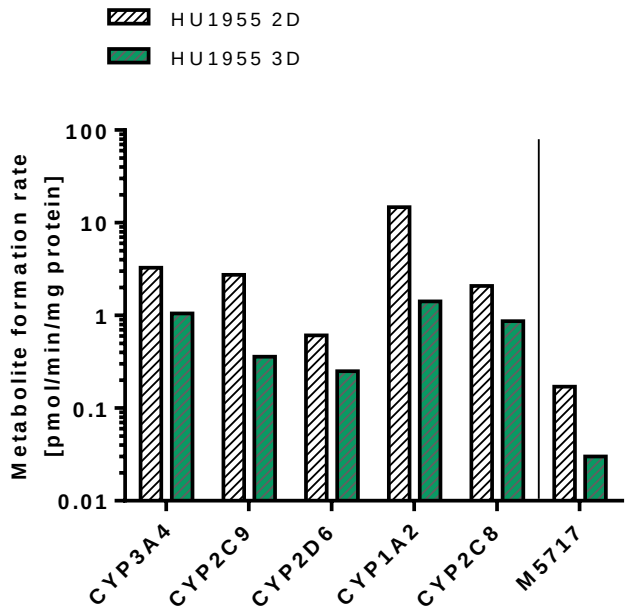

Figure IV.5 - Assessment of drug metabolism capacity of 3D co-cultures of cryopreserved primary human hepatocytes (PHH) lot 1955 and

HepaRG. Metabolite formation rate determined by LC-MS. Results are represented as the mean±S.D of 2 (drug cocktail, 3D) or 3 (drug cocktail, 3D) independent experiments; for 2D, bars represent mean±S.D. of 2 technical replicates.

Similar to HU8287, the HU1955 PHH lot showed a comparable drug metabolization profile in 3D and 2D cultures, for prototypical drugs and M5717. The HU8287 lot showed a tendency for higher metabolite formation rate than HU1955, but additional experiments will be required to ascertain the intra- and inter-lot tendencies observed.

Overall, these data show that the co-culture strategy developed sustained PHH spheroid aggregation in 30 mL spinners and maintained hepatocyte polarity, phenotype and metabolism capacity along a course of at least 4 weeks. PHH:HepaRG spheroid co-cultures derived from two distinct donors showed metabolic activity for five main phase I metabolizing enzymes, namely CYP450 3A4, 2C9, 1A2, 2D6 and CYP2C8. The metabolization of prototypical drugs and M5717, the anti-plasmodial drug under clinical development, demonstrates the potential of these cultures as a platform for anti-plasmodial drug discovery

The novel 3D co-culture strategy can be directly applied to other cryopreserved primary human hepatocyte lots

To assess the robustness of the aggregation and long-term culture strategy optimized in 30 mL stirred-tank culture systems, i.e., co-culture of PHH and HepaRG cells in a 4:1 ratio, we employed a panel of 13 lots of cryopreserved PHH. These lots were acquired from different donors, varying in demographics and commercial sources (Table IV.1). All PHH lots have been pre-validated by the suppliers for plating capacity (in collagen type-I-coated surfaces) and characterized for phase I metabolizing enzyme gene expression (CYP3A4, CYP1A2 and CYP2D6). The aggregation profile and cell viability were monitored

along culture time, as exemplified in Figure IV.6 for 4 lots from different vendors.

Table IV.1 - Panel of the cryopreserved primary human hepatocyte lots tested, and results obtained for 3D co-cultures with HepaRG cells, in stirred-tank culture systems. The different colors indicate distinct vendors. Pre-validations performed by the vendors can include spheroid formation (in ultra-low adherence plates), metabolism in 2D (metabolite formation of CYP450 substrates when plated in collagen-type I-coated surfaces) and induction ability (of CYP450 activity induced by prototypical drugs). The table also depicts the aggregation success rate (assessed as spheroid formation by day 3 or 4 of culture), maximum culture time and the number of independent cultures performed reaching the maximum culture time.

PHH Lot	Race	Age (years)	Gender	BMI	Pre-validations (vendor)	Successful agg at day 3/4	Max. culture time (days)	Total cultures performed
M00995-P	Caucasian	50	Male	20.4	-	✓	14	3/3
HHM01008	Hispanic	1	Male	N.A	-	✓	25	1/2
HUM182411	Hispanic	5	Male	19.3	spheroid formation	✓	25	1/2
HUM183121	African American	49	Male	30.7	spheroid formation	X	-	-
HUM182351*	Caucasian	28	Male	27.6	-	✓	14	1/1
HUM182701	Caucasian	31	Male	22.1	spheroid formation	✓	20	1/1
HUM182851	Caucasian	54	Male	32.2	spheroid formation	✓	21	1/1
HU1955	Caucasian	71	Male	21.5	plated metabolism	✓	15	2/3
HU8287	Caucasian	49	Female	19.6	plated metabolism	✓	25	10/15
HU8295	Caucasian	19	Male	21.9	plated metabolism	✓	10	1/2
HU8340	Caucasian	45	Male	19	induction activity	✓	31	2/2
HU8360	Caucasian	37	Female	32.3	plated metabolism	✓	31	2/2
HU8373	Caucasian	26	Female	18.6	induction activity	✓	28	2/2

N/A – not applicable *Elevated ALT (Alanine Aminotransferase) and AST (Aspartate aminotransferase) levels

BMI – body max index

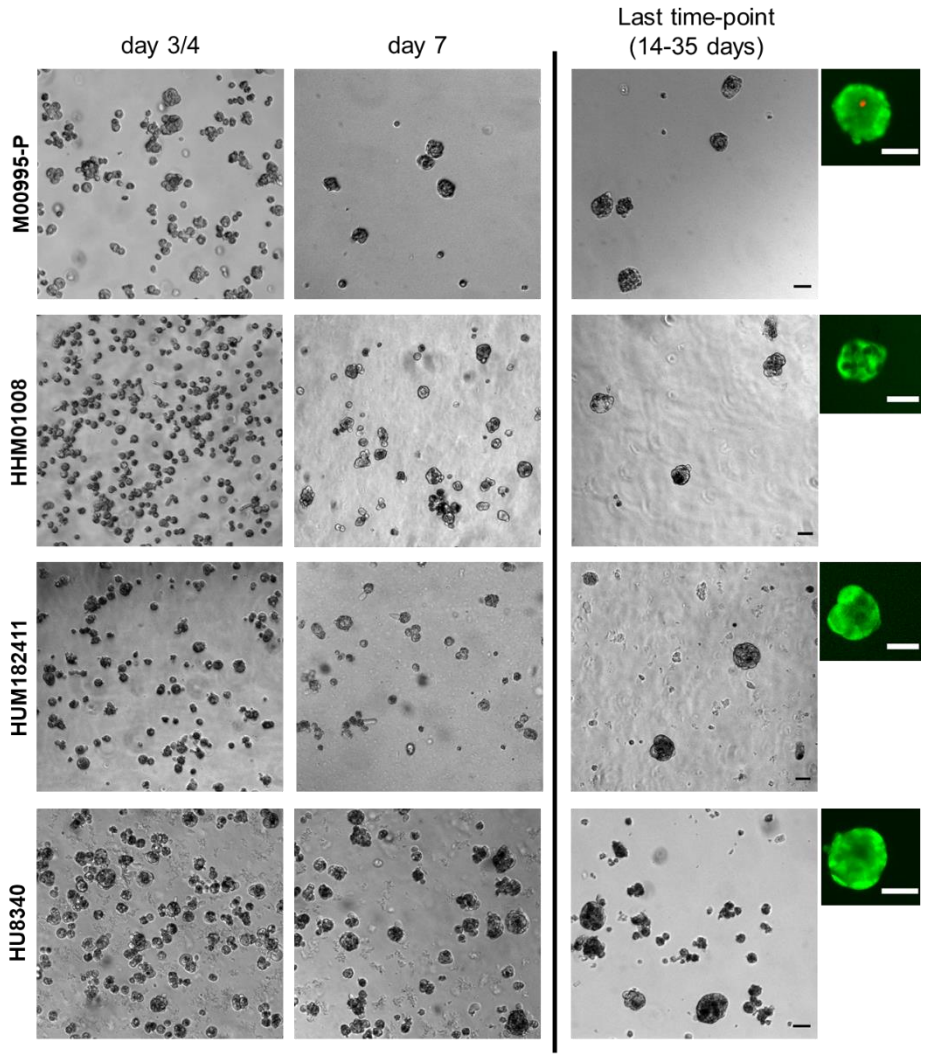

Figure IV.6 - Aggregation of different cryopreserved PHH lots employing the 3D co-culture strategy. Phase contrast and fluorescence microscope images representative of the aggregation ability and cell viability of cryopreserved PHH lots from different sources). Phase contrast images depict the day of culture at which cells formed compact spheroids (between day 3 and 4 of culture), day 7 of culture and last day of culture for each of the lots (day 14 for M00995-P; day 21 for HHM182411 and HHM01008; Day 31 for HU8340). Representative images of fluorescence microscopy of live/dead assay (Fluorescein – green, live; Propidium iodide – red, dead) at the last day of culture for each lot. Scale bars: 50 µm.

Cryopreserved PHH from different commercial sources were successfully aggregated employing the optimized culture strategy, and their aggregation profile was comparable to that previously observed for the HU8287 lot (Figure IV.6). At day 3 after inoculation, PHH from 12 out of 13 lots aggregated into small compact spheroids (Figure IV.6 and Table IV.1). A daily medium exchange regimen (from day 3 onwards) allowed the removal of the single cells remaining in suspension. The HepaRG distribution assessed in the co-culture of two of the lots tested, confirmed the presence of small number of HepaRG cells within spheroids mostly composed of PHH, and HepaRG maintenance up to the fourth week of culture (Supplementary Figure IV.S1).

The spheroids generated from the different lots were maintained with high cell viability for up to 2 to 5 weeks in culture (Table IV.1). For most of the PHH lots tested, additional experiments will be required to confirm these data, as some of the cultures (e.g., M00995-P and HU1955) were terminated due to spheroid retrieval for analytical purposes. Overall, our data suggest that the 3D culture strategy developed is a promising platform that may mitigate the impact of cryopreserved PHH lot variability associated with different donors and commercial sources.

This was further highlighted when 10/13 lots previously employed were assessed for their susceptibility to *Plasmodium falciparum* infection.

An additional source of variability when developing infection models is the restricted permissiveness of PHH to *Plasmodium* species and strains (March et al. 2013; Roth et al. 2018). So far, it was not possible to pinpoint the mechanisms underlying these differences, so we

screened our panel of PHH lots, employing *P. falciparum* strain NF54 and PHH monolayer cultures (Figure IV.7).

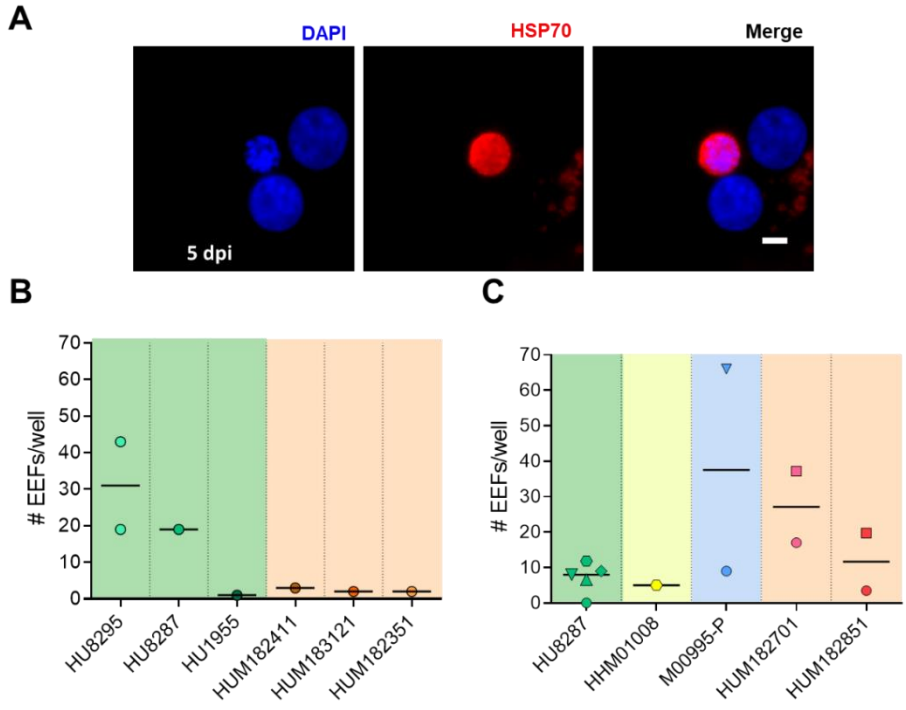

Figure IV.7 - Assessment of the susceptibility to *P. falciparum* infection of a panel of cryopreserved PHH lots cultured in monolayer. Different PHH lots were plated in collagen I-coated surfaces and assessed for their susceptibility to *P.* falciparum (*Pf*) infection. **(A)** Representative images of developed exoerythrocytic forms (EEFs), at day 5 post-infection (dpi). EEFs were detected by the co-localization of heat-shock protein 70 (HSP70, red) and nuclei, stained with DAPI (blue). Scale bar: 5µm. **(B-C)** Quantification of EEFs *per* well. Cells were plated on glass coverslips coated with collagen I: **(B)** in 24 well plates, at $4x10^5$ cell/well and exposed to *Pf* sporozoites at cell-to-sporozoite ratio of 4:1 or **(C)** at $6.4x10^4$ cell/well and incubated with *Pf* sporozoites at 1:1 cell-to-sporozoite ratio. In both graphs each individual data point corresponds to one independent infection experiment (1 to 8 technical replicates) and the mean of biological replicates is also presented. Each symbol

indicates one batch of sporozoites, identifying lots that were tested in parallel. The graph colors indicate lots from different vendors.

The susceptibility of infection was assessed by the detection of exoerythrocytic forms (EEFs), developed forms of the parasites, at 5 days post-infection (dpi). EEFs were identified by the co-localization of a protein abundantly expressed in the parasites, such as the heat-shock protein 70 (HSP70) or circumsporozoite protein (CSP) and nuclei staining (Figure IV.7A). The quantification of the infection was performed and represented by the number of EEFs detected *per* well in a 24-well plate format (Figure IV.7B) or a 96-well format (Figure IV.7C) for the PHH lots tested. Of note, these results were obtained in experiments performed along two years, with different *Pf* NF54 strains, obtained from different sources (from Leiden and other produced at a Lisbon facility, Portugal); the operation procedures of mosquito handling and dissection was also different, due to optimizations along time. Hence, direct comparisons can only be performed between lots infected in parallel (identified by similar symbols in Figure IV.7).

An overall variability of susceptibilities to *Pf* infection was observed among the lots tested (Figure IV.7 B-C). There was not one specific commercial source rendering consistently lots with permissive to *Pf* infection although one of our best lots was from a vendor of PHH with previous reports of higher development rates by both *Pf* and *Pv* (Roth et al. 2018). Nevertheless, at least one lot of each of the four different vendors tested, showed to be infected by *Pf* and sustain EEFs development in 2D PHH monolayers, with at least 5 EEFs/well (4/11 lots, Figures IV.7 B and C). Neither these 4 nor the remaining 7 lots showed common feature in terms of demographics (age, race, gender or BMI).

Among the lots that can be directly compared (tested in parallel with the same batch of sporozoites), similar number of EEFs were detected

in HU8287 and HHM01008 lots (Figure I.7C, ⎔) at 5 dpi. Moreover, HU8287 presented lower #EEFs than M00995-P, HUM182701 and HUM182851 (Figure IV.7C, ○). The highest infection rates (measured as the % of EEFs relatively to the total of sporozoites inoculated), obtained in these lots was of 0.1% for M00995-P (one experiment) and 0.05% for HUM182701 (one experiment) (Supplementary material Figure IV.S2). Comparing these values with the infection rates of *Pf* in PHH monolayers reported in the literature, the highest infection rates obtained in this work were similar to the lowest infection rates obtained from *Pf* NF54 strains, as reported from others (March et al. 2013; Roth et al. 2018).

Overall, the infection rates obtained were highly variable, even within the same lot and the same *Pf* strain. Such inconsistency and low levels of *Pf* development detected restricted the development of a 3D infection platform in 3D setting.

Discussion

Primary human hepatocytes (PHH) are the gold standard cell source to address liver function, as they are originated from the native tissue. They are also reported to sustain the development of both *Pf* and *Pv* sporozoites *in vitro* (March et al. 2013), as well as other hepatotropic pathogens (Arez et al. 2021). The availability of cryopreserved PHH is an advantage for their application in drug discovery pipelines. However, cells derived from different donors and processed using different isolation and cryopreservation procedures present differences in terms of viability post-thawing, plating and aggregation capabilities, and culture longevity, as well as different susceptibilities to infection by human *Plasmodium* species (Roth et al. 2018). Although PHH are the preferred cell source to address liver function, scarce studies have

systematically addressed the aggregation potential of different cryopreserved PHH batches and assessed their applicability for metabolic studies as well as the stability of liver function over time (Solanas et al. 2022). Therefore, our aim was to develop a robust method for 3D culture of cryopreserved PHH. We present a spheroid-based platform for cryopreserved PHH culture that maintained the metabolism capacity and phenotype of hepatocytes for up to 4 weeks in culture, in agitation-based culture systems. PHH were co-cultured with HepaRG, which improved aggregation efficiency and culture longevity. The metabolic performance of the PHH:HepaRG co-cultures was studied, showing that that the 5 most relevant metabolizing enzymes CYP450 metabolized specific substrates. This platform can potentially be applied in the discovery of drugs targeting the liver-stage infection of human infectious *Plasmodium species (Pf* and *Pv)* or other hepatotropic pathogens.

Spheroid models of hepatic immortalized cell lines or primary monkey hepatocytes have shown predictive potential in drug discovery targeting the liver-stage of *Plasmodium* infection. Specifically, the pre-erythrocytic activity of standard-of-care therapies (Chua et al. 2019; Arez et al. 2019) and exploratory drugs (Chua et al. 2019) or drug candidates under clinical development for malaria, such as M5717 (Arez et al. 2019; Fontinha et al. 2022) were predictive of the *in vivo* outcomes. For M5717, the predictive potential was further demonstrated into the clinics (Khandelwal et al. 2022). Despite promising, these spheroid models were so far employed to *Plasmodium* surrogate species *P. berghei* (for *P. falciparum-Pf* and *P. vivax-Pv* schizontal phase) and *P. cynomolgi* (for *Pv*). Furthermore, they exploit hepatic cell sources not fully recapitulative of the human drug response, due to the poor metabolism capacity of immortalized cell lines and the species difference of primate hepatocytes (Olson et al. 2000; Gerets et al. 2012) over human hepatocytes. PHH are permissive to *Pf* and *Pv* infection,

however, hepatocytes derived from different donors present different susceptibilities to infection by these human *Plasmodium* species (Roth et al. 2018). Furthermore, besides the inter-donor variability of the human hepatic cell source, *Plasmodium* strains within the same species (e.g., *Pf* NF54, NF135 and NF175 from *P. falciparum* species) or within the same strain (e.g. NF54-WT and NF54-GFP) also present different infectivity rates towards human hepatocytes (Roth et al. 2018; Yang et al. 2021). Aiming to minimize the inter-donor variability of infection platforms, in this work we present a spheroid-based platform with cryopreserved PHH that maintained the metabolism capacity and phenotype of hepatocytes for up to 4 weeks in culture. This platform has the potential to be further employed in drug discovery targeting the liver-stage infection of human infectious *Plasmodium species (Pf* and *Pv)*.

Spheroid cultures are now widely accepted to allow the maximization of cell-cell and cell-extracellular matrix (ECM) interactions, improving PHH cell polarization and metabolic activity *in vitro* for up to 3 weeks (Tostões et al. 2012; Bell et al. 2016; Rebelo et al. 2017), for longer culture times than PHH sandwich cultures from the same donors (Bell et al. 2018). We have previously employed 200 to 500 mL stirred-tank bioreactors, operating in perfusion mode, to generate robust spheroid cultures of freshly isolated PHH (Tostões et al. 2012; Rebelo et al. 2017). These systems present increased mass transfer coefficients over static cultures, minimizing the formation of hypoxic centers in the spheroids. Furthermore, the continuous agitation and the perfusion of nutrients and small molecules, while clearing the single cells and toxic by-products in culture, allows an increase in culture longevity (Tostões et al. 2012; Rebelo et al. 2017). However, these, or other stirred-tank culture systems were never employed in the generation of 3D cultures from cryopreserved PHH. The large scale of the bioreactor systems requires a large quantity of PHH, which beyond the high cost associated, is also not feasible for *Plasmodium* infection, as the amount

of sporozoites from a same batch is limited. Hence, 30 mL spinner vessels were employed. While the scale is advantageous, as the system has been recently developed, parameters defining the hydrodynamic characteristics are not fully characterized (e.g., impeller power number, and power input). Nevertheless, the trapezoid shaped impeller, which was reported to be favorable to aggregate formation in other stirred-tank vessel configurations by our group and others (Olmer et al. 2012; Simão et al. 2016). We have already reported the infection of HepG2 spheroids by *P. berghei* and subsequent culture for at least 4 days, using culture volumes below 20 mL (Arez et al. 2019). Hence, the optimization of PHH aggregation in this stirred-tank culture system was performed empirically, fine tuning culture parameters such as cell concentration and stirring rate. In previous works, optimization of these parameters allowed, the control over spheroid size, while minimizing detrimental effects of shear stress (Miranda et al. 2010; Kinney et al. 2011; Santo et al. 2016). In this work, the manipulation of these parameters was not sufficient to render consistent aggregation and long-term culture of cryopreserved PHH as monocultures. By employing a co-culture approach with the hepatocarcinoma cell line HepaRG, we could improve the aggregation and maintenance of hepatic spheroids composed mainly of PHH, for at least 7 days in culture. Culture longevity could be extended up to more than 30 days when we increased the HepaRG proportion in the co-cultures (PHH:HepaRG of 4:1). Co-culture with HepaRG cells has been previously shown to extend the culture longevity of primate primary hepatocytes in a collagen-sandwich model (Dembélé et al. 2014). In the latter, Dembélé et al. reported the lack of permissiveness of HepaRG cells to *P. cynomolgi* (Dembélé et al. 2014), which we demonstrated to be true also for *P. berghei* (Arez et al. 2019). Hence, the presence of HepaRG in these co-cultures is not expected to interfere in the *Plasmodium* infection rates to be obtained, having solely a supportive role in PHH adhesion/self-assembly and long-term

maintenance. The improvement of PHH aggregation and longevity in co-culture has been previously reported to be a consequence of ECM deposition by the supporting cell types. PHH co-cultured with rat epithelial cells showed stable biosynthetic functions for longer periods of time consistent with the accumulation of collagen I and III between both cell types (Clement et al. 1984), and the same effect was observed in co-cultures with 3T3-J2 fibroblasts consistent with the induction of decorin expression (Khetani et al. 2004; Leite et al. 2011). Ever since, co-culture approaches have been successfully employed in the development of hepatocyte cell models for infectious diseases and drug toxicity studies (Kostadinova et al. 2013; Dembélé et al. 2014; March et al. 2015; Rebelo et al. 2017). We detected an accumulation of collagen type-I in the intercellular space of the spheroids, suggesting the built up of a liver microenvironment in these co-cultures. As this type of collagen is very poorly expressed in hepatocytes, in the normal liver (Chojkier et al. 1988), we hypothesize that the HepaRG cell mediate aggregation and spheroid stability along time via production of this ECM protein. Further studies will be required to test this hypothesis.

The heterotypic spheroids obtained showed high cell viability and preserved hepatocyte phenotype for up to 4 weeks in culture, similarly or even longer culture times than the ones obtained in the larger scale bioreactors (Tostões et al. 2012; Rebelo et al. 2017). Specifically, hepatocyte nuclear factor 4-apha (HNF4-α) was detected in the cells composing the spheroids, and the accumulation of F-actin in cell-cell contact areas demonstrated the repolarization of PHH and formation of bile canalicular-like structures (BC). HNF4-α is known to regulate genes crucial for the functionality of mature hepatocytes, such as albumin production, glucose, fatty acid, cholesterol and drug metabolism functions (Gonzalez 2008), as well as for the formation of functional tight junctions an essential feature of hepatocytes polarization (Chiba et al. 2003). Establishment and maintenance of hepatocyte polarization is

critical for many hepatocyte functions, from drug metabolism, e.g., as the apical membrane delineating BC harbors the drug transporters responsible for the phase III of xenobiotic metabolism. Furthermore, the BC are small lumens into which hepatocytes excrete by-products, including drug metabolites and bile (Treyer and Müsch 2013). Assessment of drug receptors localization in the heterotypic PHH:HepaRG spheroids is still pending. Nonetheless CD81, one of the host cell receptors involved in the entry of *Pf* and hepatitis C virus in hepatocytes, was detected in the 3D cultures, with membrane localization as soon as spheroids were formed. Moreover, Roth et al reported that BC formation was associated with higher susceptibility to *Plasmodium* infection (Roth et al. 2018). Altogether, the maintenance of hepatocyte identity, the hepatocyte repolarization, BC formation and the presence and correct localization of CD81 are good indicators of the potential ability of our spheroids to sustain *Plasmodium* infection.

Besides the structural and functional organization, the hepatic cells in spheroids showed metabolite formation catalyzed by at least five of the six CYP450 isoforms responsible for 90% of xenobiotic metabolism (Manikandan and Nagini 2018). Among them were CYP3A4, the most abundant isoform that is responsible for the metabolism of over 50% of marketed drugs, and CYP2D6, which although less expressed is responsible for the metabolism of 30% of marketed drugs (Fraczek et al. 2013). Included in these 30% is primaquine, one of the two available anti-plasmodial drugs with hypnozoidal activity, which is metabolized by CYP2D6 into the active compound. Moreover, the intermediate metabolite of M5717, an anti-plasmodial drug candidate under clinical development by Merck (Baragaña et al. 2015), was also detected. The CYP isoform responsible for M5717 metabolism is not yet uncovered and the current platform may thus be employed for such studies for M5717 across the anti-plasmodial drug pipeline.

PHH are normally derived from patient biopsies or liver resections, being of limited availability and presenting large variability between donors (Zeilinger et al. 2016). Commercially available cryopreserved PHH lots, typically derived from deceased donors, provide a higher number of cells from the same donor and from a panel of donors, being isolated, processed, characterized and cryopreserved employing robust and standardized procedures. In this work we evaluated a total of 13 lots of cryopreserved PHH, from 4 different vendors, for which there was availability of at least 50 vials from a single donor (a total of approximately 1-5x10^8 cells *per* lot), sufficient for longitudinal studies and drug screening. Furthermore, nowadays the cryopreserved PHH are characterized and pre-validated for different features, such as spheroid formation, long-term viability and metabolism, to facilitate lot selection and to reduce the effects of inter-donor variability. Nevertheless, variability between different vendors is also observed. Herein, we benchmarked our 3D platform by applying it to distinct PHH lots from diverse suppliers. We showed successful aggregation of 12/13 lots from 4 different vendors. Importantly, for most of the lots, successful aggregation into compact spheroids was consistently observed by day 3 to 4 (12/12), without further optimization (10/12), demonstrating the robustness of the platform. Additionally, for the two lots evaluated in further detail, the spheroid concentration by day 7 of culture was consistent (1.1x10^5 cell/mL), despite the difference in the average spheroid diameter.

Employing a regimen of partial medium exchange daily, mimicking the perfusion mode previously employed in bioreactors, most of the single cells were cleared out, rendering cultures mostly composed of spheroids with diameter of maximum 80 µm by day 7. This is within the size range of PHH spheroids previously cultured in stirred-tank bioreactors to be devoid of hypoxic centers (Tostões et al. 2012). Finally, the 12 lots that successfully aggregated could be maintained

from a minimum of 2 weeks up to a maximum of 5 weeks in culture, demonstrating the long-term stability of these cultures and therefore potential suitability for drug repeated toxicity studies. We showed the drug metabolism capacity of two PHH lots after one week of culture. The next step will be to expand the analysis to the phase II and III of xenobiotic metabolism, later timepoints, and additional lots. Other potential applications are chronic infections and latent *P. vivax* hypnozoites. The latter have been shown to take 21 days for activation and development into schizonts *in vitro*, after the primary infection (Dembélé et al. 2014; Gural et al. 2018).

Despite the consistent results on the establishment of 3D cultures of the different PHH lots, the same was not observed for their plating efficiency in 2D. As an example, the HU8287 lot consistently rendered high viability and plating efficiency post-thawing than other lots (data not shown), highlighting the typical limitations of 2D cultures of PHH.

Moreover, the results in terms of susceptibility to *Pf* infection in 2D were also highly variable. Overall, the infection rates were highly variable between the 10 PHH lots tested, and even within the same lot. This was probably due to the batch-to-batch variability typical of sporozoites, the use of different sources of *Pf* NF54 and, on top of sporozoite variability, also the differences in plating efficiency of the different PHH lots (Smith et al. 1984; March et al. 2013; Roth et al. 2018). For all these reasons, it was not possible to make quantitative comparisons, even when the infection was done in parallel, with the same sporozoite batch. This indicates that the 3D platform herein described could surpass the variability obtained by monolayer cultures and raises the question unanswered in this work if less variability on the infection susceptibility would be seen in the spheroids generated from different lots.

The 13 PHH lots tested in this work covered a wide range of genetic backgrounds, representing ethnicities of both American and European

populations (Hispanic, African American and majority Caucasian). Furthermore, a wide range of donor demographics was represented such as age (from 1 to 71 years old), gender (10 male and 3 female donors), body mass index, cause of death, alcohol and drug histories, all addressed in different previous studies for their influence on the yield, viability, functionality and plating efficiency (only recently) of hepatocytes after isolation (Lee et al. 2014; Geerts et al. 2019; Solanas et al. 2022). Although the main aim was not to correlate the donor characteristics with the aggregation efficiency of the PHH in the developed platform, as no reports on the effect of these demographics exist on aggregation capacity, we briefly report some important considerations as follow-up work. In the developed platform, the high success rate eliminates the effect of the donor demographics abovementioned in the success of aggregation in stirred-tank culture systems. Only one PHH lot could not be aggregated in the current system (fruit of 1 attempt), which was derived from an African American individual. Although no conclusions can be withdrawn given the uneven portion of ethnicities herein represented, it does not pass unnoticed that one ethnicity as abundant in the malaria endemic areas could not be established in the platform developed, being imperative to address this observation further. Additionally, based in this lot results, the pre-validation of PHH for a specific application in different systems from which they will be employed does not guarantee their successful application (e.g. this lot pre-validated for spheroid formation in ultra-low-adherent plates could not aggregate in the stirred-tank culture system). The gender has been recently reported to affect yield and viability of hepatocytes isolated from liver resections, but no plating efficiency in 2D cultures (Solanas et al. 2022). The results herein showed no differences on aggregation capacity of male *versus* female donors, however, interestingly, the 3 lots tested derived from female donors are within the 6 lots maintained at least 4 weeks in culture. Furthermore, differences

of CYP450 expression between male and female hepatocytes have been reported in mice (Ullah et al. 2021) and different susceptibilities of female human hepatocytes for hepatotoxicants have been recently reported (Mennecozzi et al. 2015). Here, the two donors assessed for their metabolism capacity varied in the gender and showed a tendency for lower metabolism capacity for the female hepatocytes. However, this is based in very preliminary results and would need a much larger number of samples assessed for any conclusion in this regard.

In conclusion, the platform herein described allows the robust generation of spheroids from cryopreserved PHH representing a wide variety of genetic backgrounds that can reproduce the liver phenotype for a course of 4 weeks and are metabolically active for 5/6 of the most relevant phase I metabolizing enzymes. The stirred-tank cultures herein employed can be used for the infection of hepatic spheroids by *Plasmodium* sporozoites and the 3D cultures were able to metabolize M5717, an anti-plasmodial drug candidate against liver-stage Plasmodium infection. These systems allow non-destructive sampling, being especially useful for drug repeated toxicity studies and infections that require long-term cultures, such as from human infectious *Plasmodium species* and *P. vivax* hypnozoites. By employing PHH, this platform has the potential to be extended to other infectious diseases such as hepatitis (e.g. HBV and HCV).

Acknowledgments

We acknowledge Ana Filipa Teixeira and Ana Parreira for mosquito production and infection. This work was funded by the healthcare business of Merck KGaA, Darmstadt, Germany (CrossRef Funder ID: 10.13039/100009945). M.P. is a recipient of a “Concurso de Estímulo ao Emprego Científico” Principal Investigator award of Fundação para a Ciência e Tecnologia, Portugal (FCT), with Ref. N. CEECIND/03539/2017. D.F. is funded by FCT project

CRCNA/BRB/0281/2019. F.A. is recipient of PhD fellowship PD/BD/128371/2017 followed by COVID/BD/151635/2021, funded by FCT.

Supplementary Material

Table IV.S1 - Panel of the cryopreserved primary human hepatocyte lots tested, and results obtained for 3D co-cultures with HepaRG cells, in stirred-tank culture systems. The different colors indicate distinct vendors. Pre-validations performed by the vendors can include spheroid formation (in ultra-low adherence plates), metabolism in 2D (metabolite formation of CYP450 substrates when plated in collagen-type I-coated surfaces) and induction ability (of CYP450 activity induced by prototypical drugs). The table also depicts the aggregation success rate (assessed as spheroid formation by day 3 or 4 of culture), maximum culture time and the number of independent cultures performed reaching the maximum culture time.

Vendor	PHH Lot	Race	Age (years)	Gender	BMI	Cause of Death	Drug/Alcohol	Pre-validated (by the vendor)
BioIVT	M00995-P	Caucasian	50	Male	20.4	Stroke (CVA)	Yes/Yes	metabolic activity
Yecuris	HHMM01008	Hispanic	14 mo	Male	N/A	Head Trauma	No/No	metabolic activity
Lonza	HUM182411	Hispanic	5	Male	19.3	N.D	No/No	spheroid formation Long-term culture
	HUM183121	African American	49	Male	30.7	N.D	Yes/No	spheroid formation Long-term culture metabolic activity
	HUM182351*	Caucasian	28	Male	27.6	N.D	Yes/occasionally	Long-term culture metabolic activity
	HUM182701	Caucasian	31	Male	22.1	N.D	Yes/No	spheroid formation Long-term culture metabolic activity
	HUM182851	Caucasian	54	Male	32.2	N.D	No/occasionally	spheroid formation Long-term culture metabolic activity
Thermo	HU1955	Caucasian	71	Male	21.48	Colorectal cancer	No/current	plated metabolism
	HU8287	Caucasian	49	Female	19.6	Head trauma	Yes/Yes	plated metabolism
	HU8295	Caucasian	19	Male	21.9	Head Trauma	Yes occasionally last few years)/Yes (6mo)	plated metabolism
	HU8340	Caucasian	45	Male	19	Anoxia	Yes/2-3 beers/day	plated metabolism
	HU8360	Caucasian	37	Female	32.3	Anoxia	N.A/No	plated metabolism
	HU8373	Caucasian	26	Female	18.6	Asphyxiation	Yes/2-4drinks/mo	plated metabolism

N.D – not disclosed N/A – not applicable *ALT and AST levels elevated mo – months d - days N.A – not assessed

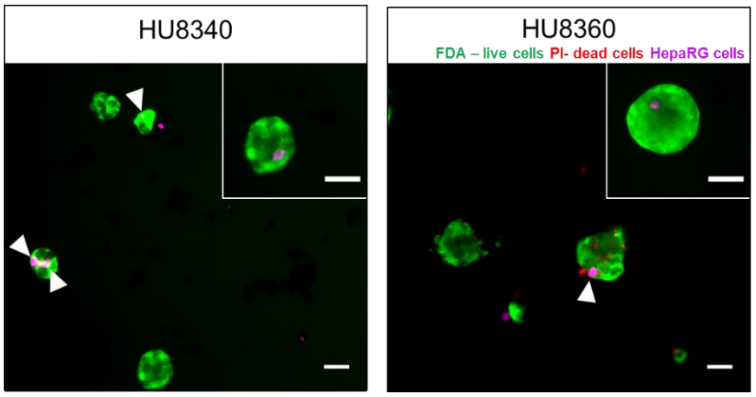

Figure IV.S1 - Assessment of HepaRG distribution in HU8340 and HU8360 3D cultures. Representative images of Fluorescence microscopy live/dead assay (Fluorescein – green; Propidium iodide – red) and HepaRG labeled by cell tracker (magenta and identified by white arrows) in PHH spheroids of week 4 of culture. Zoom in of one spheroid for better visualization of HepaRG cells within the spheroids. Scale bars: 50 µm.

A

PHH Lot	*Pf* development (%)
M00995-P	0.06±0.04
HUM182701	0.03±0.02
HUM182851	0.02±0.01

B

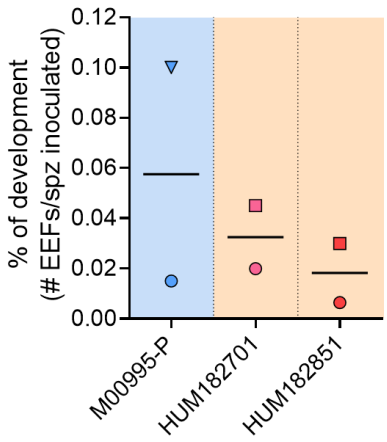

Figure IV.S2 - *Plasmodium falciparum* development in M00995-P, HUM182701 and HUM182851 lots cultured as monolayers. Quantification of the of the *Pf* development in the PHH lots cultured as monolayers measured by the % of exoerythrocytic forms (EEFs) at day 5 post-infection relatively to the number of sporozoites inoculated (spz). **(A)** Results as mean ± S.D are presented in table of at least two biological replicates. **(B)** Graph representation of each biological replicate (each batch of sporozoites) as mean of at least two experiments. Each symbol indicates one batch of sporozoites, identifying lots that were tested in parallel. The color of the background of the graphs indicates lots from different vendors.

References

Arez F, Rebelo SP, Fontinha D, et al (2019) Flexible 3d cell-based platforms for the discovery and profiling of novel drugs targeting plasmodium hepatic infection. ACS Infect Dis 5:1831–1842. https://doi.org/10.1021/acsinfecdis.9b00144

Arez F, Rodrigues AF, Brito C, Alves PM (2021) Review bioengineered liver cell models of hepatotropic infections. Viruses 13:1–25. https://doi.org/10.3390/v13050773

Aycock RS, Seyer JM (1989) Collagens of Normal and Cirrhotic Human Liver. Connect Tissue Res 23:19–31. https://doi.org/10.3109/03008208909103901

Baragaña B, Hallyburton I, Lee MCS, et al (2015) A novel multiple-stage antimalarial agent that inhibits protein synthesis. Nature 522:315–320. https://doi.org/10.1038/nature14451

Bell CC, Dankers ACA, Lauschke VM, et al (2018) Comparison of hepatic 2D sandwich cultures and 3d spheroids for long-term toxicity applications: A multicenter study. Toxicol Sci 162:655–666. https://doi.org/10.1093/toxsci/kfx289

Bell CC, Hendriks DFG, Moro SML, et al (2016) Characterization of primary human hepatocyte spheroids as a model system for drug-induced liver injury, liver function and disease. Sci Rep 6:25187. https://doi.org/10.1038/srep25187

Chattopadhyay R, Velmurugan S, Chakiath C, et al (2010) Establishment of an In vitro Assay for Assessing the Effects of Drugs on the Liver Stages of Plasmodium vivax Malaria. PLoS One 5:1–8. https://doi.org/10.1371/journal.pone.0014275

Chiba H, Gotoh T, Kojima T, et al (2003) Hepatocyte nuclear factor (HNF)-4α triggers formation of functional tight junctions and establishment of polarized epithelial morphology in F9 embryonal carcinoma cells. Exp Cell Res 286:288–297. https://doi.org/10.1016/S0014-4827(03)00116-2

Chojkier M, Lyche KD, Filip M (1988) Increased production of collagenin Vivo by hepatocytes and nonparenchymal cells in rats with carbon tetrachloride-induced hepatic fibrosis. Hepatology 8:808–814. https://doi.org/10.1002/hep.1840080419

Chua ACY, Ananthanarayanan A, Ong JJY, et al (2019) Hepatic spheroids used as an in vitro model to study malaria relapse. Biomaterials 216:119221. https://doi.org/10.1016/j.biomaterials.2019.05.032

Clement B, Guguen-Guillouzo C, Campion J -P, et al (1984) Long-Term Co-Cultures of Adult Human Hepatocytes with Rat Liver Epithelial Cells: Modulation of Albumin Secretion and Accumulation of Extracellular Material. Hepatology 4:373–380. https://doi.org/10.1002/hep.1840040305

Dembélé L, Franetich J-F, Lorthiois A, et al (2014) Persistence and activation of malaria hypnozoites in long-term primary hepatocyte cultures. Nat Med 20:307–312. https://doi.org/10.1038/nm.3461

Dumoulin PC, Trop S a., Ma J, et al (2015) Flow cytometry based detection and isolation of Plasmodium falciparum liver stages in vitro. PLoS One 10:1–24. https://doi.org/10.1371/journal.pone.0129623

Fontinha D, Arez F, Gal IR, et al (2022) Pre-erythrocytic Activity of M5717 in Monotherapy and Combination in Preclinical Plasmodium Infection Models. ACS Infect Dis 8:721–727. https://doi.org/10.1021/acsinfecdis.1c00640

Fraczek J, Bolleyn J, Vanhaecke T, et al (2013) Primary hepatocyte cultures for pharmaco-toxicological studies: at the busy crossroad of various anti-dedifferentiation strategies. Arch Toxicol 87:577–610. https://doi.org/10.1007/s00204-012-0983-3

Geerts S, Ozer S, Chu C, et al (2019) Exploring donor demographics effects on hepatocyte yield and viability: Results of whole human liver isolation from one center. Technology 07:1–11. https://doi.org/10.1142/s2339547819500018

Gerets HHJ, Tilmant K, Gerin B, et al (2012) Characterization of primary human hepatocytes, HepG2 cells, and HepaRG cells at the mRNA level and CYP activity in response to inducers and their predictivity for the detection of human hepatotoxins. Cell Biol Toxicol 28:69–87. https://doi.org/10.1007/s10565-011-9208-4

Gonzalez FJ (2008) Regulation of Hepatocyte Nuclear Factor 4α-mediated Transcription. Drug Metab Pharmacokinet 23:2–7. https://doi.org/10.2133/dmpk.23.2

Gural N, Mancio-Silva L, Miller AB, et al (2018) In Vitro Culture, Drug Sensitivity, and Transcriptome of Plasmodium Vivax Hypnozoites. Cell Host Microbe 23:395-406.e4. https://doi.org/10.1016/j.chom.2018.01.002

Karnasuta C, Pavanand K, Chantakulkij S, et al (1995) Complete development of the liver stage of Plasmodium falciparum in a human hepatoma cell line. Am J Trop Med Hyg 53:607–611. https://doi.org/10.4269/ajtmh.1995.53.607

Khandelwal A, Arez F, Alves PM, et al (2022) Translation of liver stage activity of M5717, a Plasmodium elongation factor 2 inhibitor: from bench to bedside. Malar J 21:151. https://doi.org/10.1186/s12936-022-04171-0

Khetani SR, Szulgit G, Del Rio JA, et al (2004) Exploring interactions between rat hepatocytes and nonparenchymal cells using gene expression profiling. Hepatology 40:545–554. https://doi.org/10.1002/hep.20351

Kinney M a, Sargent CY, McDevitt TC (2011) The multiparametric effects of hydrodynamic environments on stem cell culture. Tissue Eng Part B Rev 17:249–262. https://doi.org/10.1089/ten.teb.2011.0040

Kostadinova R, Boess F, Applegate D, et al (2013) A long-term three dimensional liver co-culture system for improved prediction of clinically relevant drug-induced hepatotoxicity. Toxicol Appl Pharmacol 268:1–16. https://doi.org/10.1016/j.taap.2013.01.012

Landry J, Bernier D, Ouellet C, et al (1985) Spheroidal aggregate culture of rat liver cells: Histotypic reorganization, biomatrix deposition, and maintenance of functional activities. J Cell Biol 101:914–923. https://doi.org/10.1083/jcb.101.3.914

Lee SML, Schelcher C, Laubender RP, et al (2014) An algorithm that predicts the viability and the yield of human hepatocytes isolated from remnant liver pieces obtained from liver resections. PLoS One 9:. https://doi.org/10.1371/journal.pone.0107567

Leite SB, Teixeira AP, Miranda JP, et al (2011) Merging bioreactor technology with 3D hepatocyte-fibroblast culturing approaches: Improved in vitro models for toxicological applications. Toxicol Vitr 25:825–832. https://doi.org/10.1016/j.tiv.2011.02.002

Li J, Ning G, Duncan SA (2000) Mammalian hepatocyte differentiation requires the transcription factor HNF-4α. Genes Dev 14:464–474. https://doi.org/10.1101/gad.14.4.464

Manikandan P, Nagini S (2018) Cytochrome P450 Structure, Function and Clinical Significance: A Review. Curr Drug Targets 19:38–54. https://doi.org/10.2174/1389450118666170125144557

March S, Ng S, Velmurugan S, et al (2013) A microscale human liver platform that supports the hepatic stages of plasmodium falciparum and vivax. Cell Host Microbe 14:104–115. https://doi.org/10.1016/j.chom.2013.06.005

March S, Ramanan V, Trehan K, et al (2015) Micropatterned coculture of primary human hepatocytes and supportive cells for the study of hepatotropic pathogens. Nat Protoc 10:2027–2053. https://doi.org/10.1038/nprot.2015.128

Mennecozzi M, Landesmann B, Palosaari T, et al (2015) Sex differences in liver Toxicity-Do female and male human primary hepatocytes react differently to toxicants in vitro? PLoS One 10:1–23. https://doi.org/10.1371/journal.pone.0122786

Miranda JP, Rodrigues A, Tostões RM, et al (2010) Extending hepatocyte functionality for drug-testing applications using high-viscosity alginate-encapsulated three-dimensional cultures in bioreactors. Tissue Eng - Part C Methods 16:1223–1232. https://doi.org/10.1089/ten.tec.2009.0784

Olmer R, Ph D, Lange A, et al (2012) Suspension Culture of Human Pluripotent Stem Cells in Controlled , Stirred Bioreactors. 18:772–784. https://doi.org/10.1089/ten.tec.2011.0717

Olson H, Betton G, Robinson D, et al (2000) Concordance of the Toxicity of Pharmaceuticals in Humans and in Animals. Regul Toxicol Pharmacol 32:56–67. https://doi.org/10.1006/rtph.2000.1399

Prudêncio M, Mota MM, Mendes AM (2011) A toolbox to study liver stage malaria. Trends Parasitol 27:565–574. https://doi.org/10.1016/j.pt.2011.09.004

Ramaiahgari SC, Waidyanatha S, Dixon D, et al (2017) Three-dimensional (3D) HepaRG spheroid model with physiologically relevant xenobiotic metabolism competence and hepatocyte functionality for liver toxicity screening. Toxicol Sci 159:124–136. https://doi.org/10.1093/toxsci/kfx122

Raphemot R, Posfai D, Derbyshire ER (2016) Current therapies and future possibilities for drug development against liver-stage malaria. J Clin Invest 126:2013–2020. https://doi.org/10.1172/JCI82981

Rebelo SP, Costa R, Silva MM, et al (2017) Three-dimensional co-culture of human hepatocytes and mesenchymal stem cells: improved functionality in long-term bioreactor cultures. J Tissue Eng Regen Med 11:2034–2045. https://doi.org/10.1002/term.2099

Roth A, Maher SP, Conway AJ, et al (2018) A comprehensive model for assessment of liver stage therapies targeting Plasmodium vivax and Plasmodium falciparum. Nat Commun 9:. https://doi.org/10.1038/s41467-018-04221-9

Santo VE, Estrada MF, Rebelo SP, et al (2016) Adaptable stirred-tank culture strategies for large scale production of multicellular spheroid-based tumor cell models. J Biotechnol 221:118–129. https://doi.org/10.1016/j.jbiotec.2016.01.031

Sattabongkot J, Yimamnuaychoke N, Leelaudomlipi S, et al (2006) Establishment of a human hepatocyte line that supports in vitro development of the exo-erythrocytic stages of the malaria parasites Plasmodium falciparum and P. vivax. Am J Trop Med Hyg 74:708–715. https://doi.org/74/5/708 [pii]

Serra M, Brito C, Correia C, Alves PM (2012) Process engineering of human pluripotent stem cells for clinical application. Trends Biotechnol 30:350–359. https://doi.org/10.1016/j.tibtech.2012.03.003

Silvie O, Rubinstein E, Franetich J-F, et al (2003) Hepatocyte CD81 is required for Plasmodium falciparum and Plasmodium yoelii sporozoite infectivity. Nat Med 9:93–96. https://doi.org/10.1038/nm808

Simão D, Arez F, Terasso AP, et al (2016) Perfusion Stirred-Tank Bioreactors for 3D Differentiation of Human Neural Stem Cells. In: Methods in Molecular Biology. pp 129–142

Smith J., Meis JFG., Ponnudurai T, et al (1984) IN-VITRO CULTURE OF EXOERYTHROCYTIC FORM OF PLASMODIUM FALCIPARUM IN ADULT

HUMAN HEPATOCYTES. Lancet 324:757–758. https://doi.org/10.1016/S0140-6736(84)92670-9

Solanas E, Sanchez-fuentes N, Serrablo A, Lue A (2022) How Donor and Surgical Factors Affect the Viability and Functionality of Human Hepatocytes Isolated From Liver Resections. 9:1–9. https://doi.org/10.3389/fmed.2022.875147

Tostões RM, Leite SB, Serra M, et al (2012) Human liver cell spheroids in extended perfusion bioreactor culture for repeated-dose drug testing. Hepatology 55:1227–1236. https://doi.org/10.1002/hep.24760

Treyer A, Müsch A (2013) Hepatocyte polarity. Compr Physiol 3:243–287. https://doi.org/10.1002/cphy.c120009

Ullah I, Shin Y, Kim Y, et al (2021) Effect of sex-specific differences on function of induced hepatocyte-like cells generated from male and female mouse embryonic fibroblasts. Stem Cell Res Ther 12:1–14. https://doi.org/10.1186/s13287-020-02100-z

Yang ASP, Waardenburg YM, Vegte-Bolmer M, et al (2021) Zonal human hepatocytes are differentially permissive to Plasmodium falciparum malaria parasites. EMBO J 40:. https://doi.org/10.15252/embj.2020106583

Zeilinger K, Freyer N, Damm G, et al (2016) Cell sources for in vitro human liver cell culture models. Exp Biol Med 241:1684–1698. https://doi.org/10.1177/1535370216657448

Chapter V

Concluding remarks and Perspectives

Author contributions: Chapter writing, FA; Chapter revision and editing, MP, CB and PMA

Table of contents

Discussion

Malaria is a high incidence infectious disease still causing more than half a million deaths yearly, of which most are caused by *P. falciparum* (*Pf*) and *P. vivax* (*Pv*) (WHO 2021). The lack of a truly efficacious vaccine against malaria reinforces the need for the discovery of effective prophylactic drugs against this disease. The liver-stage of infection is the first step of the *Plasmodium* life cycle in the mammalian host, obligatorily preceding the phase associated to the clinical symptoms. Thus, it constitutes an attractive target towards malaria chemoprevention. However, the low availability of human *Plasmodium* species (*Pf* and *Pv*) and the restricted *in vitro* tropism of these pathogens to mature human hepatocytes, have hampered the development of cell models that mimic the liver-stage of *Plasmodium* infection. The scarcity of *in vitro* models has also limited the knowledge on the liver-stage of the *Plasmodium* life cycle, which is reflected in the malaria drug pipeline. Most anti-plasmodial drugs target the erythrocytic stage and share the same therapeutic target, leading to cross-resistance. Very few approved therapies have pre-erythrocytic activity and only two clinically approved drugs target the hypnozoites, the latent hepatic forms of the *Pv,* responsible for malaria relapses.

The work developed in this thesis aimed to tackle the scarcity of preclinical cell models that can recapitulate hepatic infection by *Plasmodium* sporozoites and predict drug metabolism and hepatotoxicity of anti-plasmodial drugs, hence, contributing to the development of anti-plasmodium drugs targeting the liver-stage of the infection. To this end, hepatoma cell lines susceptible to *Pv* (HepG2 and HC-04) and to *Pf* (HC-04) infection and cryopreserved primary human hepatocytes (PHH) were cultured in small-scale stirred-tank culture systems (30 mL), to generate long-term 3D cultures potentially capable of sustaining *Plasmodium* infection and reproducing human drug

response. The 3D cultures generated with both cell sources maintained cell viability, polarization, phenotype, and biosynthetic functions **(Chapters 2 and 4)**. Importantly, the culture method was successfully implemented for a variety of cryopreserved PHH lots, from different vendors **(Chapter 4)**. The hepatoma-derived spheroids sustained the *P. berghei* sporozoites differentiation into blood infective merozoites and were successfully employed in the evaluation of the pre-erythrocytic activity of M5717, a drug candidate under clinical development by Merck. The drug was assayed as monotherapy **(Chapter 2)**, or in combination with a drug partner effective against the blood-stage of the infection **(Chapter 3)**. Importantly, the data obtained for the M5717 monotherapy was applied to a pharmacokinetics population model and simulations that defined the dose of a Phase Ib clinical trial (*Pf*-induced volunteer infection study - NCT04250363). Finally, the metabolism of M5717 was assessed in the PHH spheroid model (**Chapter 4)**. The platforms developed in this thesis overcome some of the limitations of the area: long-term 3D cultures in which longitudinal drug assays can be performed, including evaluation of recrudescence **(Chapter 2)**, and can potentially be applied to human *Plasmodium* species, such as *Pf* and species generating long-lasting hypnozoites such as *Pv*. We could also tackle the lack of robustness of spheroid generation from cryopreserved PHH, reducing the typical inter-donor and inter-vendor variability associated with this cell source. Altogether, we have demonstrated that the platforms developed in thesis are a valid tool for successful clinical translational of the drug discovery pipeline targeting the hepatic phase of *Plasmodium* infection.

Spheroid-based models for anti-plasmodial drug discovery

By the time the objectives of this thesis were defined, the few available models to study the liver-stage of *Pf* and *Pv* infection *in vitro* relied on PHH cultures (Mazier et al. 1984; Smith et al. 1984; March et

al. 2013). PHH cultured *in vitro* as monolayers display a widely described phenotypic decay from 48h of culture onwards (Maurel 1996). Furthermore, in such cultures the infection rate reported for *Pf* after 72h post-infection was only 0.007%, an extremely low percentage (Smith et al. 1984). These infection rates were improved in a bioengineered culture format consisting of micropatterned co-cultures of PHH in islands surrounded by murine fibroblasts (MPCC), in which infection rates up to 0.18% were obtained (March et al. 2013). MPCC culture has extended PHH viability sufficiently to capture the complete liver stage development of *Pf* and *Pv,* and the persistence of hypnozoites for up to 21 days post-infection (March et al. 2013). The infection rates reported for *Pf* were similar to those described for the hepatoma cell line HC-04 (Dumoulin et al. 2015), despite inconsistent observations in the literature for the latter. HC-04 were also reported to sustain the full development of *Pf* sporozoites (Sattabongkot et al. 2006). These improved infection rates were still lower compared to those reported for surrogate *species* in human hepatic cell lines (Calvocalle et al., 1994; Hollingdale et al., 1983 as cited in Sattabongkot et al., 2006). Moreover, the availability of PHH is limited and is has high inter-donor variability, which adding up to the variability associated with *Plasmodium* sporozoite batches, constitutes a major bottleneck in the development of robust hepatic infection models suitable for drug discovery and development applications.

As such, the first objective of this thesis was to develop a platform suitable for drug discovery that could mimic the *Plasmodium* liver-stage infection while overcoming the low availability, the high variability and the low infection rates of PHH. For this, we took advantage of hepatoma cell lines presenting different susceptibility to infection by human *Plasmodia* and metabolism capacity, in addition to *Plasmodium* surrogate species. Specifically, we employed HepG2 cells, known to

sustain the development of *Pv* sporozoites *in vitro*, and that possess low metabolism capacity (Chattopadhyay et al. 2010; Gerets et al. 2012); HC-04, reported to sustain *Pf* development, and similarly to HepG2 lacking the expression of important phase I metabolizing enzymes (Sattabongkot et al. 2006; Lim et al. 2007); and HepaRG cells, uncharacterized at the time for their susceptibility to *Plasmodium* infection, except for the simian *P. cynomolgi* (*Pc*), to which it was not susceptible in co-culture with primary hepatocytes (Dembélé et al. 2014). The HepaRG cell line has been reported to retain a drug metabolism capacity closer to that of PHH than the other two cell lines, overcoming inter-donor variability (Gerets et al. 2012), and has been widely employed for drug toxicity purposes (Leite et al. 2012; Rebelo et al. 2015; Pasqua et al. 2020). Specifically, the low expression of CYP450 but not of the phase II metabolizing enzymes reported for HepG2 and HC-04, makes them suitable for screening the toxicity of the parent drugs, or drugs that do not require metabolic activation (Gerets et al. 2012), which is the case of most of the anti-plasmodial drugs discovered by target-based screens. Despite their restricted permissiveness to infection by *Pf* and *Pv* (Sattabongkot et al. 2006; Prudêncio et al. 2011), cell lines are highly permissive to surrogate species, which share many of the features of liver-stage infection with human parasites. As surrogate species, we employed the rodent *P. berghei* (*Pb*), which is a surrogate model of *Pf* (Prudêncio et al. 2011). *Pb* is more amenable to maintain *in vitro,* than its human counterpart, which makes this a more easily available source of sporozoites (Prudêncio et al. 2011). This availability fostered the development of *Pb* reporter strains expressing constitutively reporter genes, such as luciferase (Ploemen et al. 2009) and eGFP (Prudêncio et al. 2007; Dumoulin et al. 2015), which facilitate the assessment of sporozoite progression throughout the liver-stage and allow direct quantification of infection rates. We took advantage of these tools, implementing direct

fluorescence microscopy and flow cytometry readouts for *Pb* infection rate (Chapter 2 and Chapter 3). The short hepatic life cycle of *Pb in vitro* (~48 h to complete the proliferation and differentiation phases and ~60 h for merosome release) circumvents the short time allowed by hepatic cell lines to assess infection, before the cellular overgrowth masks the infection rates obtained (Dumoulin et al. 2015). Despite this, to be able to move to parasite species with longer liver stages, such as *Pf* and *Pv*, in hepatoma cell lines, we employed spheroid cultures. Hepatic spheroids circumvent the overgrowth issue by maximizing cell–cell interactions, which has been reported to result in contact inhibition of growth of HepG2 and HepaRG cells (Ramaiahgari et al. 2014; Rebelo et al. 2015). Additionally, in this thesis we generated spheroid cultures in stirred-tank culture systems of 125 mL, previously optimized by our group for the maintenance of HepaRG spheroids for up to 4 weeks in culture (Leite et al. 2012; Rebelo et al. 2015). This is a culture time appropriate for long-term studies. Hence, the characterization of the hepatocyte phenotype was focused on HepG2 and HC-04 in such systems. These spheroids maintained the hepatocyte identity over a course of 4 weeks, characterized in this thesis by the detection of HNF4α. This is a transcription factor critical for hepatocyte maturity, functionality (Gonzalez 2008), and has been reported to be important in the establishment of hepatocyte polarization (Chiba et al. 2003). The cell polarization typical of hepatocytes, with the formation of bile canaliculi on the apical membrane domain, as well as the biosynthetic function, were recapitulated, up to at least 4 weeks in these 3D cultures of hepatoma cell lines.

So far, besides the work presented in this thesis, the application of spheroid cell models to replicate the *Plasmodium* life cycle has been very limited. There is only one other report of spheroid-based hepatocyte cultures sustaining *Plasmodium* liver-stage infection (Chua

et al. 2019). In that work, the authors reported the infection of primary simian hepatocytes with *Pc* sporozoites prior to, and after, spheroid formation in cellulosic sponges (Chua et al. 2019). The authors highlighted the difficulty in infecting and imaging spheroids entrapped in scaffolds, which posed a physical barrier to *Plasmodium*.

The models presented in this thesis circumvent the bottlenecks outlined above. The spheroids generated are compatible with several imaging techniques commonly used for other organotypic cultures (Gualda et al. 2014; Simão et al. 2016; Estrada et al. 2016). Furthermore, we successfully developed two infection platforms in which *Pb* sporozoites are incubated after spheroid formation, in two different culture systems. The **static platform** takes advantage of the large amounts of spheroids obtained in stirred-tank culture systems, that can potentially be used to feed medium-throughput systems (e.g., 96-well plates), where the incubation with *Pb* sporozoites is performed. The infected cultures are then maintained under static conditions until the end of the liver-stage of the *Pb* life cycle. This platform is appropriate for short-term assays, and adequate to test several conditions in parallel. On the other hand, in the **dynamic platform,** infection of the spheroids with *Pb* sporozoites is performed in 30 mL stirred-tank culture systems, under continuous agitation. The homogeneous access to fresh nutrients and oxygen achieved in this culture system is expected to contribute for the long-term maintenance of the infected cultures. We and others have previously shown that these conditions are favorable for the long-term maintenance of hepatocyte viability and functionality, in non-infected cultures (Tostões et al. 2012; Leite et al. 2012; Rebelo et al. 2015, 2017; Pasqua et al. 2020). The dynamic infection platform is thus suitable for long-term assays.

The culture systems to employ in the implementation of both platforms were carefully considered. In the establishment of the static

platform, the use of low-adherence plates avoided spheroid fusion for the period of the assay (up to 60 h). On the other hand, for the establishment of the dynamic infection platform, 30 mL stirred-tank culture systems were employed, as the limited number of *Plasmodium* sporozoites attained in each batch of mosquitos hampers the use of the 125 mL scales used for the generation of the hepatic spheroids. The infection rates were optimized by manipulating the cell density, cell-to-sporozoite (cell:spz) ratios and cell:spz mode of contact; all of these parameters have been reported to influence the infection rates in 2D cultures (Prudêncio et al. 2007; Ploemen et al. 2009; Swann et al. 2016). The cell and sporozoite densities were optimized in the static and dynamic culture formats to maximize their accessibility to the sporozoites, while avoiding spheroid fusion or contaminations from the non-sterile mosquitoes. Different culture systems also required different modes of promoting cell:spz contact. In the static infection platform, the centrifugation step employed in the 2D models (Prudêncio et al. 2007; Ploemen et al. 2009) was optimized to promote the sedimentation of sporozoites, while avoiding spheroid fusion. Specifically, spheroids were plated in the central area of the plate and accelerating and stopping brakes were employed to reduce the impact of the centrifugal force on the spheroids. For the dynamic infection, reducing the volume of the culture during the period required for the parasite invasion (2h), was sufficient to achieve infection rates comparable to those obtained in the static infection conditions. The reduction of culture volume, or incubation with the pathogen in discrete agitation conditions, have been reported to efficiently promote the infection of neurospheroids with viral vectors (Brito et al. 2012; Simão et al. 2016). Another strategy that increased infection efficiency of neurospheroids with canine adenoviral vectors was increasing the multiplicity of infection, or pathogen-to-cell ratio (Simão et al. 2016). However, due to the limited availability of *Plasmodium* sporozoites, which will be even more restricted when

employing *Pf* and *Pv* sporozoites, the strategy of increasing cell:spz ratios was not pursued.

The 3D cultures of HepG2 and HC-04, but not HepaRG cells, were susceptible to *Pb* infection and sustained the invasion and development of *Pb* sporozoites into merozoites. As this was the first report of exoerythrocytic forms (EEFs), i.e., developed forms of the parasites, in 3D cultures, we characterized the parasite growth profile, from 24 to 60 h post-infection (hpi). EEFs presented their typical proliferative profile that peaked at 48 hpi. At this time, the EEFs within hepatic cells of spheroids had a diameter of approximately 10 µm, which is in agreement with other *Pb*-infected hepatic cells cultured in 2D (Ng et al. 2015; Grand et al. 2020). Importantly, EEFs were found in hepatocytes throughout the spheroid layers, showing that unlike in the porous scaffolds (Chua et al. 2019), the 3D architecture of spheroids does not constitute a barrier to the sporozoite. The infection platforms developed in this thesis can potentially be employed to unveil specific aspects of the *Plasmodium* biology. The spheroid architecture, which generates gradients of nutrients, soluble factors and oxygen which typically underly the hepatocyte functional zonation in the liver lobule (Rebelo et al. 2015; Gaskell et al. 2016). Thus, these cultures could be employed to uncover the mechanisms underlying the higher susceptibility of hepatocytes from zone 3 (under low levels of oxygen) to *Pf* infection, observed in PHH monolayers (Yang et al. 2021). Another process not yet completely understood is the hepatocyte invasion by the *Plasmodium*. CD81, and the scavenger receptor class B type I (SRBI) were identified as the hepatocyte receptors for *Plasmodium* species; interestingly, they are described to have different relevance for infection by distinct *Plasmodium* species (Silvie et al. 2003, 2006; Manzoni et al. 2017; Langlois et al. 2020). Although the presence of these receptors was not assessed, it has been previously reported that HepG2 do not express

CD81 (Zhang et al. 2004). We detected CD81 in PHH spheroids, hence complementing their potential to address these particular mechanisms across the several *Plasmodium* species.

In both platforms, higher cell:spz ratios (1:1 and 1:2), and consequently higher sporozoite loads, yielded higher infection rates. The infection rates of spheroids in the static platform ranged from 0.1 to 0.8% of infected cells for HepG2 and from 0.05 to 0.5% of infected cells for HC-04. These values are higher than those observed for PHH cultures infected with human *Plasmodium* parasites (March et al. 2013; Roth et al. 2018), and lower than the ones reported for cell lines infected with surrogate species (Calvocalle et al., 1994; Hollingdale et al., 1983 as cited in Sattabongkot et al., 2006). Furthermore, the continuous agitation did not impair *Pb* infection. The dynamic platform was established with the 1:1 cell:spz ratio and the reduction of this ratio to 2:1 (half of the parasite amount for the same number of cells) did not compromise the assessment of the infection rates. Importantly, the infection rates obtained in the spheroids were compatible with bioluminescence-based estimation of infection loads, an assay suitable for high-throughput screenings and in drug testing, to which microscopy- or cytometry-based techniques may be less appropriate (Swann et al. 2016).

The *Pb* sporozoites developing in the HepG2 cells in spheroids fully matured into blood-infective merozoites, able to cause blood-stage infection in 100% of the mice injected with the cultures supernatants. These results demonstrate the suitability of these 3D models to mimic the complete liver-stage development of *Pb* infection. The short duration of *Pb* liver infection did not justify the follow-up of the infected culture beyond the 60 hpi. However, the assessment of the maximum culture time demonstrate that the dynamic platform can maintain infected spheroids during the time required to model *Pv* liver stages and

hypnozoite persistence. *Pc* and *Pv* hypnozoites have been demonstrated to persist *in vitro* for at least 21 days in primary hepatocyte cultures, and their activation could be observed within that time-frame (Dembélé et al. 2014; Gural et al. 2018; Chua et al. 2019). At day 21, spheroid cultures in the stirred-tank culture systems presented high cell viability and stable hepatocyte phenotype. Furthermore, these culture systems allow the non-destructive sampling, which facilitates the monitoring and follow-up of one infected culture. Hence, the dynamic infection platform herein described, represents an attractive alternative to the previous models including for the assessment of genetic changes demonstrated to happen throughout the hypnozoite persistence and activation in MPCC cultures (Gural et al. 2018). The possibility of non-destructive sampling is very attractive for long-term drug assays, as it enables assessing the same infected culture throughout the different stages of the parasite hepatic development and different time-points of the drug incubation.

In this thesis both static and infection platforms were employed in drug discovery targeting the pre-erythrocytic stage of *Pb*. As a proof-of-concept, the static infection platform was successful employed to assess the half-inhibitory concentration (IC50) of atovaquone (ATO), a standard-of-care anti-plasmodial drug with pre-erythrocytic activity (Baggish and Hill 2002). The results obtained in the 3D cultures were in agreement with the IC50 determined in monolayer cultures employing the same mode of exposure (24 h of drug exposure during the hepatic development of the parasites) (Baragaña et al. 2015). The 3D cultures were further employed in drug discovery using M5717, as case study **(Chapters 2 and 3)**. M5717 is a drug candidate under clinical development by Merck, that fulfills the criteria for the next-generation of anti-plasmodial drugs (Burrows, et al., 2013). Specifically, it exploits a novel mechanism of action, avoiding the cross-resistance affecting the

malaria drug pipeline. The fast activity and long-lasting half-life makes M5717 suitable for single-dose regimens and to combine with complementary drug partners with similar pharmacokinetic properties, such as pyronaridine (pyro) (Baragaña et al. 2015; Rottmann et al. 2020). The work presented in this thesis was part of the preclinical phase of this drug's development, more specifically in the use of *in vitro* and *in vivo Pb* infection models to address the safety and efficacy of M5717 as monotherapy **(Chapter 2)** and in combination with pyro **(Chapter 3)**. With the static infection platform a range of concentrations could be employed and the IC50 (non-curative dose) and IC99 (curative dose) determined. The IC50 obtained for M5717 in spheroids was concordant with what was reported in the literature in 2D models (Baragaña et al. 2015). The comparison between M5717 and ATO confirmed the higher potency of M5717's pre-erythrocytic activity compared to the standard-of-care (Baragaña et al. 2015). When employed in combination with pyro, a standard-of-care exclusively targeting the erythrocytic stage of infection, the efficacy of M5717 against liver-stage parasites was not decreased, rather enhanced. These results were corroborated by a mouse model of *Pb* liver-stage infection commonly employed in anti-plasmodial preclinical drug development (Prudêncio et al. 2011). The enhanced effect of M5717-pyro that we observed for the liver-stage, was not observed for the blood-stage by Rottman et al. employing a humanized mouse model of *Pf* infection (Rottmann et al. 2020). The authors reported non-detrimental pharmacodynamic interactions for these drugs in combination, against the blood-stage of *Pf* infection (Rottmann et al. 2020). Altogether, these results suggest that M5717-pyro constitutes a promising combination therapy, with a multi-stage anti-plasmodial effect. The similar half-lives of the two drugs circumvent possible drug resistance derived from the exposure of remaining parasites to a single compound (Burrows, et al., 2013). Despite that, complementary studies

on drug-drug interactions will be important to characterize this combination therapy, as previously performed for the blood-stage (Rottmann et al. 2020). An experimental set up of that nature, using a set of drug concentrations and ratios of both compounds *vs* monotherapy would be feasible and interesting to address, also in the static infection platform. The dynamic platform was employed to address if the curative and non-curative doses of M5717 monotherapy determined *in vitro* could completely inhibit the schizont development after the 48 h of infection. In this assay, the dynamic infection platform allowed the maintenance of the infected spheroids with cell viability for up to 84 h, at least. Longer periods of time were not assessed, as the M5717 effect did not delay further the development of *Pb* sporozoites. This experiment was performed in parallel in the mice model of *Pb* liver-stage infection. Both *in vitro* and *in vivo*, the non-curative doses did not inhibit the schizont development after 48 h, whereas a dose higher than the IC99 (curative) completely inhibited schizont development, avoiding parasite recrudescence up to 84 hpi. Parasite recrudescence has been identified as a consequence of suboptimal drug exposure, contributing to *Plasmodium* drug resistance (Burrows, et al., 2013). Importantly, the complete clearance of the liver-stage infection prevents the progression into the blood-stage associated to the pathology, rendering prevention of malaria. Together, these results demonstrate the predictive power of the spheroids cultures, which gained more confidence after a simulation study employing a pharmacokinetics (PK) model fed with phase I clinical data (Khandelwal et al. 2022). In this study, the dose-responses of M5717 determined *in vitro* and *in vivo* were fed to the mathematical model describing the PK of the human population. The results of the simulation showed that both data generated in the 3D *in vitro* platform herein developed and *in vivo,* predicted similar minimal doses of M5717 to prevent the blood-stage infection in humans with an ongoing *Plasmod*ium liver-infection (Khandelwal et al. 2022). The predictive

power demonstrated in this thesis highlights the potential of these platforms to potential to reduce in some extent the animal models required in the drug development process. The translation of the *in vitro* data into clinical studies was subsequently pursued, as a follow-up of the work presented in this thesis. The dose predicted by the *in vitro* model was administered to healthy volunteers after direct venous injection of *Pf* sporozoites, in a phase Ib clinical trial (NCT04250363), which was recently concluded. Therefore, this thesis constitutes a pivotal study on the integration of scaffold-free spheroids in the preclinical development of a drug candidate targeting the liver-stage of *Plasmodium* infection.

PHH-based platform for drug toxicity studies targeting hepatotropic infectious pathogens

While the use of rodent malaria parasites has been, and will continue to be, undoubtedly crucial in host–parasite research and drug development, disparities have been identified between the rodent- and human-infectious *Plasmodium species* (Silvie et al. 2006; Prudêncio et al. 2011). Furthermore, a widely recognized bottleneck in drug development are the divergences between the human and rodent host drug responses (Olson et al. 2000), contributing for high drug attrition rates (Lowe 2019). Hence, the second main aim of this thesis was to expand the 3D infection platform to include PHH to better predict the human drug metabolism, while being able to support the infection of human *Plasmodium* species. To this end, we employed cryopreserved PHH spheroids, which more closely reflect the liver phenotype and functionality. Moreover, the cryopreservation does not impair the metabolic activity when compared with freshly isolated hepatocytes (Smith et al. 2012). In fact, it allows to extend the availability of cells derived from the same donor, which otherwise would have to be employed at a single time (Stéphenne et al. 2010). Furthermore,

cryopreservation allows the development of a donor cell bank, comprehending diverse genetic backgrounds and distinct metabolic profiles (Stéphenne et al. 2010). Biotech companies are nowadays taking advantage of this to commercialize lots of PHH pooled or from individual donors, characterized for their functionality. More recently, PHH lots pre-validated for specific applications are also available, as it is the case of the ones employed in this thesis, which were either metabolism qualified, or pre-validated for their capacity for spheroid formation. This facilitates the choice of appropriate donors depending on the intended purpose. However, it is only suitable if the platform adopted fits the exact design/layout in which such validation was performed (e.g. culture systems for spheroid formation; enzymatic activity assessed). This was shown in this thesis for one of the lots pre-validated for spheroid formation in 96-well plates that could not be established in the stirred-tank culture system. The spheroid cultures of cryopreserved PHH were generated in the previously employed 30 mL spinner vessels, taking advantage of the scale-down and proof-of-concept of their suitability for infection studies, presented in Chapter 2. The cryopreserved lot used to implement the aggregation of this cell source in the stirred-tank culture systems, did not aggregate in the 30 mL spinner vessels, unless in co-culture with a supportive cell type. In this case, we co-cultured the PHH with HepaRG cells as these were previously shown effective in extending the culture longevity of non-human primate hepatocytes in sandwich models (Dembélé et al. 2014). No other reports were found in the literature on the aggregation of cryopreserved PHH in stirred-tank culture systems, which most likely results from the large scales available in these systems, incompatible with the low availability and high costs of this cell source. Hence, by implementing this 3D cultures in 30 mL spinner vessels we are contributing with a novel platform suitable for biological material of limited availability. Consistently with the advantage of using three-

dimensional models for recapitulating aspects of the tissue microenvironment and for longer periods of time over the conventional 2D cell cultures (Tostões et al. 2012; Simão et al. 2015, 2018; Estrada et al. 2016; Bell et al. 2016, 2018; Rebelo et al. 2017, 2018), the accumulation of specific extracellular matrix components (e.g., collagen type I) and the correct localization of membrane receptors (e.g., CD81) were observed. Furthermore, the spheroid cultures were maintained up to 6 weeks, across several PHH lots, retaining hepatocyte identity and cellular polarization for at least 4 weeks. Six weeks is longer than the maximum culture time achieved in the previously reports from our group, employing freshly isolated PHH in 200 mL or 500 mL, computer-controlled bioreactors (Tostões et al. 2012; Rebelo et al. 2017). Importantly, PHH donors employed varied in the donor demographics (age, race, gender, and body mass index), genetic backgrounds, and the susceptibility to *Pf* infection. Many advantages emerge from establishing a platform that can reproduce this variability for drug discovery applications. CYP450 gene expression and activity, have been reported to differ between races and genders (Wijnen et al. 2007). In particular, lower activity of the CYP2C9 variants present at a higher percentage in Caucasians than in African Americans or Asians (Wijnen et al. 2007), higher CYP3A4 gene expression was observed in women (samples from European cohort) than in men, and higher activity of CYP1A2 was observed in men than in women within the Chinese population (Ou-Yang et al. 2000). Despite this, the inter-donor variability did not affect the parameters measured for the successful establishment of the platform, developed, namely its aggregation capacity or the maximum culture time achieved in these culture systems. Twelve out of thirteen lots deriving from different commercial vendors were successfully employed in the developed platform. Testing the metabolism capacity of two donors varying in the gender revealed metabolite formation of the substrates specific for the major CYP450

involved in xenobiotic metabolism (e.g., 3A4, 2C9, 1A2, 2D6, 2C19 and 2E1) as well as the intermediate metabolite of M5717. An overall tendency for increased metabolic activity of female hepatocytes was detected, although the cohort represented by the PHH lots tested and the biological replicates performed are enough for withdrawing conclusions in this matter.

Importantly, the metabolic competence demonstrated in the platform employing cryopreserved PHH complements the infection and drug discovery applications achieved in the platforms employing the hepatoma cell line spheroids. A clear example would be evident in the *in vitro* evaluation of primaquine, which requires metabolic activation into the active compound for the anti-plasmodial activity against liver-stage development, including against *Pv* hypnozoites.

Finally, the stirred-tank culture systems (30 mL spinners) employed in this thesis are relatively new and not well characterized. Nevertheless, they showed a versatile potential to be employed to several cell sources and PHH donors with different genetic backgrounds, generating reproducibly spheroids with well-preserved hepatic functionality. Such technology has therefore the potential to be employed with other cell sources, such as derived from pluripotent stem cells, or patient-derived explants to apply in a personalized medicine approach. Coupled with the advanced gene editing technologies such as CRISPR–Cas9, and the possibility of creating the ultimate patient-specific ‘control chips’ for drug testing, in which disease mutations are corrected in an otherwise identical genetic background, it is a need that could yet become reality.

Conclusions and Future Perspectives

In recent years, the advance on bioengineering approaches to improve hepatocyte cultures functionality and culture longevity has triggered the interest of private investment from biotechnology and

pharmaceutical companies. To achieve the common goal of integrating in drug development more predictive models it is common for private companies to employ advanced *in vitro* models to explore the pharmacology of drug candidates and to screen candidates for specific toxicities early in drug discovery. The development of characterization techniques compatible with 3D cultures have placed spheroids among the most promising tools in disease modeling and drug discovery (Baran 2022). Nevertheless, this exponential development and application of 3D models is not reflected in the field of malaria, as reviewed by Arez et al. 2021.

The work developed in this thesis describes the development of 3D human hepatic cell models to be employed in malaria drug development, specifically targeting the liver-stage of *Plasmodium* infection. We firstly developed one of the first 3D culture models able to reproduce the complete *Plasmodium* liver-stage infection employing stirred-tank culture systems and spheroid models.

Integrated with what was discussed above, but not pursued in this thesis, spheroid-based models provide a biological system better in resembling the host-pathogen interactions, allowing the discovery of novel drug targets to be explored in the drug discovery process, a demanding need in the malaria field.

Spheroids in computer–controlled bioreactors, in which the control of dissolved oxygen in culture is strictly controlled may help to understand the factors (e.g.,the oxygen concentration (Ng et al. 2014; Yang et al. 2021) involved in the *Plasmodium* invasion and development of hepatocytes. Although the stirred-tank culture systems mentioned are of large scales for drug screening, in this thesis we reported the down-scale to 30mL. This down-scale process herein describe can be translated to lower scale systems, such as to miniaturized bioreactors

(e.g ABMR, 15 mL) developed for bioprocess screening applications, and , which allow the tightly control culture conditions in smaller scales (Sandner et al. 2019). One of the advantages of spheroid cultures is the straightforward co-culture of different cell types. A co-culture with KC would allow to address the initial interaction between the parasite and the endothelial and KC lining barrier (Tweedell et al. 2018). This interaction is thought to mediate an immune response that involves the later recruitment of CD8 T cells to which the parasite can evade (Tweedell et al. 2018)(Cockburn et al. 2013). Addressing both oxygen and co-culture with KC is important for hepatocytes drug metabolism (Lee-Montiel et al. 2017). Oxygen-driven hepatocyte zonation influences the metabolic activity of hepatocytes and KC. KC are reported to possess phase I metabolizing enzymes and mediate drug-metabolism immune responses, highlighting the important integration of such non-parenchymal cells in the *in vitro* model.

We show the application and the integration of the 3D *in vitro* models developed, in the preclinical development of a novel drug candidate, using as case study, the M5717.

Additionally, spheroids derived from stirred-tank culture systems are robust and compatible with the use of multi-well plates or higher throughput platforms. Together, with the ability to assess the inhibitory anti-plasmodium activity through a bioluminescence assay, assessed in this thesis, spheroids are useful in early-stage drug screenings, to test a high number of drugs.

In this work the predictive potential of 3D *in vitro* models was extensively demonstrated by comparison with *in vivo* models. Not only we confirmed the utility of 3D *in vitro* and their human context, to replace animal models in specific assays along the preclinical drug development, namely the pharmacodynamic drug interactions, but with

the availability of clinical data after this work, the possibility of validating these *in vitro* platforms against clinical data, will soon be possible.

As previously mentioned, the development of more complex platforms composed of spheroids from different tissue origins is being explored to mimic the systemic delivery and drug metabolism with higher predictive power in drug efficacy and safety on multiple organs of the body. These can be achieved in miniaturized controlled environments such as chip-based platforms, highly attractive to pharmaceutical companies due to their commercial suitability, of ‘plug-and-play’ potential. However, they are not yet integrated in the drug pipeline. The application of the developed spheroids in a platform of this kind, connected with erythrocytes to neurospheroids, constitutes a promising platform to address not only the malaria disease progression into cerebral malaria, but interesting in the malaria drug development. Nevertheless, due to more technical demand of spheroid generation from different tissues, this would be promising to be used in later stages of the drug discovery pipeline, when few drugs are being better characterized.

References

Arez F, Rodrigues AF, Brito C, Alves PM (2021) Review bioengineered liver cell models of hepatotropic infections. Viruses 13:1–25. doi: 10.3390/v13050773

Baggish AL, Hill DR (2002) Antiparasitic Agent Atovaquone. Antimicrob Agents Chemother 46:1163–1173. doi: 10.1128/AAC.46.5.1163-1173.2002

Baragaña B, Hallyburton I, Lee MCS, et al (2015) A novel multiple-stage antimalarial agent that inhibits protein synthesis. Nature 522:315–320. doi: 10.1038/nature14451

Baran S (2022) Perspectives on the evaluation and adoption of complex in vitro models in drug development: Workshop with the FDA and the pharmaceutical industry (IQ MPS Affiliate). ALTEX 39:297–314. doi: 10.14573/altex.2112203

Bell CC, Dankers ACA, Lauschke VM, et al (2018) Comparison of Hepatic 2D Sandwich Cultures and 3D Spheroids for Long-term Toxicity Applications: A Multicenter Study. Toxicol Sci 162:655–666. doi: 10.1093/toxsci/kfx289

Bell CC, Hendriks DFG, Moro SML, et al (2016) Characterization of primary human hepatocyte spheroids as a model system for drug-induced liver injury, liver function and disease. Sci Rep 6:25187. doi: 10.1038/srep25187

Brito C, Simão D, Costa I, et al (2012) Generation and genetic modification of 3D cultures of human dopaminergic neurons derived from neural progenitor cells. Methods 56:452–60. doi: 10.1016/j.ymeth.2012.03.005

Burrows JN, Hooft van Huijsduijnen R, Möhrle JJ, et al (2013) Designing the next generation of medicines for malaria control and eradication. Malar J 12:187. doi: 10.1186/1475-2875-12-187

Calvocalle JM, Moreno A, Eling WMC, Nardin EH (1994) In Vitro Development of Infectious Liver Stages of P. yoelii and P. berghei Malaria in Human Cell Lines. Exp Parasitol 79:362–373. doi: 10.1006/expr.1994.1098

Chattopadhyay R, Velmurugan S, Chakiath C, et al (2010) Establishment of an In vitro Assay for Assessing the Effects of Drugs on the Liver Stages of Plasmodium vivax Malaria. PLoS One 5:1–8. doi: 10.1371/journal.pone.0014275

Chiba H, Gotoh T, Kojima T, et al (2003) Hepatocyte nuclear factor (HNF)-4α triggers formation of functional tight junctions and establishment of polarized epithelial morphology in F9 embryonal carcinoma cells. Exp Cell Res 286:288–297. doi: 10.1016/S0014-4827(03)00116-2

Chua ACY, Ananthanarayanan A, Ong JJY, et al (2019) Hepatic spheroids used as an in vitro model to study malaria relapse. Biomaterials 216:119221. doi: 10.1016/j.biomaterials.2019.05.032

Cockburn I a, Amino R, Kelemen RK, et al (2013) In vivo imaging of CD8+ T cell-mediated elimination of malaria liver stages. Proc Natl Acad Sci U S A 110:9090–5. doi: 10.1073/pnas.1303858110

Dembélé L, Franetich J-F, Lorthiois A, et al (2014) Persistence and activation of malaria hypnozoites in long-term primary hepatocyte cultures. Nat Med 20:307–312. doi: 10.1038/nm.3461

Dumoulin PC, Trop S a., Ma J, et al (2015) Flow cytometry based detection and isolation of Plasmodium falciparum liver stages in vitro. PLoS One 10:1–24. doi: 10.1371/journal.pone.0129623

Estrada MF, Rebelo SP, Davies EJ, et al (2016) Modelling the tumour microenvironment in long-term microencapsulated 3D co-cultures recapitulates phenotypic features of disease progression. Biomaterials 78:50–61. doi: 10.1016/j.biomaterials.2015.11.030

Gaskell H, Sharma P, Colley HE, et al (2016) Characterization of a functional C3A liver spheroid model. Toxicol Res (Camb) 5:1053–1065. doi: 10.1039/c6tx00101g

Gerets HHJ, Tilmant K, Gerin B, et al (2012) Characterization of primary human hepatocytes, HepG2 cells, and HepaRG cells at the mRNA level and CYP activity in response to inducers and their predictivity for the detection of human hepatotoxins. Cell Biol Toxicol 28:69–87. doi: 10.1007/s10565-011-9208-4

Gonzalez FJ (2008) Regulation of Hepatocyte Nuclear Factor 4α-mediated Transcription. Drug Metab Pharmacokinet 23:2–7. doi: 10.2133/dmpk.23.2

Grand M, Waqasi M, Demarta-Gatsi C, et al (2020) Hepatic Inflammation Confers Protective Immunity Against Liver Stages of Malaria Parasite. Front Immunol 11:. doi: 10.3389/fimmu.2020.585502

Gualda EJ, Simão D, Pinto C, et al (2014) Imaging of human differentiated 3D neural aggregates using light sheet fluorescence microscopy. Front Cell Neurosci 8:. doi: 10.3389/fncel.2014.00221

Gural N, Mancio-Silva L, He J, Bhatia SN (2018) Engineered Livers for Infectious Diseases. Cmgh 5:131–144. doi: 10.1016/j.jcmgh.2017.11.005

Khandelwal A, Arez F, Alves PM, et al (2022) Translation of liver stage activity of M5717, a Plasmodium elongation factor 2 inhibitor: from bench to bedside. Malar J 21:151. doi: 10.1186/s12936-022-04171-0

Langlois A-C, Manzoni G, Vincensini L, et al (2020) Molecular determinants of SR-B1-dependent Plasmodium sporozoite entry into hepatocytes. Sci Rep 10:13509. doi: 10.1038/s41598-020-70468-2

Lee-Montiel FT, George SM, Gough AH, et al (2017) Control of oxygen tension recapitulates zone-specific functions in human liver microphysiology systems. Exp Biol Med 242:1617–1632. doi: 10.1177/1535370217703978

Leite SB, Wilk-Zasadna I, Zaldivar JM, et al (2012) Three-Dimensional HepaRG Model As An Attractive Tool for Toxicity Testing. Toxicol Sci 130:106–116. doi: 10.1093/toxsci/kfs232

Lim PLK, Tan W, Latchoumycandane C, et al (2007) Molecular and functional characterization of drug-metabolizing enzymes and transporter expression in the novel spontaneously immortalized human hepatocyte line HC-04. Toxicol Vitr 21:1390–1401. doi: 10.1016/j.tiv.2007.05.003

Lowe D (2019) The Latest on Drug Failure and Approval Rates. In: In The Pipeline. https://www.science.org/content/blog-post/latest-drug-failure-and-approval-rates

Manzoni G, Marinach C, Topçu S, et al (2017) Plasmodium P36 determines host cell receptor usage during sporozoite invasion. Elife 6:. doi: 10.7554/eLife.25903

March S, Ng S, Velmurugan S, et al (2013) A Microscale Human Liver Platform that Supports the Hepatic Stages of Plasmodium falciparum and vivax. Cell Host Microbe 14:104–115. doi: 10.1016/j.chom.2013.06.005

Maurel P (1996) The use of adult human hepatocytes in primary culture and other in vitro systems to investigate drug metabolism in man. Adv Drug Deliv Rev 22:105–132. doi: 10.1016/S0169-409X(96)00417-6

Mazier D, Landau I, Druilhe P, et al (1984) Cultivation of the liver forms of plasmodium vivax in human hepatocytes. Nature 307:367–369

Ng S, March S, Galstian A, et al (2014) Hypoxia promotes liver-stage malaria infection in primary human hepatocytes in vitro. 215–224. doi: 10.1242/dmm.013490

Ng S, Schwartz RE, March S, et al (2015) Human iPSC-Derived Hepatocyte-like Cells Support Plasmodium Liver-Stage Infection In Vitro. Stem Cell Reports 4:348–359. doi: 10.1016/j.stemcr.2015.01.002

Olson H, Betton G, Robinson D, et al (2000) Concordance of the Toxicity of Pharmaceuticals in Humans and in Animals. Regul Toxicol Pharmacol 32:56–67. doi: 10.1006/rtph.2000.1399

Ou-Yang DS, Huang SL, Wang W, et al (2000) Phenotypic polymorphism and gender-related differences of CYP1A2 activity in a Chinese population. Br J Clin Pharmacol 49:145–151. doi: 10.1046/j.1365-2125.2000.00128.x

Pasqua M, Pereira U, Messina A, et al (2020) HepaRG Self-Assembled Spheroids in Alginate Beads Meet the Clinical Needs for Bioartificial Liver. Tissue Eng Part A 26:613–622. doi: 10.1089/ten.tea.2019.0262

Ploemen IHJ, Prudêncio M, Douradinha BG, et al (2009) Visualisation and quantitative analysis of the rodent malaria liver stage by real time imaging. PLoS One 4:1–12. doi: 10.1371/journal.pone.0007881

Prudêncio M, Mota MM, Mendes AM (2011) A toolbox to study liver stage malaria. Trends Parasitol 27:565–574. doi: 10.1016/j.pt.2011.09.004

Prudêncio M, Rodrigues CD, Ataíde R, Mota MM (2007) Dissecting in vitro host cell infection by Plasmodium sporozoites using flow cytometry. Cell Microbiol 10:070816152918001-??? doi: 10.1111/j.1462-5822.2007.01032.x

Ramaiahgari SC, den Braver MW, Herpers B, et al (2014) A 3D in vitro model of differentiated HepG2 cell spheroids with improved liver-like properties for repeated dose high-throughput toxicity studies. Arch Toxicol. doi: 10.1007/s00204-014-1215-9

Rebelo SP, Costa R, Estrada M, et al (2015) HepaRG microencapsulated spheroids in DMSO-free culture: novel culturing approaches for enhanced xenobiotic and biosynthetic metabolism. Arch Toxicol 89:1347–1358. doi: 10.1007/s00204-014-1320-9

Rebelo SP, Costa R, Silva MM, et al (2017) Three-dimensional co-culture of human hepatocytes and mesenchymal stem cells: improved functionality in long-term bioreactor cultures. J Tissue Eng Regen Med 11:2034–2045. doi: 10.1002/term.2099

Rebelo SP, Pinto C, Martins TR, et al (2018) 3D-3-culture: A tool to unveil macrophage plasticity in the tumour microenvironment. Biomaterials 163:185–197. doi: 10.1016/j.biomaterials.2018.02.030

Roth A, Maher SP, Conway AJ, et al (2018) A comprehensive model for assessment of liver stage therapies targeting Plasmodium vivax and Plasmodium falciparum. Nat Commun 9:. doi: 10.1038/s41467-018-04221-9

Rottmann M, Jonat B, Gumpp C, et al (2020) Preclinical antimalarial combination study of M5717, a Plasmodium falciparum elongation factor 2 inhibitor, and pyronaridine, a hemozoin formation inhibitor. Antimicrob Agents Chemother 64:1–9. doi: 10.1128/AAC.02181-19

Sandner V, Pybus LP, McCreath G, Glassey J (2019) Scale-Down Model Development in ambr systems: An Industrial Perspective. Biotechnol J 14:1700766. doi: 10.1002/biot.201700766

Sattabongkot J, Yimamnuaychoke N, Leelaudomlipi S, et al (2006) Establishment of a human hepatocyte line that supports in vitro

development of the exo-erythrocytic stages of the malaria parasites Plasmodium falciparum and P. vivax. Am J Trop Med Hyg 74:708–715. doi: 74/5/708 [pii]

Silvie O, Greco C, Franetich JF, et al (2006) Expression of human CD81 differently affects host cell susceptibility to malaria sporozoites depending on the Plasmodium species. Cell Microbiol 8:1134–1146. doi: 10.1111/j.1462-5822.2006.00697.x

Silvie O, Rubinstein E, Franetich J-F, et al (2003) Hepatocyte CD81 is required for Plasmodium falciparum and Plasmodium yoelii sporozoite infectivity. Nat Med 9:93–96. doi: 10.1038/nm808

Simão D, Pinto C, Fernandes P, et al (2016) Evaluation of helper-dependent canine adenovirus vectors in a 3D human CNS model. Gene Ther 23:86–94. doi: 10.1038/gt.2015.75

Simão D, Pinto C, Piersanti S, et al (2015) Modeling Human Neural Functionality In Vitro : Three-Dimensional Culture for Dopaminergic Differentiation. Tissue Eng Part A 21:654–668. doi: 10.1089/ten.tea.2014.0079

Simão D, Silva MM, Terrasso AP, et al (2018) Recapitulation of Human Neural Microenvironment Signatures in iPSC-Derived NPC 3D Differentiation. Stem Cell Reports 11:552–564. doi: 10.1016/j.stemcr.2018.06.020

Smith CM, Nolan CK, Edwards MA, et al (2012) A comprehensive evaluation of metabolic activity and intrinsic clearance in suspensions and monolayer cultures of cryopreserved primary human hepatocytes. J Pharm Sci 101:3989–4002. doi: 10.1002/jps.23262

Smith J., Meis JFG., Ponnudurai T, et al (1984) IN-VITRO CULTURE OF EXOERYTHROCYTIC FORM OF PLASMODIUM FALCIPARUM IN ADULT HUMAN HEPATOCYTES. Lancet 324:757–758. doi: 10.1016/S0140-6736(84)92670-9

Stéphenne X, Najimi M, Sokal EM (2010) Hepatocyte cryopreservation: Is it time to change the strategy? World J Gastroenterol 16:1–14. doi: 10.3748/wjg.v16.i1.1

Swann J, Corey V, Scherer C a., et al (2016) High-Throughput Luciferase-Based Assay for the Discovery of Therapeutics That Prevent Malaria. ACS Infect Dis 2:281–293. doi: 10.1021/acsinfecdis.5b00143

Tostões RM, Leite SB, Serra M, et al (2012) Human liver cell spheroids in extended perfusion bioreactor culture for repeated-dose drug testing. Hepatology 55:1227–1236. doi: 10.1002/hep.24760

Tweedell R, Qi L, Sun Z, Dinglasan R (2018) Kupffer Cells Survive Plasmodium berghei Sporozoite Exposure and Respond with a Rapid Cytokine Release. Pathogens 7:91. doi: 10.3390/pathogens7040091

WHO (2021) World malaria report 2021

Wijnen PAHM, Op Den Buijsch RAM, Drent M, et al (2007) Review article: The prevalence and clinical relevance of cytochrome P450 polymorphisms. Aliment Pharmacol Ther 26:211–219. doi: 10.1111/j.1365-2036.2007.03490.x

Yang ASP, Waardenburg YM, Vegte-Bolmer M, et al (2021) Zonal human hepatocytes are differentially permissive to Plasmodium falciparum malaria parasites. EMBO J 40:. doi: 10.15252/embj.2020106583

Zhang J, Randall G, Higginbottom A, et al (2004) CD81 Is Required for Hepatitis C Virus Glycoprotein-Mediated Viral Infection. J Virol 78:1448–1455. doi: 10.1128/jvi.78.3.1448-1455.2004

ITQB NOVA, Avenida da República, 2780-157 Oeiras, Portugal | Tel +351 214 469 100 | itqb.unl.pt